공학박사학위논문

정적연소실을 이용한 부분 예혼합 조건에서의 저옥탄 연료의 화염 가시화 및 분석 – 연소 컨셉 모델 제시와 스프레이 내부 현상에 대한 이해

Understanding the spray combustion of low octane fuel under partially premixed condition in constant volume chamber - Conceptual model and inner stochastic behaviors

2017 년 2 월

서울대학교 대학원

기계항공공학부

이 종 혁

Abstract

Understanding the spray combustion of low octane fuel under partially premixed condition in constant volume chamber - Conceptual model and inner stochastic behaviors

Jonghyeok Lee
School of Mechanical and Aerospace Engineering
The Graduate School
Seoul National University

Compression ignition (CI) engines are widely used in transportation field, especially for high duty vehicles, because of their high thermal efficiency and torque. However, they have emission problems with soot (particulate matter) and NOx (nitrogen oxide). Many countries make effort to reduce the environmental problems resulted by vehicle emissions by strengthening regulation. Among the several attempts to satisfy the new regulation, partially premixed compression ignition (PPCI) is being given attention. In CI type

engines, fuel-rich zone during combustion duration is cause of soot production. Therefore, to reduce the soot production, it is important to lead to more mixing of direct injected fuel and ambient air to decrease local equivalence ratio before start of combustion (SOC). In PPCI strategy, by adjusting injection timing or adopting alternative fuels, it is possible to induces enough mixing time, and then makes more premixed charge before SOC.

Among the various commercial fuels, gasoline-like fuels having high resistance to auto-ignition have advantages of mixing because they have longer ignition delay than conventional diesel fuel. Especially, low octane fuels having 70 – 80 octane numbers are more effective than high octane gasolines in low load, high RPM and high EGR conditions.

To apply low octane fuels and develop optimized CI engines, it is necessary to understand fundamental characteristics of fuel spray and combustion, because they are dominant factors to determine efficiency, emissions, and geometry of CI engines. Recently, although there are several works to demonstrate the superiority of low octane fuel in CI engines, those works are conducted with conventional diesel engine with little optimization. Thus, there is not enough physical information and spray combustion model of low octane fuel yet.

In this study, to understand the spray combustion of low octane fuel in

PPCI condition as a precedent step to develop new type of CI engine, fundamental researches were conduct on fuel spray. Instead of commercial fuel, spray combustion of primary reference fuel 70 (surrogate fuel for low octane fuel) was analyzed empirically in constant volume chamber by high speed imaging including filtered natural luminosity and shadowgraph.

Firstly, from the comparison of combustion modes in operating regime, it is verified that there exists new combustion mode. This new combustion mode is designated as 'partially premixed combustion zone'. This new combustion mode has longer injection duration than conventional low temperature combustion (LTC) model and combustion occurs at more downstream than quasi-steady diesel combustion model. As different with conventional diesel combustion where flame goes forward with high momentum, this mode shows expansion of combustion zone to all radial direction in downstream region where momentum is low enough. When combustion zone expands and finally passes the certain upstream location, soot with intensive luminosity begins to appear. In some cases, there is little soot or no radiation signal during combustion duration even at same operating condition. From the stochastic analysis, it is verified that whether soot intensity is high or low comes from variation in initial combustion location.

To understand these stochastic behaviors, validated 1-D computational

model was used to calculate the thermodynamic properties of mixture in spray. From the combination of experimental and computational results, it is verified that case by case variation in temperature near the injector tip has significant effects on first ignition location. Namely, as temperature near the tip is high, combustion location becomes close to injector tip and then chance of intensive soot production becomes high. If it is possible to control temperature in upstream region in reasonable range, it is also possible to predict initial combustion. Additionally, if combustion zone is restricted to downstream enough not to expand to certain upstream location, soot production can be reduced. It general, to reduce the soot during combustion duration, short injection duration is recommended, but it is shown that it is possible to limit the soot production even with extreme long injection duration.

In this work, it is confirmed that it is possible to achieve distinctive combustion mode with low octane fuel. When low octane fuel is injected with low injection pressure and long injection duration, expansion of initial combustion zone in downstream is dominant mechanism to determine soot production. In this case, temperature in front of injector tip has significant effect on initial combustion location and resultant soot production. If temperature is well regulated and combustion zone can be restricted to downstream, it prevents reaction zone from producing soot in upstream.

Keywords: Partially premixed compression ignition, Low octane fuel, Primary reference fuel, Spray, Soot, Constant volume chamber, One dimensional model

***Student Number*: 2011-20740**

Contents

List of Figures

List of Tables

Chapter 1. Introduction

1.1 Research background

There are two kinds of typical internal combustion (IC) engines; compression ignition (CI) engine and spark ignition (SI) engine. CI engines use diesel fuel prone to be auto-ignited easily, in contrast to CI engine, SI engines use gasoline fuel which is not easy to be auto-ignited. Each type has different in-cylinder process to get thermal energy from fuel. CI engines get power from auto-ignition of direct-injected diesel near top dead center (TDC). In SI engines, fuel is ignited passively by spark plug in cylinder head and flame propagates and covers the cylinder volume (Figure 1.1) [1]. Among the two types of IC engines, CI engines are usually used in heavy-duty vehicles because of high torque from their explosive auto-ignition process. Also, CI engines have higher thermal efficiency than SI engines because they have higher compression ratio to lead to auto-ignition of fuel. Recently, because of superiority in torque and thermal efficiency, CI engines are widely used in small passenger cars and light-duty vehicles as well as heavy-duty vehicles. Now, in field of light-duty vehicles, motor-electric hybrid and electric vehicles are beginning to substitute for gasoline fueled SI engine, not for heavy-duty because of limitation of power and electric capacity. As shown in Figure 1.2, gasoline consumption is decreasing in light-duty vehicles as portion of hybrid sector becomes large. On the other hands, diesel consumption continues increasing slightly as shown Figure 1.3 [2]. World Energy Council also predicted that the similar trend that

as total demand of transportation fuel becomes large in the coming few decades, relative amount of heavy-duty vehicles (diesel + jet) to gasoline also becomes large, shown in Figure 1.4 [3].

As explained above, diesel fueled CI engines will be used widely in transportation industry in future. However, there is critical issue about whether CI engines can maintain important position in vehicle power source. That is emission problem. Because of physical and chemical characteristics of combustion process in CI engines, particulate matters (called soot) and nitrogen oxide (NOx) are contained in exhaust gas of CI engines. In conventional CI engines, diesel fuel is directly injected to cylinder near TDC during compression stroke. Because of high temperature and pressure in-cylinder condition, liquid fuel vaporizes right after injection and starts to be mixed with hot ambient air. After few crank angle degrees (CADs) corresponding to ignition delay, reaction starts and soot is produced in rich mixture. Figure 1.5 suggested by H. Kosaka et al. shows two dimensional conceptual image for diesel spray development [4].

According precedent researches, soot is produced in fuel-air mixture where local equivalence ratio is larger than 2 [5]. For diesel fuel, since ignition occurs right after start of injection, there is not enough time for mixing so that local equivalence ratio is usually high than 2. In Figure 1.6, orange line on equivalence ratio-temperature chart indicates change of mixture state during diesel compression ignition process [6]. Thus, it is inevitable that soot is produced in typical diesel CI process. Because NOx and soot are classified to detrimental matters, they are strongly regulated by government all around

world. Over the years, the regulations are being strengthened [7]. For example, Figure 1.7 shows history Euro emissions standards; current lever is much stricter than past one [8].

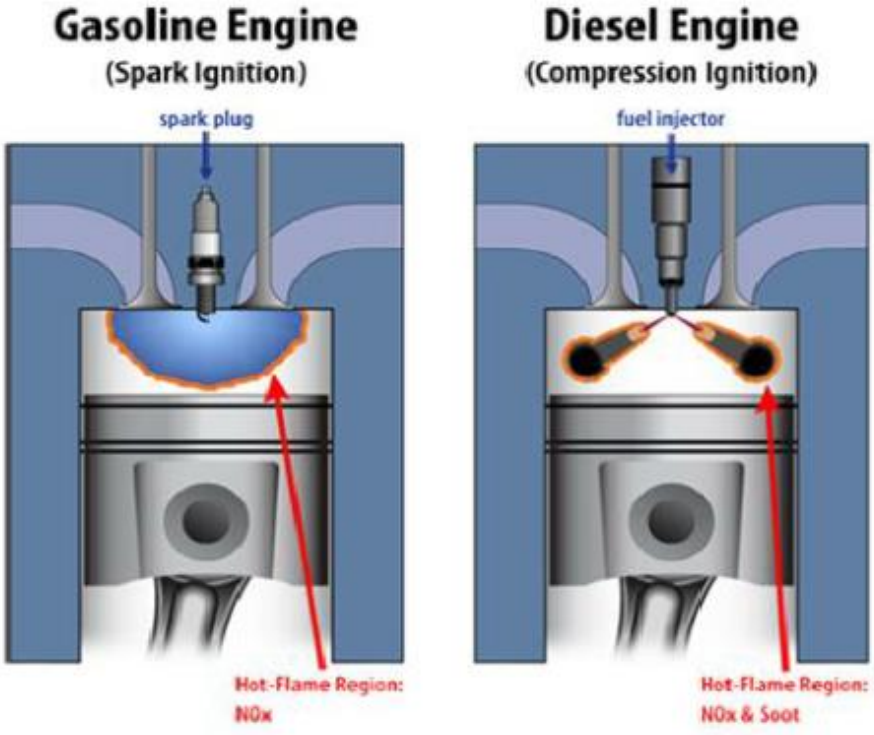

Figure 1.1 Two types of conventional internal combustion engines [1]

Left: gasoline (SI) engine

Right: diesel (CI) engine

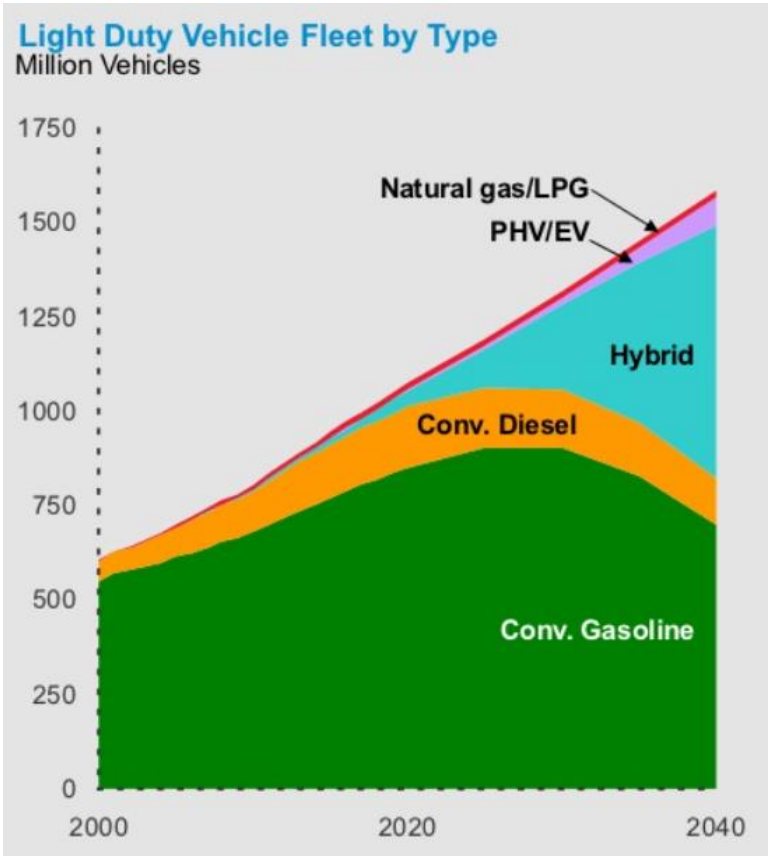

Figure 1.2 Demands of commercial fuels for light duty vehicles [2]

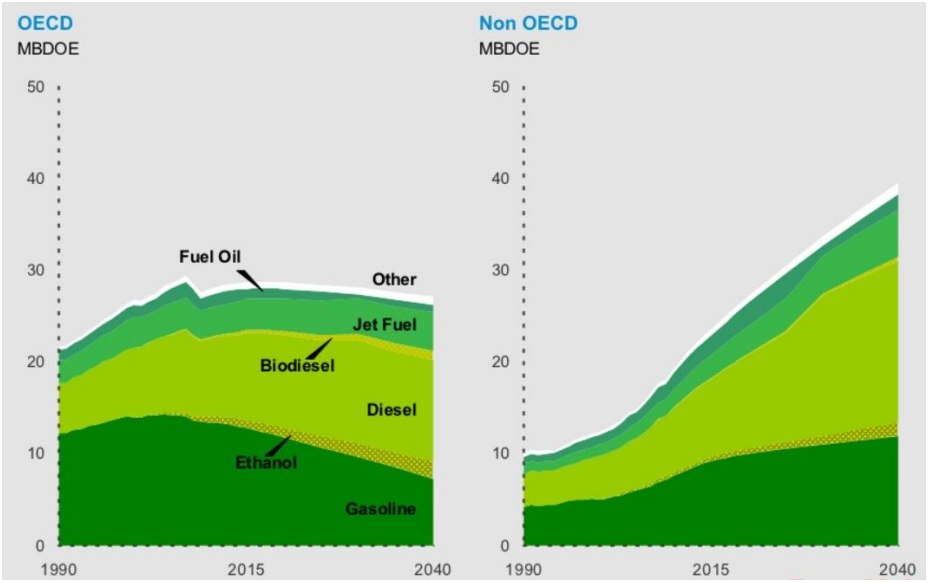

Figure 1.3 Demands of transportation fuel [2]

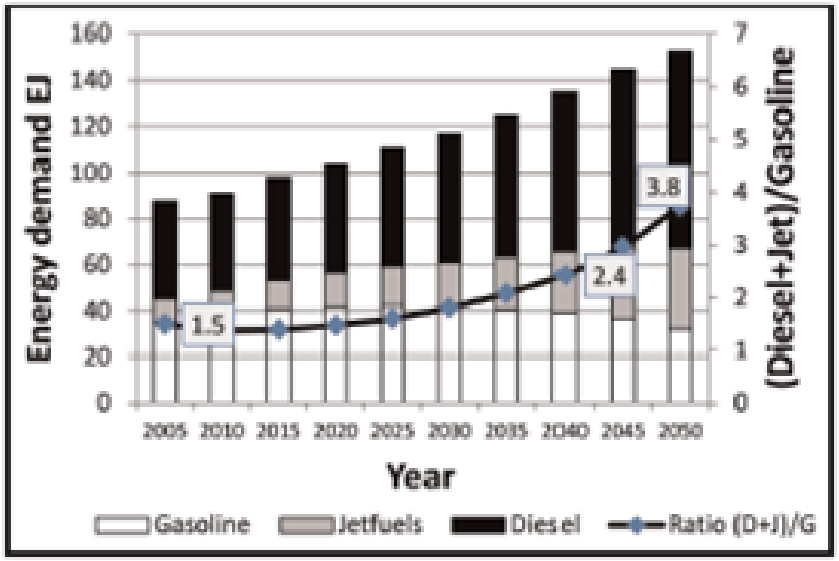

Figure 1.4 Projection for demands of gasoline, jet fuel and diesel [3]

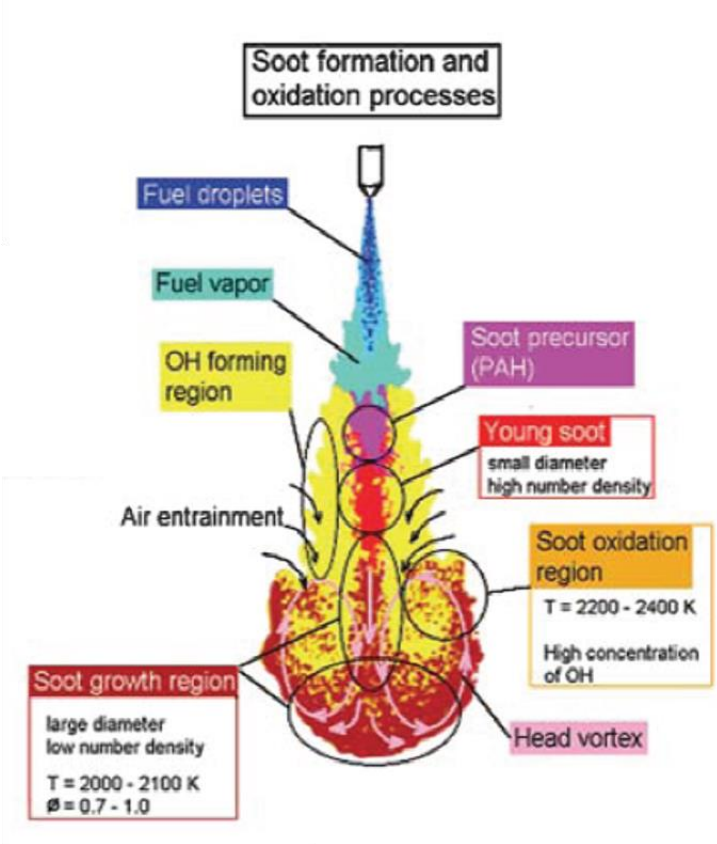

Figure 1.5 Schematic of diesel flame structure [4]

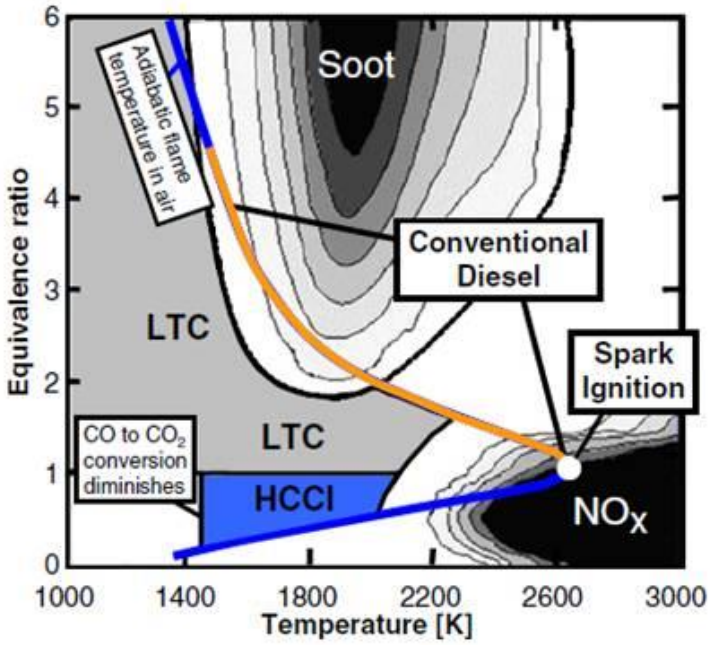

Figure 1.6 Equivalence ratio and temperature diagram indicating conditions for soot and NOx production [6]

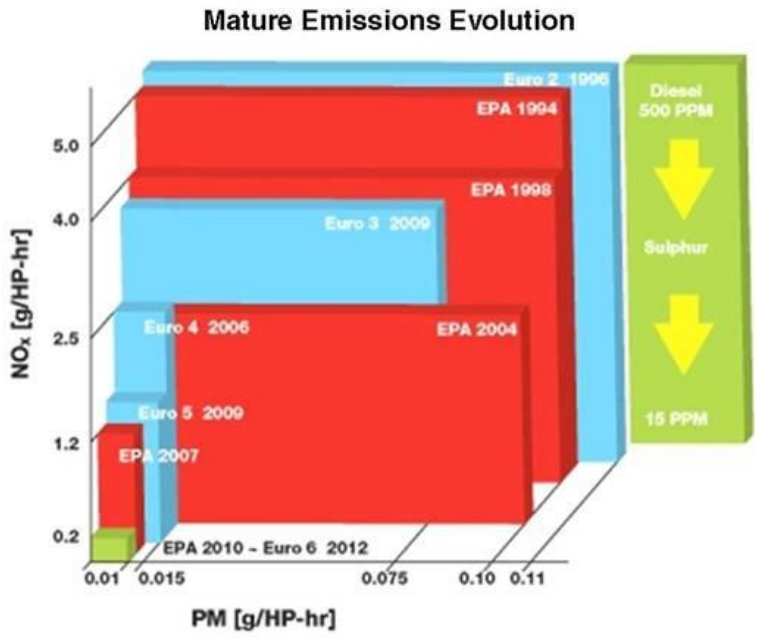

Figure 1.7 History of Euro emissions standards [8]

1.2 PPCI with low octane fuel

Among the several attempts to reduce soot and NOx emissions simultaneously, premixing strategies have been given attentions. Principle of this premixed combustion is making homogeneous mixture or partially premixed mixture before auto-ignition with higher mixing ratio to get local equivalence ratio under 2, while in-cylinder temperature is reduced by proper EGR (Exhaust Gas Recirculation) rates for NOx reduction [6].

It is known that, for conventional diesel engines, premixed concept was first introduced by Toyota Motor and Nissan Motor Corp. Toyota used multi-injection strategy where early pilot injection is used to make homogeneous mixture and ignition triggered by main injection [9]. It is called Toyota UNIBUS (Uniform Bulky Combustion System). However, this system lead to unintended combustion of pilot injected fuel at high load operation range. Nissan used high level of cooled-EGR and swirl to retard ignition timing [10]. Hashizume et al. used pilot injection to lead premixed burn before main injection [11]. All these researches focused on making combustion occurs in more lean state.

The other combustion strategy to reduce emissions is Homogeneous Charge Compression Ignition (HCCI). HCCI engines using auto-ignition of fully premixed mixture have advantages of low emission and high efficiency. However, it is difficult to control ignition timing of mixture, since the auto-ignition of homogeneous mixture solely depends on the thermodynamic state and chemical kinetics of the mixture without external combustion trigger [12].

Especially, unstable operation in low load and high load is considered as major weakness of HCCI engines.

To gain controllability on the combustion timing, Partially Premixed Compression Ignition (PPCI) was suggested, where ignition timing is can be controlled by injection timing [13, 14]. The major difference to HCCI is that PPCI requires 'partially' premixed state of fuel and air, and first ignition occurs in that region.

According to previous researches, it was suggested that injection event should be completed before ignition in PPCI operation, then flame occurs in locally formed mixture [15, 16]. If injection continues even after ignition occurs, fuel combust with form of non-premixed flame like in conventional diesel engines [15, 17]. Figure 1.8 shows example of heat release rate and needle lift profiles for gasoline and diesel in CI engine [13]. In figure, heat release occurs few crank angle degrees after needle operation, which means that injection event and combustion event are wholly separated. As needle and heat release rate profiles are more overlapped, combustion becomes non-premixed and produces more soot. If heat release goes apart from injection event, fuel has more time to mix with ambient air. This profiles imply that it is more easy to achieve PPCI operation with gasoline rather than diesel fuel. As local equivalence ratio decreases with gasoline, combustion products or emissions change. Figure 1.9 shows qualitative emission trends in premixed mixture [15]. As mixture goes lean, not only particulate matter but also NOx emission drastically decreases, because of low combustion temperature. However, there are increases of unburned hydrocarbons (HC) and carbon monoxide (CO).

Gasoline-like fuels leading to lean mixture before start of combustion, as indicated by 'High Octane' in figure, have advantages of soot and NOx emissions, but disadvantages of HC and CO emissions.

There were several researches related to PPCI in single-cylinder diesel engine. In the fuel aspect, Risberg et al. [18] studied effects of octane number of diesel fuel in premixed combustion and demonstrated that auto-ignition quality has large effect on ignition delay and resultant emission characteristics. Following the results that the fuel with higher resistance to auto-ignition has good emission characteristics in engine experiments, Kalghatgi et al. explored the potential of conventional gasoline for PPCI. In [13, 19], they demonstrated that it is possible to achieve high IMEP (~15 bar) with gasoline while maintaining low level of NOx and soot. There were also the studies on the effects of reactivity of the fuels with typical boiling range of gasoline on emission characteristics. Low octane (70~85 RON) and high octane (> 90 RON) gasoline were tested and compared with diesel fuel [14], and experimental results for various gasoline fuels are shown in [20]. From these studies, it was verified that gasoline fuels have better emission characteristics, as compared to diesel fuel. It was also confirmed by many researchers that it is more easy to achieve PPCI operation with high efficiency and low soot and NOx emissions by gasoline [21-26]. It is called gasoline PPCI or Gasoline Direct-injection Compression Ignition (GDCI) strategy. Figure 1.10 and 1.11 shows experimental results from Shell Global Solutions U.K. and Lund University [20]. They used 0.537 L single cylinder engine for various fuels including diesel and gasoline. These figures clearly show how emissions change as reactivity of

fuel changes. As explained in previous paragraph, gasoline-like fuels indicated with RON numbers have higher HC and CO emissions than diesel. However, they show absolutely low NOx emissions (< 0.3 g/kWh) with retaining low soot emissions (< 1 FSN: Filter smoke number) even at high EGR conditions. There were also researches with practical fuel like naphtha. Naphtha is less refined fuel in petroleum refinery process and has low octane number about 70. They said that naphtha has potential for reducing after-treatment cost and Well-to-Wheel CO2 emissions [27, 28]. Other research institutes like Univ. of Wisconsin or Cambridge achieved high emission performance using gasoline in CI engines. Each institute conducted research by using heavy-duty single cylinder and light-duty multi-cylinder engine, respectively [29-33].

Because gasoline has long ignition delay or low reactivity innately, mixing with air before SOC is enough to make lean combustion. Therefore, extreme high injection pressure is not necessary in PPCI. Expensive high pressure injection system can be replaced by low pressure and low cost system. Not only injection system but also after-treatment system can be simple. Because of low NOx and soot level, after-treatments can be focused on oxidation of HC and CO instead of simultaneous control of NOx and soot [7].

In those studies, it was noted that superiority of low octane fuel (or gasoline) to high octane gasoline in PPCI [22, 34, 35]. Especially at those conditions, such as low-load, high RPM and high EGR, where high resistance to auto-ignition of high octane gasoline may lead to unstable or incomplete combustion [14]. In addition, in economic aspects, low octane fuel like naphtha or straight-run gasoline classified to less refined fuel in refinery process has low

production cost. Therefore, low octane fuels have potential of replacing some portion of diesel usage in heavy-duty sector with low production cost.

Though PPCI operation with low octane fuel has a high potential of emission characteristics as mentioned in previous researches, there is not enough information about in-cylinder phenomenon. In researches mentioned above, experiments were conducted in conventional diesel engine; however, for applications of new fuels in direct-injection type engines, fuel spray characteristics are most important factors. For PPCI engines with low octane fuel, physical and chemical characteristics of fuel spray is not established yet. Though there were some researches to explore the combustion phenomenon in PPCI using constant volume vessel [36, 37], their experiments based on conventional gasoline fuel. It is clear that spray or combustion characteristics of low octane fuel in PPCI condition is not enough to be applied in engine development or optimization.

In contrast to spray combustion of gasoline-like fuel, diesel combustion with high injection pressure has been explored vigorously from old times. With the massive material from steady researches, diesel engine systems have been developed. Mechanically controlled systems begun to be controlled electrically, solenoid injector was replaced by piezo-type injector and fuel was injected more high pressure through the micro-size nozzle. Even now, researches to improve diesel engines are being conducted many companies and laboratories. Especially, study of spray characteristic with constant volume vessel has been conducted by many research labs including Sandia National Laboratory [38, 39, 40]. Recently, most of institutes are participating Engine Combustion Network

(ECN) program [41, 42, 43]. They are focusing on fully understanding of spray combustion, and applying it to real engine operation and computational model validation [44].

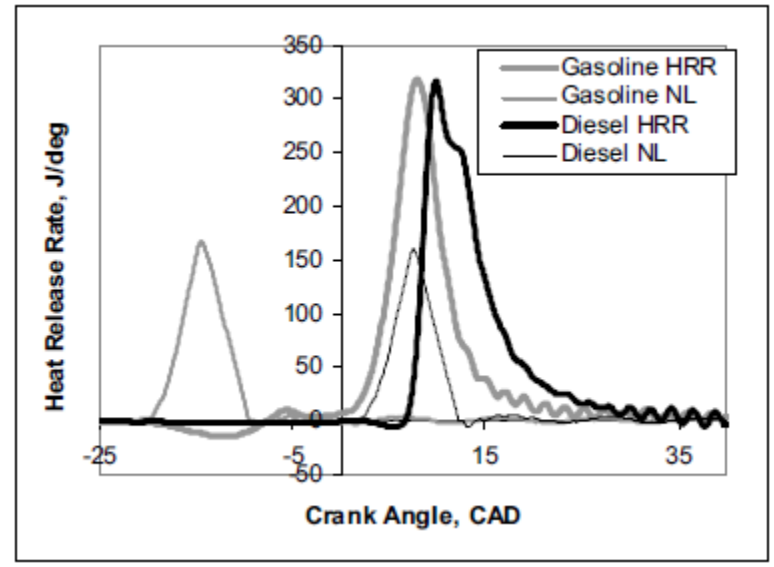

Figure 1.8 Example of needle profiles (injection event) and heat release rate for gasoline and diesel in CI engine [13]

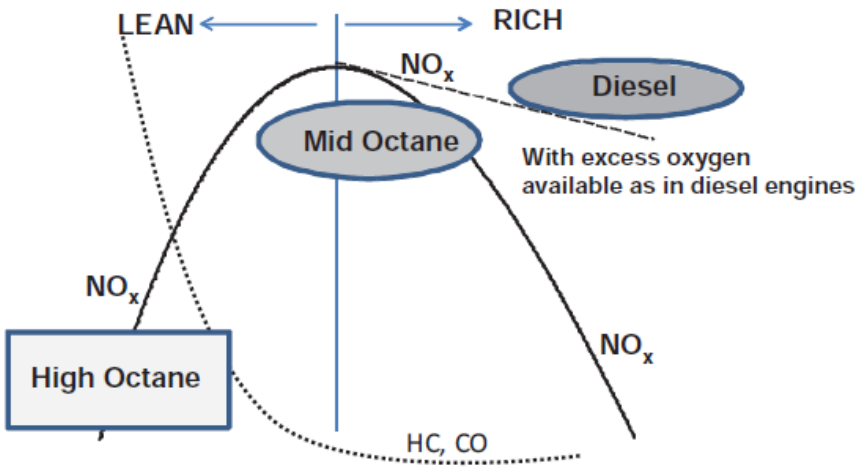

Figure 1.9 Qualitative sketch of variation of emission (NOx, HC and CO) with mixture state [15]

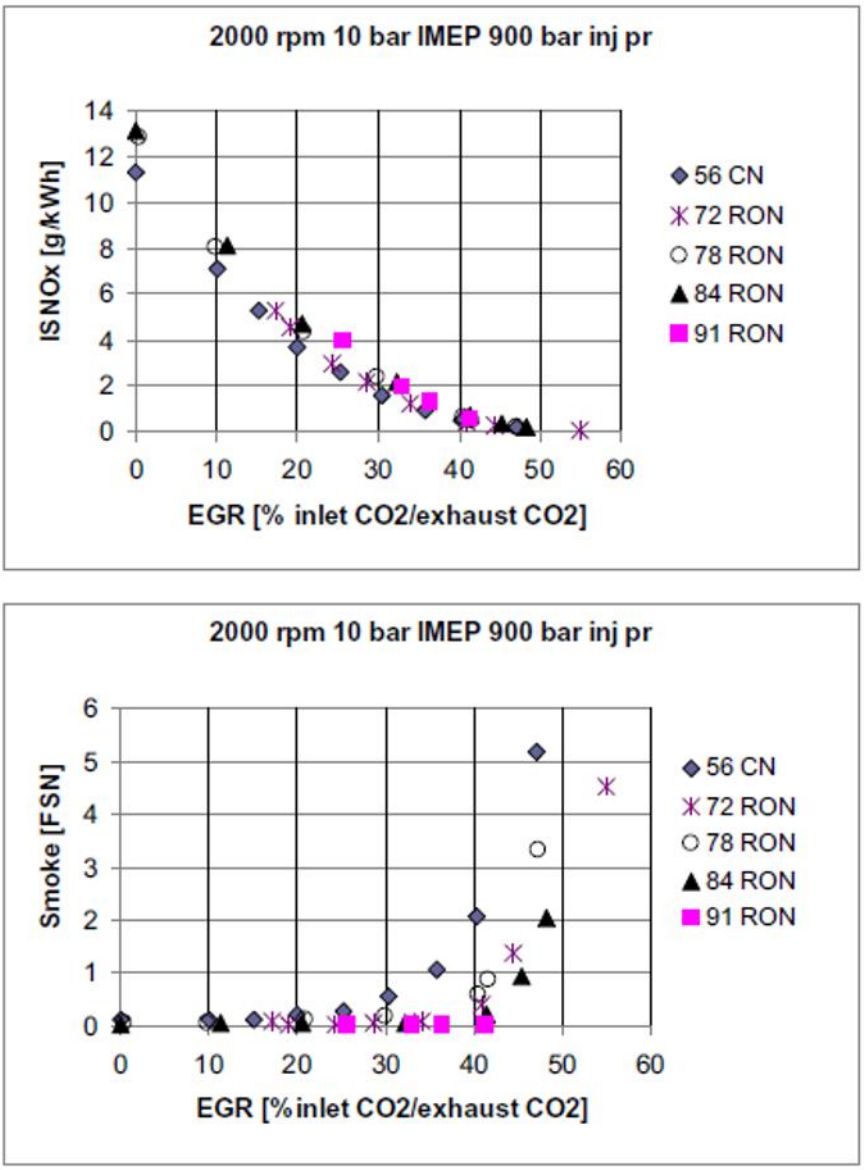

Figure 1.10 NOx and soot emission with various fuels. Experiments were conducted by Lund University and Shell Global Solutions U.K. at 2009 with 0.537 L single cylinder engine [20]

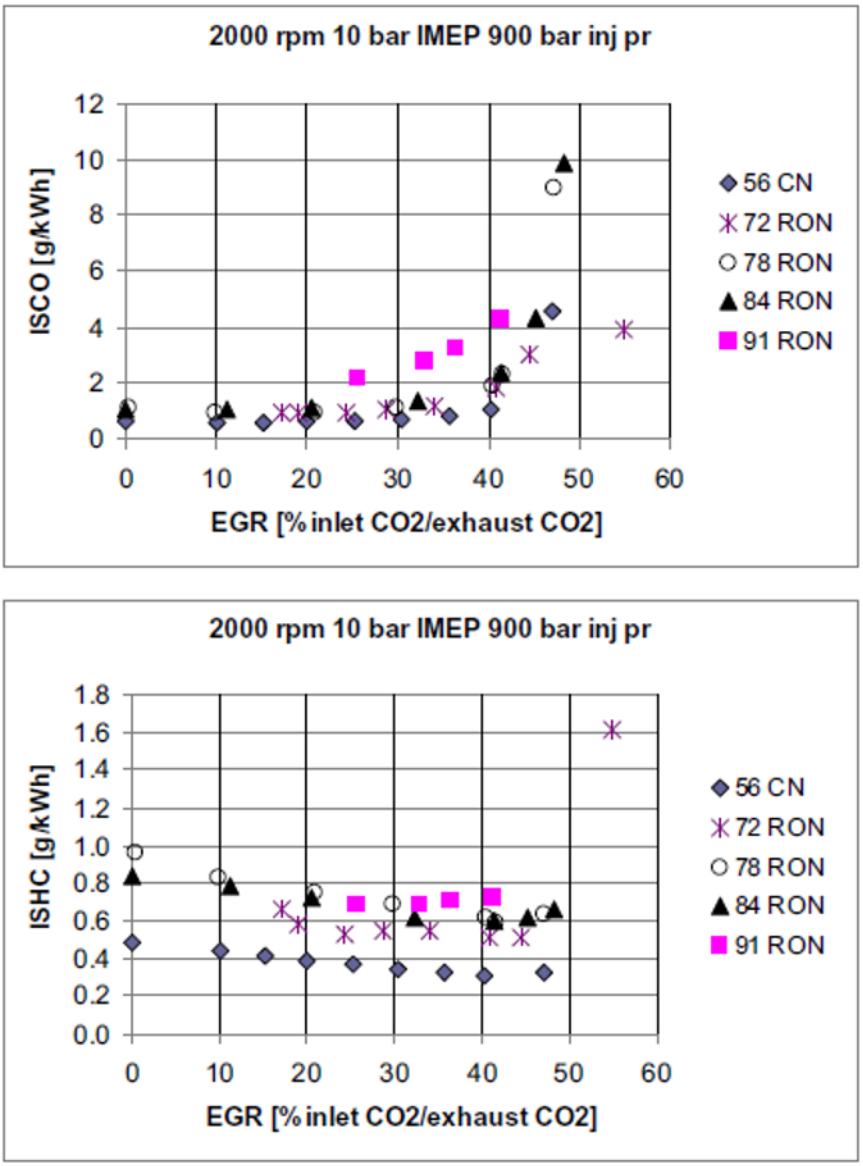

Figure 1.11 CO and HC emission with various fuels. Experiments were conducted by Lund University and Shell Global Solutions U.K. at 2009 with 0.537 L single cylinder engine [20]

1.3 Objective and motivation

In this study, as a pilot research of PPCI with low octane fuel, its combustion characteristics including spray behavior, ignition delay and soot production etc. were explored. In diesel engines, spray characteristics are most important factor to determine efficiency, geometry and emissions. In PPCI with low octane fuel, combustion properties are still coupled with spray properties and have large effects on performance. To understand the basic properties of spray combustion with low octane fuel in PPCI conditions, fundamental analysis by visualization experiments and computational study were accomplished. To reflect the reactivity of low octane fuel, primary reference fuel consisting of normal heptane and isooctane was used. Another purpose of using primary reference fuel is maintaining of fuel properties by using well known reference fuel. Properties of commercial fuel would be changed depending on when or when it was produced. With constant volume chamber and high speed imaging, fuel spray behaviors in partially premixed conditions were observed in fixed pressure and temperature condition. Captured natural luminosity and shadowgraph images during spray combustion gave information that how flame will be developed. It is expected that fundamental analysis of low octane fuel in this study gives evidence of applying gasoline-like fuel to compression ignition type engines like as if ECN has been contributed to diesel engine [45].

Chapter 2. Experimental set-up and methodology

2.1 Introduction

Firstly, to visualize the spray behavior, combustion chamber should have optically transparent windows, making optical signal from fuel spray can be detected by detector including camera. Also Chamber has to be made by durable material which can endure high pressure and temperature caused by exothermic reaction.

Secondly, to inject the liquid fuel into chamber, fuel pumping system and injection system are needed like rotary pump to pressurize fuel up to several hundred bar, common-rail system and injector control system.

And finally, optical device like light sources and detectors are necessary. Light source includes Xenon lamp for shadowgraph and high power LED for scattering and detectors includes color and monochromatic high speed camera.

In this chapter, experimental methodology including detailed introduction of main parts of rig system explained above, experimental procedure, calibration process of thermal condition, and experimental set up is presented.

2.2 Experimental apparatus

2.2.1 Constant volume chamber

To imitate the spray combustion in DI type engines, cubic-shaped chamber was built. Unlike general engines in vehicles, which involve piston motion, this new chamber has no piston and experiment is conducted under constant volume condition, so it is called constant volume chamber. Under constant volume experiments, it is possible to find the fundamental properties of spray combustion without interference of ambient flow motion like swirl or tumble flow in real engines.

Table 1. shows physical specification of this chamber. Chamber body is made by stainless steel (SUS316) and test zone volume is 2200 cm^3. Outer wall is enough thick to endure high pressure and temperature condition (~150 bar, 2000 K). It has basically cubic shape and various device can be mounted in six surface. In this study, fuel injection, magnetic fan, three quartz windows and spark plugs were installed in each surfaces. Front view of chamber and cross section of 3-D drawing are shown in Figure 2.1. Circular windows having 120mm diameter give 100mm view size for optical diagnostics. Fuel injector mounted on upper surface leans for 31.5 degrees with vertical direction to induce 45 degrees of diagonal spray direction. Two spark plugs are installed in chamber body, one is on bottom center and other is on bottom corner. Absolute pressure transducer on tube line gives filling pressure of each gas and Kistler pressure transducer (Kistler 6061B) on the chamber body give pressure information during combustion.

Table 1. Specification of constant volume chamber

Material	SUS316
Volume	2200 cc
Max. temperature	2000 K
Max. pressure	150 bar
Windows	Quartz (Φ120 x 80 mm)
Installed device	Autolite high-thread spark plug x 2 Kistler 6061B pressure sensor Magnetic fan

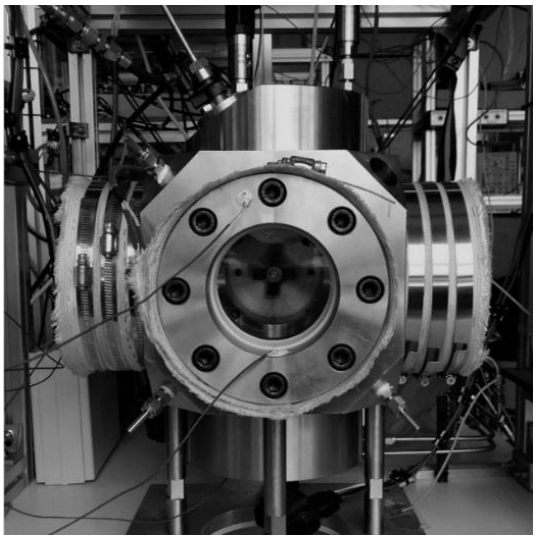

(a) Constant volume chamber (front view)

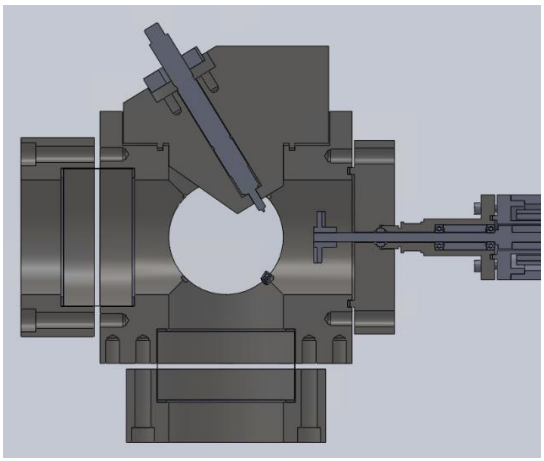

(b) 3-D drawing of constant volume chamber (cross-sectional view)

Figure 2.1 Constant volume chamber

2.2.2 Fuel pumping and injection system

To inject the fuel with high pressure, devices which pressurize and deliver fuel to common-rail and injector is needed. To apply primary reference fuel, less lubricative than diesel fuel, on common-rail & injector system, Haskel pump was used instead of commercial diesel pump system. Figure 2.2 shows detailed schematic of Haskel pumping system. Fuel in fuel tank is delivered to low pressure feed pump and pressurized to 3 bar, then pressurized again in Haskel pump up to 2000 bar for maximum pressure. In this study, injection pressures varied from 200 bar to 700 bar that is much lower than that of contemporary diesel injection to investigate the potential of using the low injection pressure with PRF70 fuel in PCI operation. Haskel pump is operated by air supply, and air supply is automatically controlled by Zenobalti Co. PCV driver. PCV driver collects the pressure information from common-rail and controls the air flow rate by solenoid valve, then fuel in common-rail becomes target injection pressure. To control the fuel injector, Zenobalti Co. injector driver was used, which can adjust injection duration, operating voltage and current shape for piezo type injector. More detailed information about pumping system is listed in Table 2.

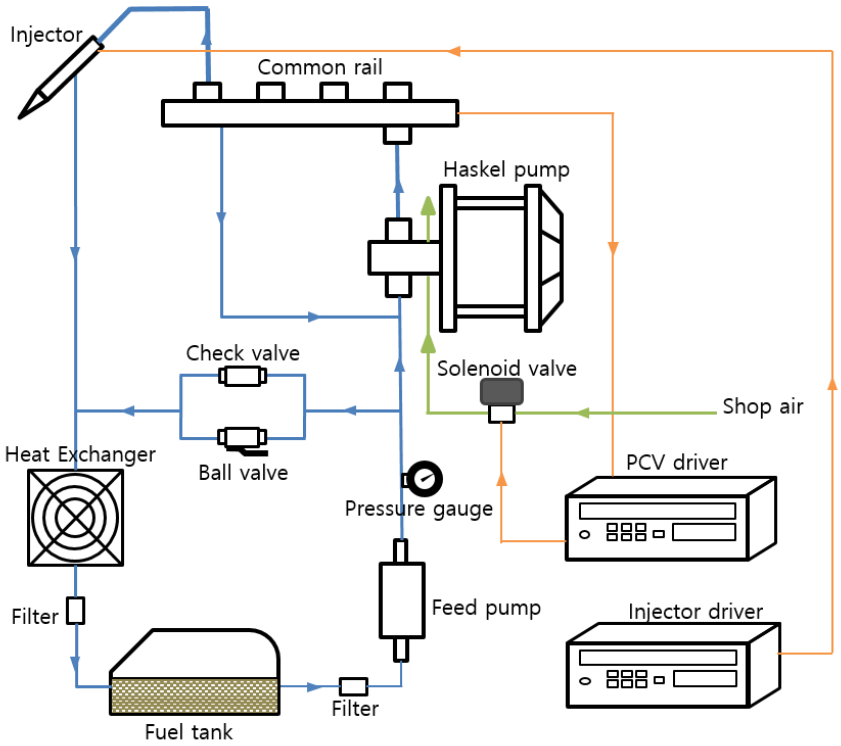

Figure 2.2 Schematic of fuel pumping system

Table 2. Specification of fuel pumping system

High pressure pump	Haskel DSHF-300	
Common-rail	Bosch 2nd generation model	
Injector	Bosch 8 holes piezo injector	
PCV driver	Zenobalti ZB-1200	
Injector driver	Zenobalti ZB-6200	
Pulse generator	Stanford Research Systems DG-535	
Actual injection duration	2.3 ms & 14 mg/shot	(TTL 1 ms)
& injection rate	5.2 ms & 18 mg/shot	(3ms)
(TTL pulse duration)	7.2 ms & 22 mg/shot	(5ms)

2.2.3 Optical diagnostics devices

In this study, three optical diagnostics were used 1) natural luminosity detection including narrow band-pass filtering 2) shadowgraph 3) Mie scattering. In addition to broadband chemiluminescence signals, 633 nm filtered signal also collected during the natural luminosity detection. Both color and monochromatic high speed camera were used to capture the chemiluminescence signal. Broadband chemiluminescence gives clue which helps to find start of combustion timing and distinguish between diffusive flame and premixed flame. 633 nm filtering signal has only flame with orange color in visible ray range, emitted from soot particle in diffusive flame generally. Combining these two kinds of chemiluminescence signal, region and position of flame or soot in spray can be determined.

For the shadowgraph analysis of spray, Z-set up shadowgraph was used with two parabolic mirror shown in Figure 2.3. Parabolic mirror is 6 inches aluminized spherical mirror having focal length of 60 inches. Shadowgraph method reflects density gradient in test zone, so it is possible to detect boundary of gas phase of spray. However, soot production cannot be acquired from this technique.

In flow visualization tests, Mie scattering is certain method to visualize particle larger than light wavelength. Mie scattering is reflection of photon from particle in test zone and its intensity increases as particle size increases. So in spray visualization, Mie scattering can be applied to detection of fuel with liquid phase before it vaporized to gas phase. Mie scattering set-up is shown in

Figure 2.4. Instead of shadowgraph Z-set up, light source and high speed camera is aligned in Mie scattering tests.

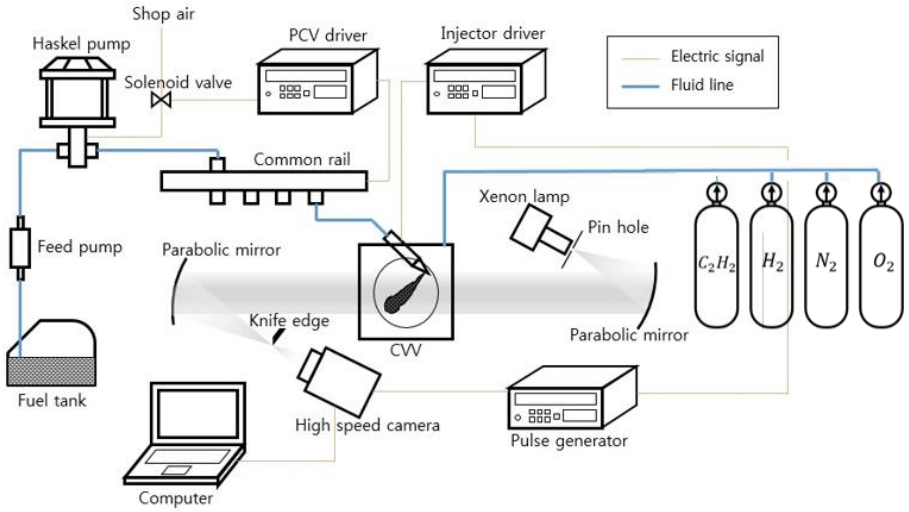

Figure 2.3 Z-type shadowgraph set-up

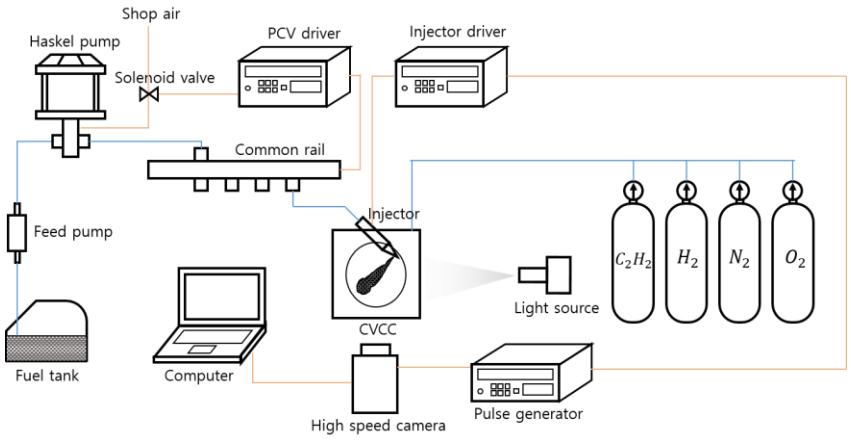

Figure 2.4 Schematic of set-up for Mie scattering imaging

2.3 Experimental procedure

2.3.1 Pre-burn process

To imitate the combustion phenomenon in real IC engines, it is important to make high pressure and temperature condition as in compression stroke in real IC engines. To make high pressure and temperature conditions in this study, pre-burn process method was applied by using hydrogen and acetylene as a fuel. During the partial pressure filling stage, acetylene, hydrogen, oxygen and nitrogen are sequentially supplied in to the chamber. After 15 minutes of mixing by magnetic fan, two spark plugs in bottom side initiate the ignition and the flame propagations inside the chamber, After the end on flame propagation, chamber is filled with high temperature and pressure product gas (CO_2, H_2O, O_2 and N_2). Then, the product gas starts cooling down during heat transfer to wall, typically by ~200K/sec drop on average, which makes nearly constant temperature pressure condition for less than 10 ms of spray combustion experiments. When the temperature and pressure reach the target state after a few seconds, injection and recording systems are triggered to perform the spray combustion and image processes. Figure 2.5 shows exemplary pressure and temperature profiles of the pre-burn process. Here, fine wire (72 μm) of k-type thermocouple was used for temperature measurement and Kistler pressure transducer for pressure measurement. Temperature was measured in center of chamber, which 45 mm away from the injection tip.

By adjusting the amount or partial pressure of four pre-burn gases, it is possible to make various compositions of product gas and ambient conditions.

However, in this study, gas composition was adjusted to protect the fine thermocouple from damage of high flame temperature and quartz windows from high pressure rise rate. Gas composition was calculated by reaction mechanism to make adiabatic pressure and temperature lower than acceptable or safety value. The composition of reactant gas and product gas are listed in Table 3. Explanation for how to determine initial pressure of reactant gases is included in next section 3.2. In experiments using constant volume chamber, besides ambient pressure and temperature, oxygen concentration in the product gas is the most important factor which can effect on fuel combustion. Oxygen concentration in constant volume chamber test corresponds to amount of exhaust gas recirculation (EGR) in real engine. Low oxygen concentration means high EGR operation, thus more inert gases exists during combustion process. Two oxygen concentrations were testes, i.e. 15% and 20%, in this study. Here, 20% corresponds nearly to the standard atmospheric state, and thus no EGR condition in an engine operation and 15% condition reflects on ~30% EGR condition, respectively.

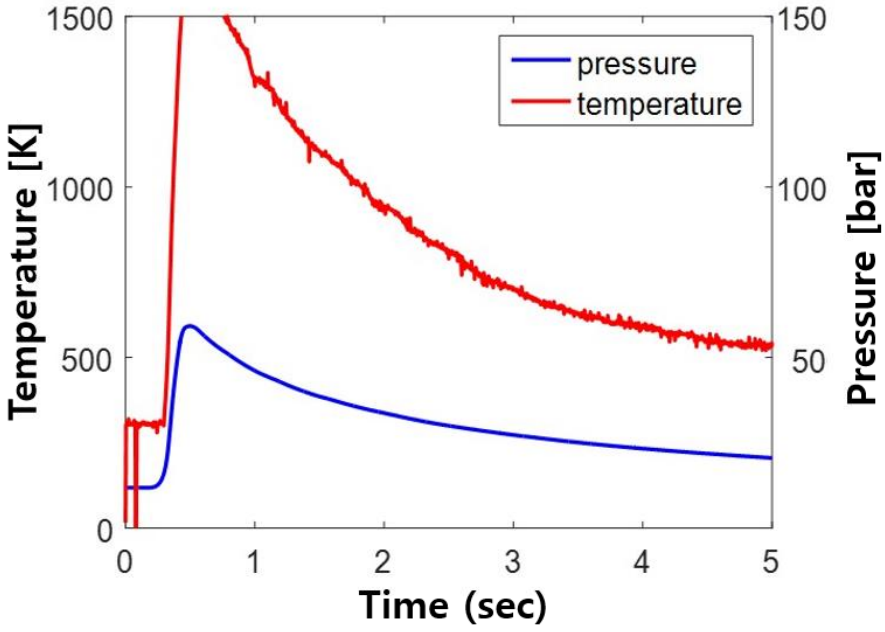

Figure 2.5 Pressure and temperature change during pre-burn process

Table 3. Gas composition of reactant gas for pre-burn and resultant product gas

	O_2 20%	**O_2 15%**
reactant		
Vol. (%) C_2H_2	3.046	2.93
Vol. (%) H_2	0.514	1
Vol. (%) O_2	27.52	22.54
Vol. (%) N_2	68.92	73.53
product		
Vol. (%) CO_2	6.2	6
Vol. (%) H_2O	3.6	4
Vol. (%) O_2	20	15
Vol. (%) N_2	70.2	75

2.3.2 Determination of target condition

Throughout the experiments in this study, pressure and temperature were fixed at 31.15 bar and 840 K. First, to determine these target values for imitation of GDCI operation with early injection timing, reference case was needed and GDCI engine in Univ. of Wisconsin was chosen as reference [35, 47]. Table 4 shows specification of reference engine. By applying these engine values in Table 4 to simulation with Matlab Cantera toolbox, the pressure and temperature profile during compression stroke were predicted. Compression was assumed as adiabatic process of air with 20% oxygen condition. Figure 2.6 shows simulation results of compression stroke. Considering that injection timing in reference case varies from 20 CAD bTDC to 10 CAD bTDC, initial pressure of reactant gas was adjusted to make cooling down profile pass this range. For 20% oxygen condition and 15% oxygen condition, initial pressure of 11.8 bar and 12 bar were selected, respectively. To assure the repeatability of pre-burn process several pre-burn processes were conducted and pressures and temperatures were averaged. Figure 2.7 shows profiles of ten pre-burn processes. From the calculation, averaged pressure and temperature were obtained with one standard deviation of 15 K. By putting the P&T profile of pre-burn process and simulation of compression stroke on same P-T plane as in Figure 2.8, it was possible to find interaction points at 31.15 bar & 840 K which correspond to values at 19 CAD bTDC of engine simulation.

Table 4. Specification of reference engine (Univ. of Wisconsin [46, 47])

Parameter	Value
Compression ratio	17.8
Bore	82 mm
Stroke	90.4mm
Connecting rod	145.4 mm

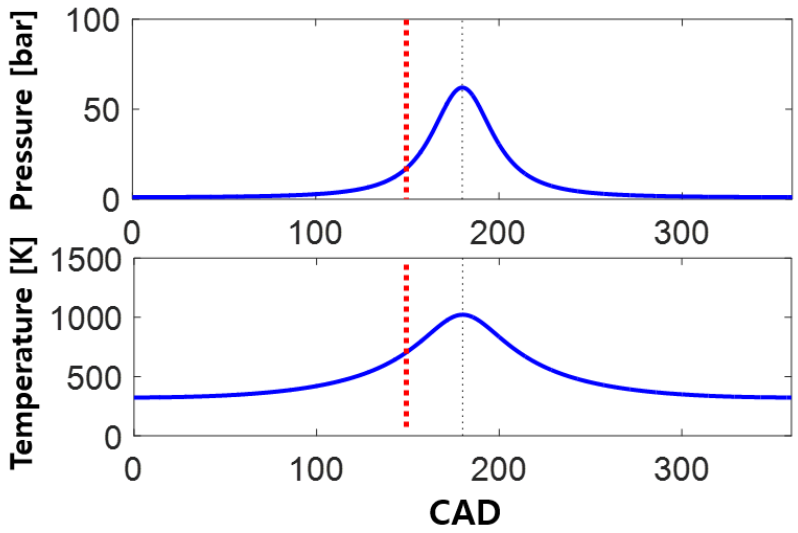

Figure 2.6 Simulation result of compression stroke reflecting specification of reference engine

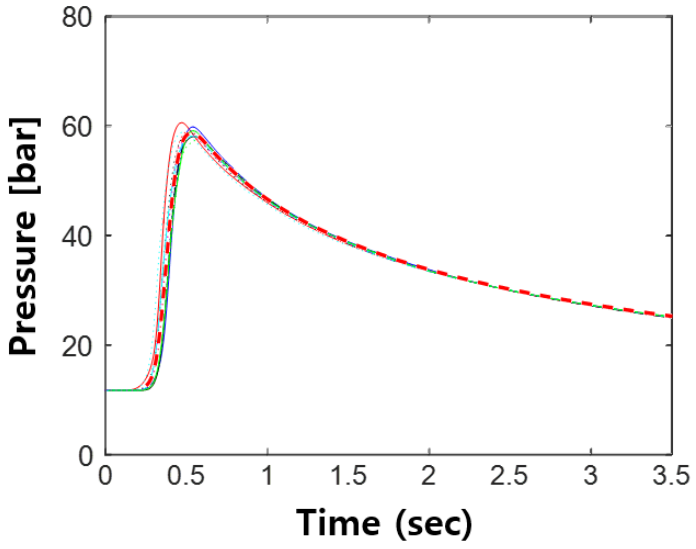

(a) Pressure

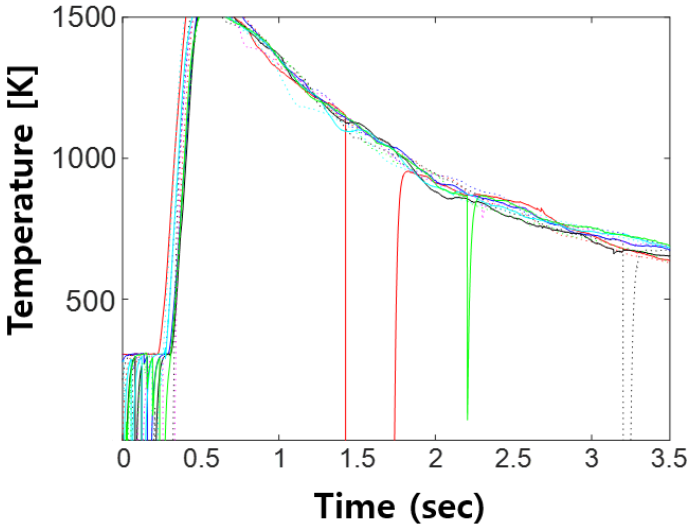

(b) Temperature

Figure 2.7 Pressure and temperature profiles of ten pre-burn processes

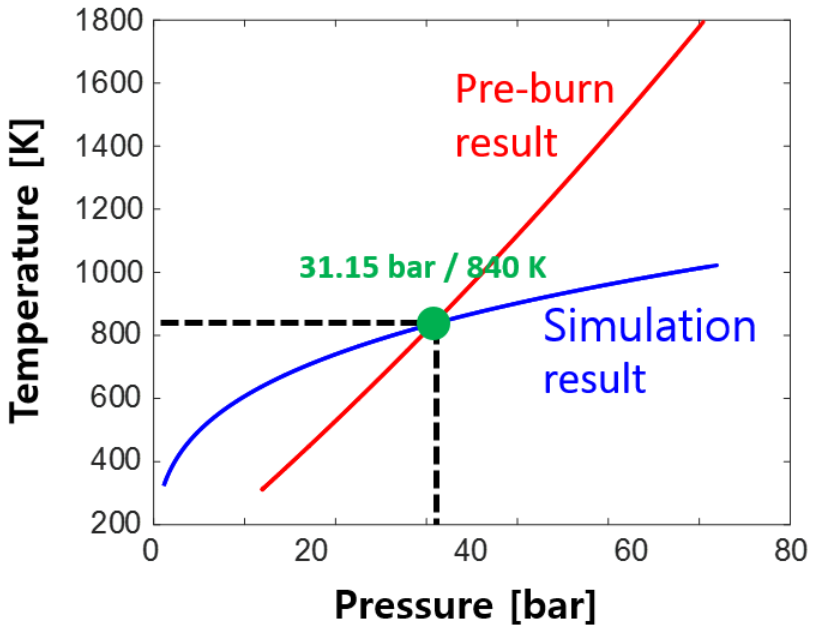

Figure 2.8 Interaction point between pre-burn process and simulation of reference engine

2.3.3 Device triggering with pressure signal

During the experiments including fuel injection, thermocouple cannot be used not to disturb fuel penetration. Thus, pressure signal from Kistler transducer is the only thing which gives information of thermodynamic states in the chamber. Because there are assurance of repeatability and averaged P&T, it is possible to predict thermodynamic state by only real-time pressure information. After mixing of four reactant gases followed by spark ignition, left procedures operate automatically. Pressure in the chamber is measured by Kistler pressure sensor during all processes. When pressure reaches target pressure of 31.15 bar during cooling down, data acquisition board linked with Labview make and send trigger signal to function generator. After function generator get trigger signal, it makes 5V digital trigger signal to injector driver and high speed camera. Then, injection and image recording start simultaneously. Figure 2.9 shows direction of electronic signal between experiment hardware.

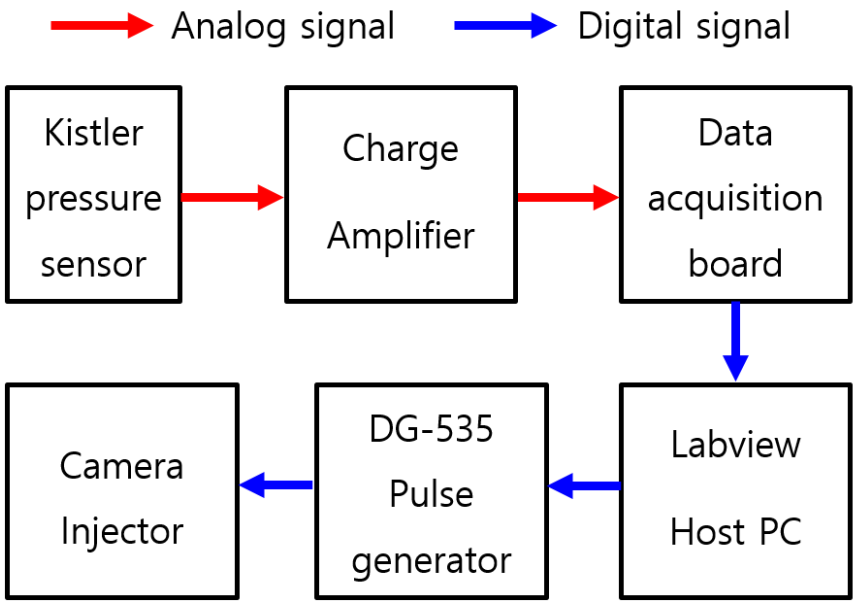

Figure 2.9 Stream of signal to control hardware and software

Chapter 3. Experimental results 1 – Operating regime of PRF70 with various injection conditions

3.1 Effects of injection pressure and duration on combustion mode change

In the first experiments, effects of injection pressure and duration on the combustion of PPCI was investigated the in 15% oxygen concentration condition. Figure 3.1(a) shows the instant of maximum natural luminosity at six representative conditions. Above 800 bar injection, ignition never occurs in a given ambient condition, because long penetration by high injection leads excessive air to enter the spray region so that mixture becomes too lean to self-ignite or fuel to interact with chamber wall. In addition to high injection pressure effect, long ignition delay (~ 5 ms) by low oxygen concentration also leads to misfire. For this reason, experiments with 15% oxygen concentration were conducted for injection pressure below 700 bar. When injection pressure is lower than 300 bar, flame begins to be intensive as injection duration is longer. Especially at 200 bar with 7.2 ms duration, ignition occurs with region of saturated luminosity signal which looks like conventional diesel flame though it locates at more downstream region. At given injection duration, as injection pressure goes higher, combustion intensity decreases, which is well shown in

injection duration of 7.2 ms cases. When the injection pressure is 700 bar with 7.2 ms duration, light flame produces in downstream of spray region. Figure 3.1(b) shows spatially integrated luminosity during the combustion stages as a function of time after start of injection (ASOI), for these six representative cases. By qualitatively comparing the results of Figs 3.1, it is speculated that the combustion process with intensity value above ~5 million becomes more non-premixed with saturated portion of soot luminosity, where the threshold value of 5 million is somewhat arbitrarily chosen from our image processing results.

In addition to six representative cases shown in Figs 3.1, total of 15 combinations of injection pressures and durations were tested, as shown in red dots in Figure 3.2. By calculating temporally-spatially integrated luminosity from each operation, the regime of the spray combustion mode of Figure 3.2 was made. Spatially integrated luminosity profiles in Fig. 3.1(b) were temporally integrated to obtain temporally-spatially integrated luminosity. The regime map can provide the guideline how the combustion mode will change as the injection pressure and duration vary. In the figure, from the lowest injection pressure tests, as injection pressure increases in given injection duration, combustion becomes more premixed. When the injection pressure is larger than 700 bar, combustion hardly appears which corresponds to white region in regime.

According to the results from injection duration variation, shorter ignition duration enables more premixed combustion in general. However, below the injection pressure of 300 bar, if the injection duration is longer than 5.2 ms, flame begins to show saturated region and might enter the non-premixed regime

with soot which is source of saturated signal. Due to the short penetration by low injection pressure, first ignition starts more close to injection tip. Thus, following injected fuel meets the reaction zone with not enough air and make soot.

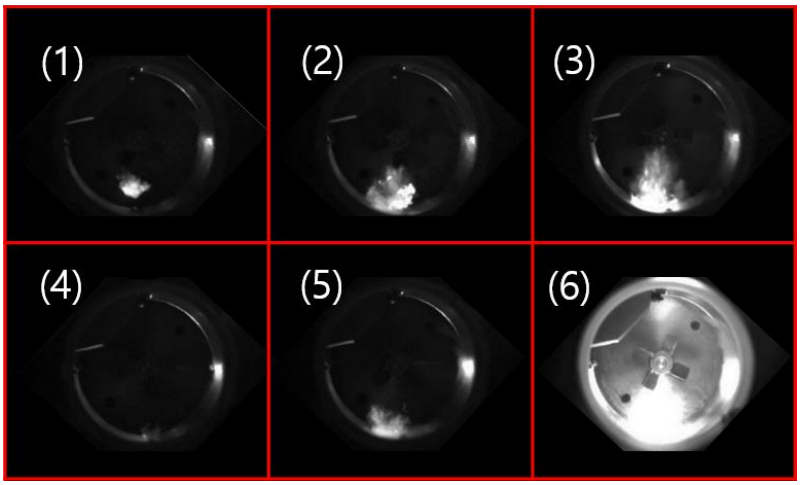

(a) (1) 300 bar / 2.3 ms (2) 300 bar / 5.2 ms (3) 300 bar / 7.2 ms

(4) 700 bar / 7.2 ms (5) 500 bar / 7.2 ms (6) 200 bar / 7.2 ms

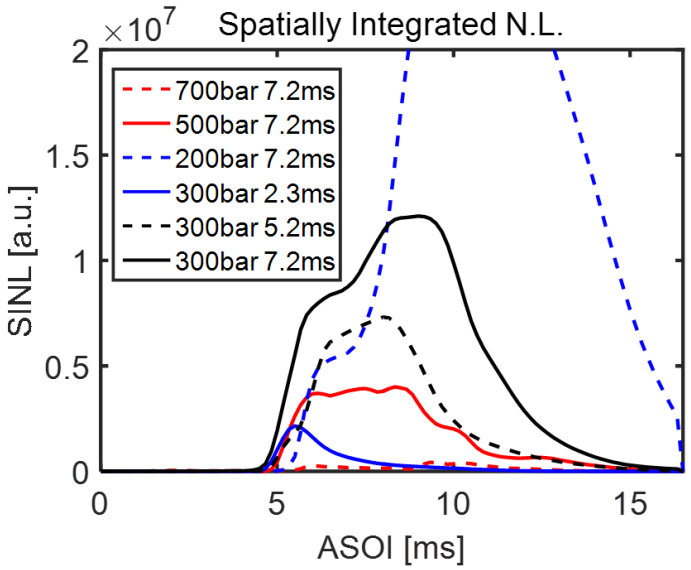

(b) Change of integrated natural luminosity

Figure 3.1 Flame intensity of six representative condition

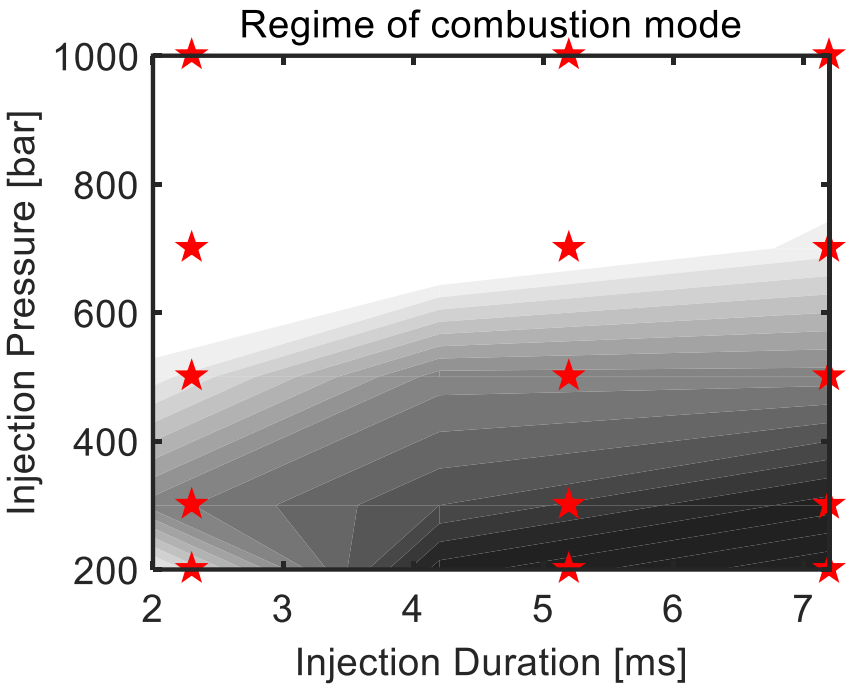

Figure 3.2 Operating regime of 15 % O_2 condition

(natural luminosity base)

3.2 Comparison of two different oxygen concentrations

To demonstrate the effect of EGR ratio or oxygen concentration on combustion of PPCI, oxygen concentration sweep test was conducted. EGR is essential strategy for NOx reduction in premixed concept engines, changing from 0% at low load to about 60% at high load, EGR ratio in engine operation stands for oxygen concentration in constant volume chamber operation. Three oxygen concentrations, 10, 15, 20%, which reflect 50, 30 and no EGR condition in real engine, respectively, were selected. However, for 10 % oxygen conditions, there was no ignition observed in the reference condition (31.15 bar and 840 K), and thus this lowest oxygen concentration case (or highest EGR case) is omitted in the following discussion. Firstly, to simply verify the effects of oxygen concentration, 500 bar injection cases in each oxygen condition were compared (Figure 3.3). Combustion with 500 bar injection pressure in 15% oxygen condition show light flame without saturated signal as shown in first raw of figure and it can be supposed that only premixed flame occurs in this conditions. However, in 20% oxygen conditions, flame shows overall white saturated region during whole combustion period, so it is impossible to distinguish whether it is premixed flame or non-premixed flame with soot. This excessive intensity of 20% oxygen concentration is caused by high temperature combustion. In general, high oxygen level leads high adiabatic temperature. To clearly show the effect of oxygen concentration on combustion mode, same experiments were conducted with 633 nm filtering set-up. 633 nm filtered signal shows existence of soot including 633 nm wavelength more clearly.

From the same experiments method, combustion images in Fig. 3.3 were reproduced. Figure 3.4 shows reproduced combustion image of two oxygen concentration conditions with 633 nm filtering. Images in first raw show absence of signal for 15% oxygen concentration when narrow-band pass filtering is applied. This result proves supposition that combustion with 500 bar injection pressure and low oxygen concentration involves only premixed flame. As different with filtered signal of 15% oxygen condition where the flame intensity is nearly zero, combustion in 20% oxygen concentration still shows locally or bulk saturated region by soot. Combustion structure looks similar with conventional diesel combustion. Other obvious difference is ignition delay, depending on the oxygen concentration. As shown in Fig. 3.3(b) to compare combustion phase between 15% and 20 % oxygen condition, it is noted that, irrespective of the injection duration, the same oxygen concentration condition leads to similar ignition delay, while at 20% oxygen conditions, ignition occurs earlier than at 15% by ~ 2 ms. Considering that the spray development, i.e. vaporization, penetration, and mixing, is similar in both conditions with same injection pressure and the background thermodynamic state except the oxygen concentration, the shorter lift-off length of the flame in 20% oxygen cases imply that the first injection portion of the fuel does not have enough time to be mixed before the ignition, leading to non-premixed combustion with soot emission. This is the direct consequence of the higher oxygen-to-fuel ratio in a given amount of entrainment into the fuel spray, and thus the shorter ignition delay of the mixture.

Based on 633 m, filtered natural luminosity, regime of combustion mode

for each oxygen concentrations were produced. Figure 3.5 shows reproduced regime for 15% oxygen concentration from Fig. 3.2. As shown in figure, non-zero-signal zone is concerned to low injection pressure and long injection duration condition. It means that intensive combustion with soot occurs at only that conditions and other conditions show only premixed flame. Figure 3.6 show the effect of high oxygen concentration or shorter ignition delay on combustion regime. Total of 18 combinations of injection pressures and durations with 20% oxygen condition were tested and plotted on combustion mode domain as in 15% oxygen concentration. Because of extremely high intensity of pure natural luminosity, regime was obtained from 633 nm filtered as already explained. As shown in the Fig. 3.6, area of combustion with 633 nm signal or soot is much wider than that of Fig. 3.5. Because of shorter ignition delay, cases with injection pressure higher than 700 bar come into combustible condition and have weak signal. Also, for lower injection pressure with 5.2 ms duration cases, combustion involves soot and has high intensity level. In short, combustible area becomes wider to high injection pressure and short injection duration region as ignition delay decreases. Therefore, present results demonstrated the higher oxygen concentration, or low EGR condition, could result shorter lift-off length of the flame and thus the sooty flame, and thus injection pressure should be increased to achieve the more premixed combustion with low soot, On the other hand, it is expected that the injection pressure needs to be lowered to make mixture rich enough to self-ignite to compensate longer ignition delay, when the oxygen concentration is lowered by EGR.

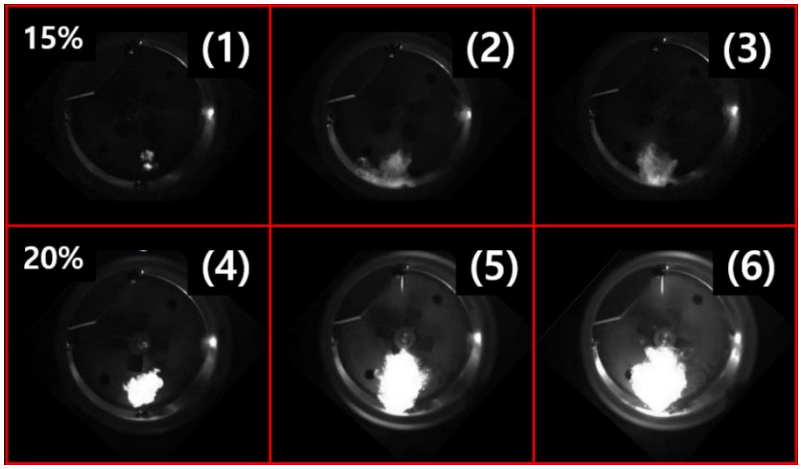

(a) (1) 500 bar / 2.3 ms (2) 500 bar / 5.2 ms (3) 500 bar / 7.2 ms

(4) 500 bar / 2.3 ms (5) 500 bar / 5.2 ms (6) 500 bar / 7.2 ms

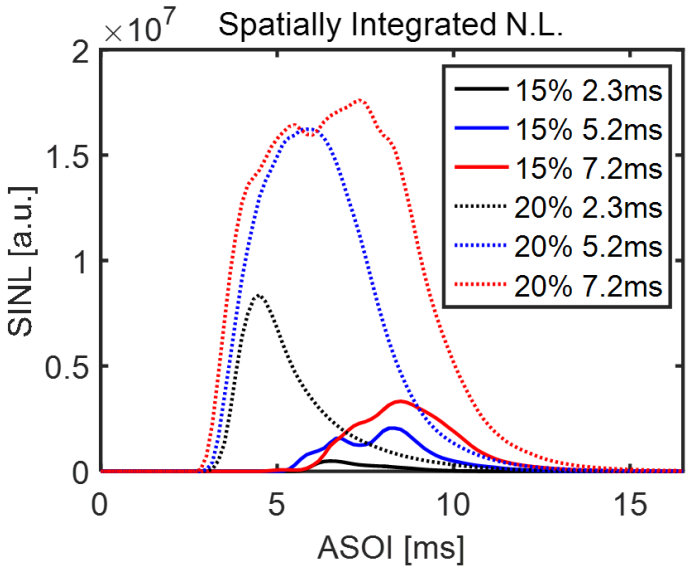

(b) Change of integrated natural luminosity

Figure 3.3 Comparison of 15 % and 20 % O_2 concentration

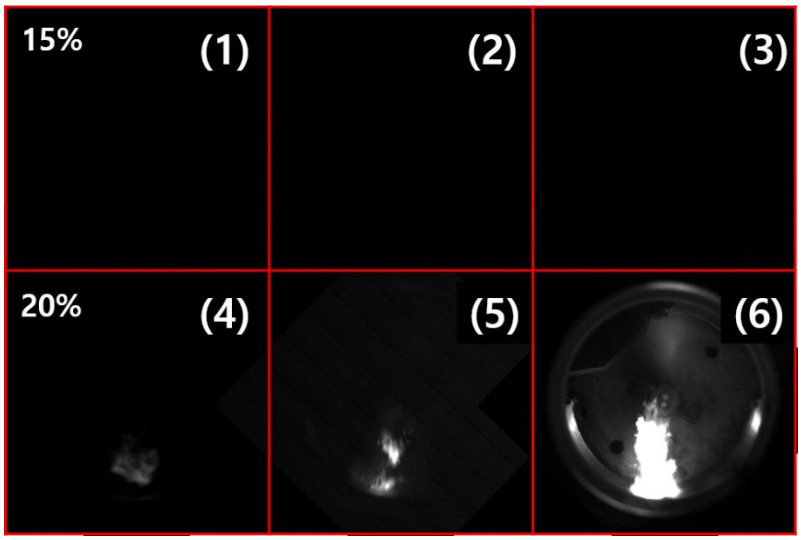

Figure 3.4 Comparison of 15 % and 20 % O_2 concentration with 633 nm filtering (same injection condition with Figure 3.4)

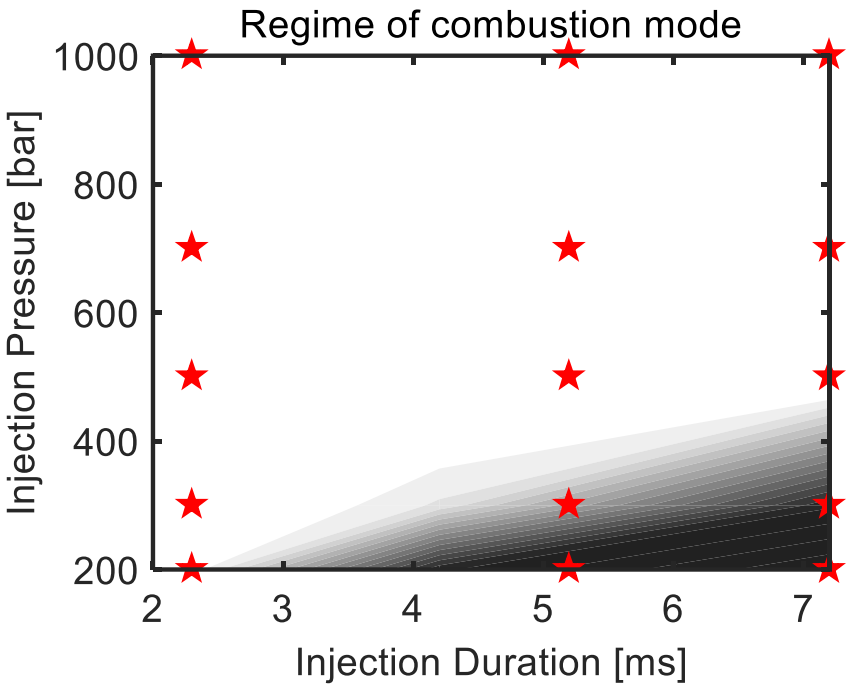

Figure 3.5 Operating regime of 15 % O_2 condition

(633 nm filtered natural luminosity base)

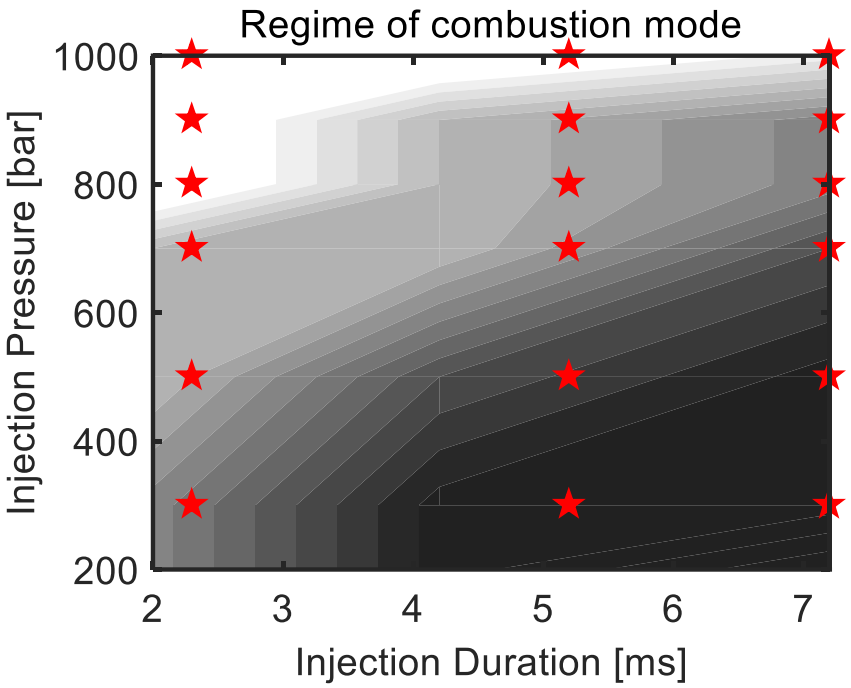

Figure 3.6 Operating regime of 20 % O_2 condition

(633 nm filtered natural luminosity base)

3.3 Summary

In this chapter including first step of this research, effects of some parameters like injection duration, injection pressure and oxygen concentration on premixed combustion were explored. At first, sweeping of injection duration and pressure shows that as injection condition goes to point where it is guessed more soot is produced, combustion intensity becomes higher and finally shows saturated signal at lower pressure and longer injection duration. Secondly, by combining the results from the parametric research for injection duration and pressure, it is possible to achieve map of combustion mode according to its signal intensity. With 15% oxygen concentration, as injection pressure decreases, combustion becomes non-premixed. At injection pressure higher than 700 bar, combustion loses its ignition, because of over-mixing or wall interaction. Especially at low injection pressure about 200 ~ 300 bar and injection duration longer than 5.2 ms, flame has saturated region by soot, which means flame begin to enter the diffusive region. Thirdly, additional tests with 20% oxygen concentration were conducted to demonstrate the effect of oxygen concentration or EGR level on PCI combustion. From comparing between 15% and 20% oxygen conditions, it was verified that ignition delay is shorter for 20% oxygen and soot was more produced. Non-premixed region in combustion mode (darker region) becomes wider and ignition becomes possible even at 700 bar injection pressure. It means oxygen concentration which effects on ignition delay has significant role in PCI operation.

Chapter 4. Experimental results 2 – Understanding of flame development by natural luminosity visualization: Physical properties of flame and resultant soot production

4.1 Introduction

In this chapter, spray combustion in each particular condition is explored. Based on physical properties of spray structure, it will be shown that how combustion zone develops and effects on soot production. In conventional diesel combustion, because of high reactivity of diesel fuel, combustion occurs right after injection. Ignition delay of diesel in typical operating condition is less than 1 ms. However, PRF 70 or gasoline-like fuel has much longer ignition delay about 3 ms for 20% oxygen condition and 5 ms for 15 % oxygen condition as shown in previous chapter. Thus, it is expected that this much longer ignition delay can effect on combustion behavior and makes it different from conventional diesel flame. For a first step of understanding of combustion process, results of parametric study in chapter 3 are reproduced.

4.2 Two combustion types in combustion regime

Regime of combustion mode in Fig. 3.6 is divided into two distinct regions. In Figure 4.1 reproduced from Fig. 3.6, two combustion regions are designated as ‘premixed combustion zone’ and ‘partially premixed combustion zone’. These two zones are roughly determined whether it has saturated intensive soot region or does not. Partially premixed combustion zone includes typically conditions of long injection duration; in contrast, premixed combustion zone includes conditions of short injection duration. Figure 4.2 shows exemplary image of both regions. Combustion in 500 bar and 2.3 ms condition shows overall faint combustion signal which means there are little soot during combustion duration, but 7.2 ms case show saturated region in spray core along the penetration. For case with shorter injection duration, it has similar combustion behavior with low temperature combustion (LTC) as shown in Figure 4.3 [48] though a little soot is detected in Sandia cases. In both tests, injection completes before start of combustion and visible combustion zone is localized in downstream region near the wall. For partially premixed combustion with long injection duration, it looks like conventional diesel combustion, but it is revealed that it is little different from conventional diesel flame because of long ignition delay and start of combustion in much downstream location. More distinct difference between this partially premixed combustion with long injection duration and conventional diesel flame is shown in Figure 4.4. The first column of figure show results of additional test with diesel fuel conducted in higher pressure and temperature (41.5 bar and 900K).

For diesel fuel, ignition delay is about 1.3 ms and 3.4 ms for PRF 70. In diesel case, first natural luminosity is detected at 35 mm from injector tip and following flame moves to downstream direction with soot generation, which follows typical development of diesel spray combustion where ignition starts at near the injector tip after short ignition delay and moves to downstream with high momentum, and finally maintain quasi-steady structure with intensive soot in core region. In contrast, for PRF 70 case, combustion with visible natural luminosity starts at 63mm from tip and combustion zone expands to opposite direction as time goes. Finally, few milliseconds after start of combustion, saturated soot signal appears in upstream and makes bulk soot motion.

In start of this chapter, two combustion zones are designated in combustion regime; premixed combustion zone and partially premixed combustion zone. In addition, from the comparing of partially premixed combustion zone with conventional diesel flame, it is turned out that flame development process in partially premixed combustion zone is unusual or new, not included in conventional diesel combustion. Therefore, there are three distinct combustion mode or zone including initial two zones on present regime and conventional diesel combustion cannot be shown in regime.

There are several conceptual models to describe the behavior of diesel combustion, basing on result from optical diagnostics. For conventional diesel combustion in heavy duty engines, John E. Dec establish concept model for development of diesel spray combustion [45, 50]. Figure 4.5 shows schematic of this conceptual model. This model shows liquid and vapor phase of fuel spray, first stage ignition containing PAHs and finally appearance of soot and thin

oxidation zone. There is also conceptual model to explain phenomenon in premixed combustion zone (Figure 4.6) [51]. This low temperature combustion model by M. P. M. Musculus [48, 51, 52] gives information about premixed combustion with positive ignition dwell in diesel engine. By detecting formaldehyde and OH indicators of first stage ignition and high temperature ignition with planar laser-induced fluorescence, combustion stages of LTC were verified. However, 'partially premixed combustion zone' in present operation regime is not fully understood by past two models. Compared to LTC operation, it has longer injection duration, so it has possibility of high temperature reaction in more upstream region. In addition, because combustion starts more downstream region, development of flame or reaction zone is quite different to conventional diesel case. Thus, it is necessary to understand the combustion in this specific zone and establish typical combustion theory. In this chapter, individual shot in 'partially premixed combustion zone' will be analyzed by experimental method and features of flame structure will be suggested.

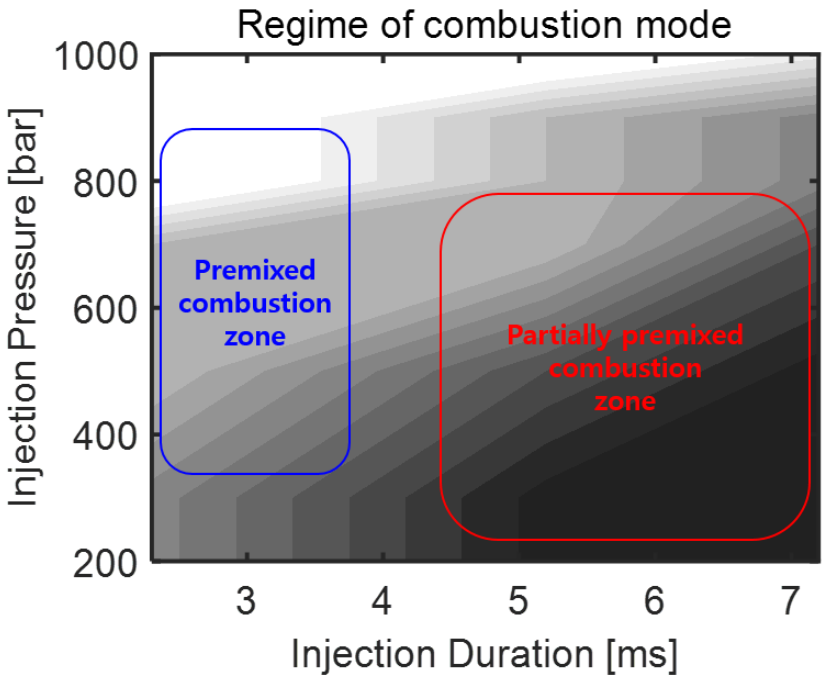

Figure 4.1 Two combustion type in operation regime

(reproduced from Fig. 3.7)

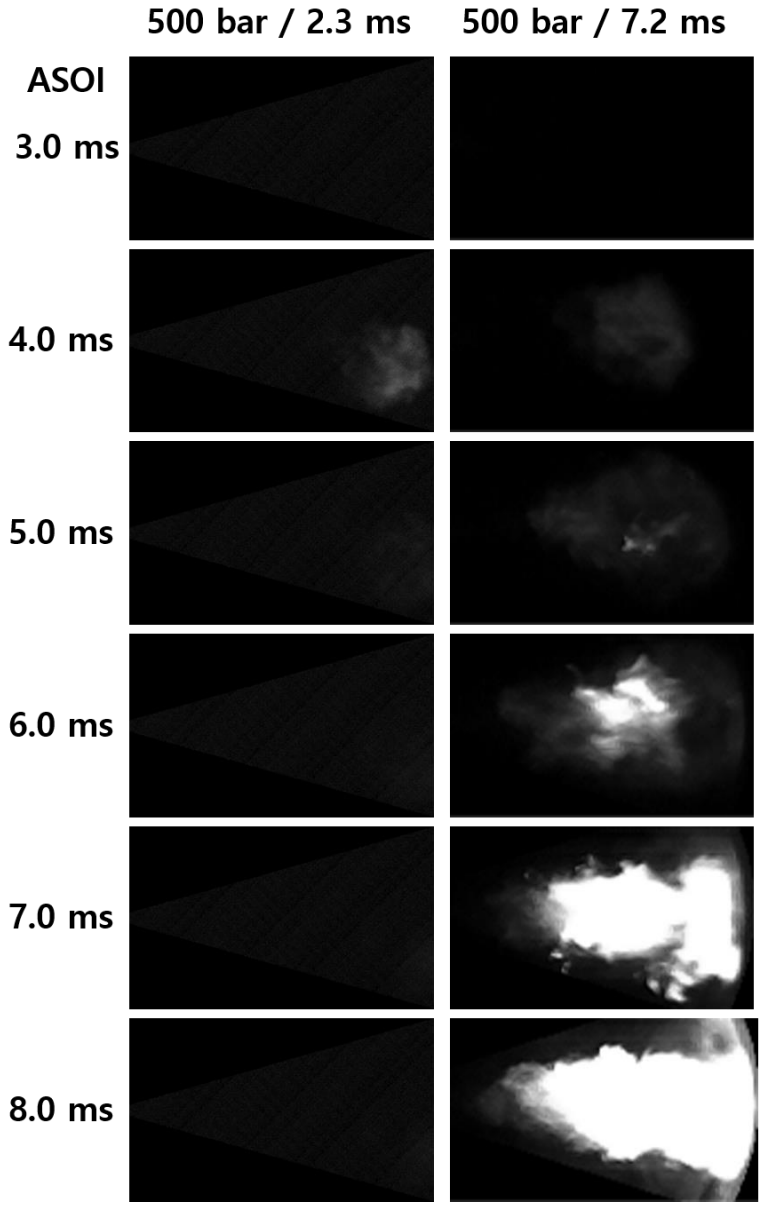

Figure 4.2 Natural luminosity of combustion in two zones

Left: premixed combustion zone

Right: partially premixed combustion zone

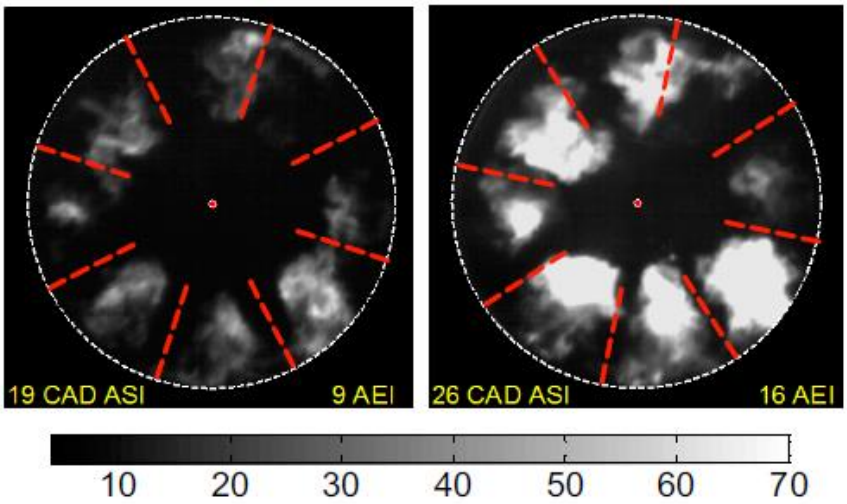

Figure 4.3 Combustion of diesel in LTC condition [48]

(apparent heat release rate occurs after end of injection)

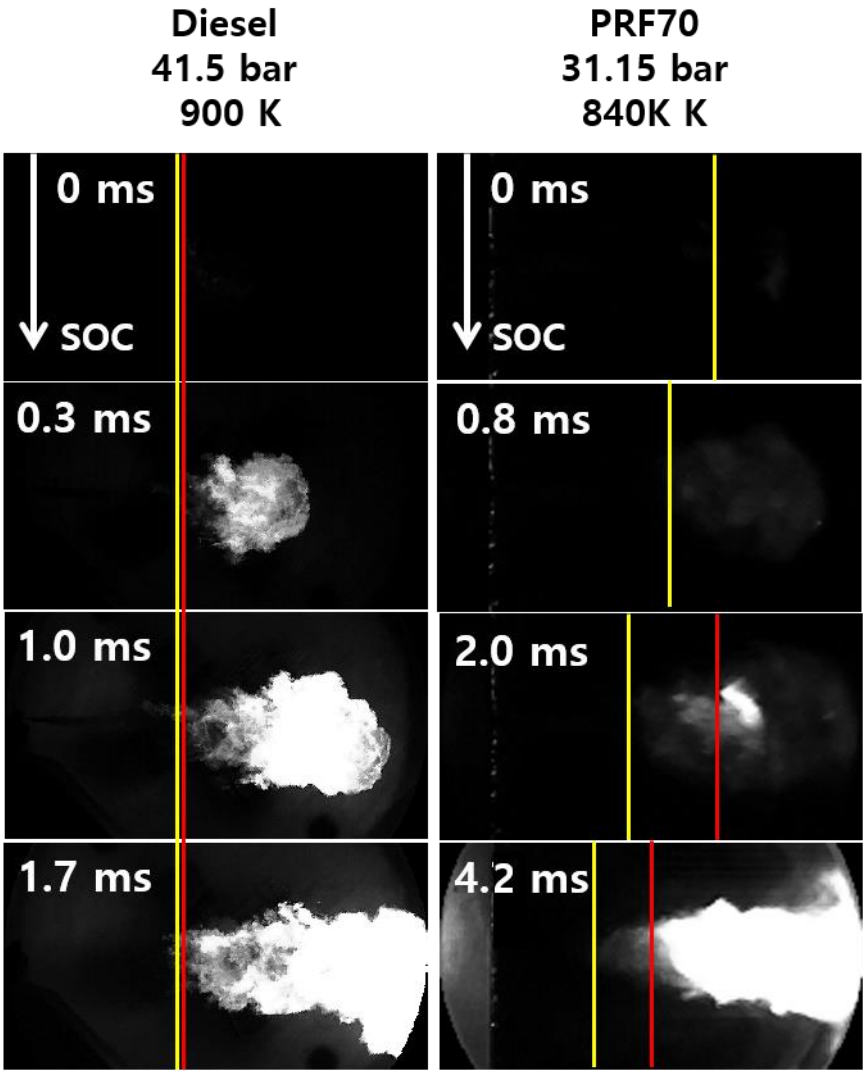

Figure 4.4 Comparison of diesel and PRF70

Left: diesel injection with 1500 bar at 41.5 bar, 900 K

Right: PRF70 injection with 500 bar at 31.15 bar, 840 K

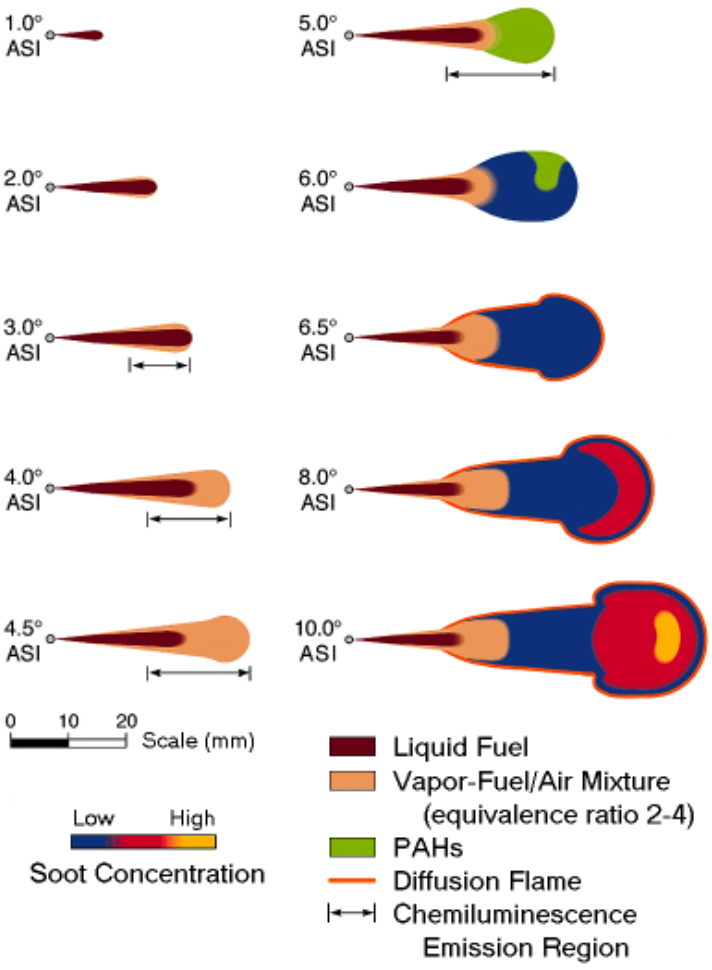

Figure 4.5 Conceptual model for diesel combustion in conventional heavy-duty by J. Dec [45, 50]

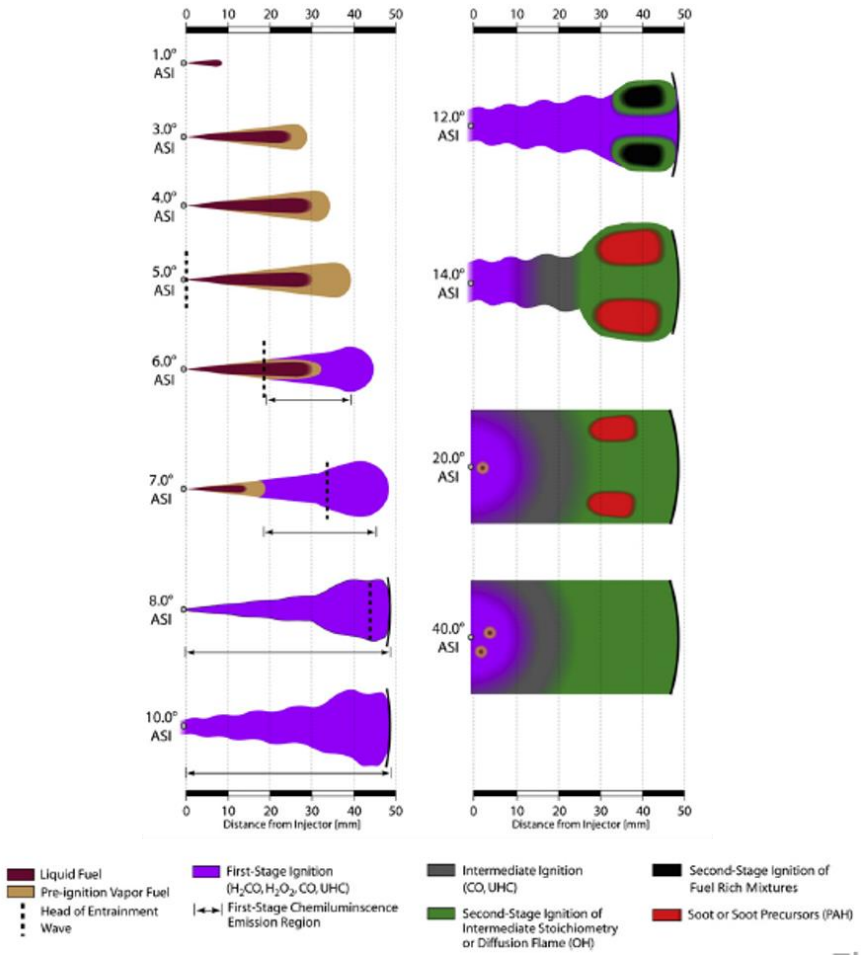

Figure 4.6 Conceptual model for diesel combustion in PPCI with LTC strategy by M.P.M. Musculus [51]

4.3 Stochastic behaviors in PRF70 spray combustion

Exploring was conducted in 20 % oxygen condition, because it has wider combustible range, so it is easy to catch how flame changes with various injection conditions. Especially, to retaining major difference to cases in premixed zone (~2.3 ms injection duration), analysis was focused on long injection duration condition (~ 7.2 ms) and injection pressure varies from 200 bar to 1000 bar.

Firstly, intensities of four injection pressures were compared. As shown in Figure 4.7, it is found that there is large intensity variation even at same condition. Especially, at 300 and 500 bar cases have standard deviation about half of their average value. For more high pressure cases, standard deviation is still large relative to average, but in these cases, average intensity is very low because of overall light premixed blue flame. Accordingly, intensity variation is so small in absolute value that it cannot change combustion mode. Briefly, combustion always maintains its premixed mode in spite of large deviation relative to average intensity. For 300 and 500 bar conditions, it is expected that large absolute deviation value would be caused by changes of combustion behavior. As a proof of my expectation, number of saturated pixel from image when intensity is maximized was derived. Saturated pixels are caused by intensive soot in spray core, so number of saturated pixel mean extent of region with soot. Figure 4.8 shows number of saturated pixel (8 shots for 300 bar and 500 bar injection). As shown in figure, maximum case has saturated pixels more than five times than minimum cases.

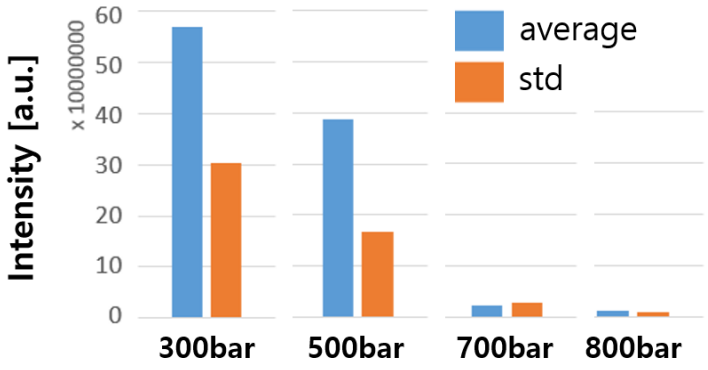

Figure 4.7 Average and standard deviation of flame intensity included in diffusive zone of operating regime)

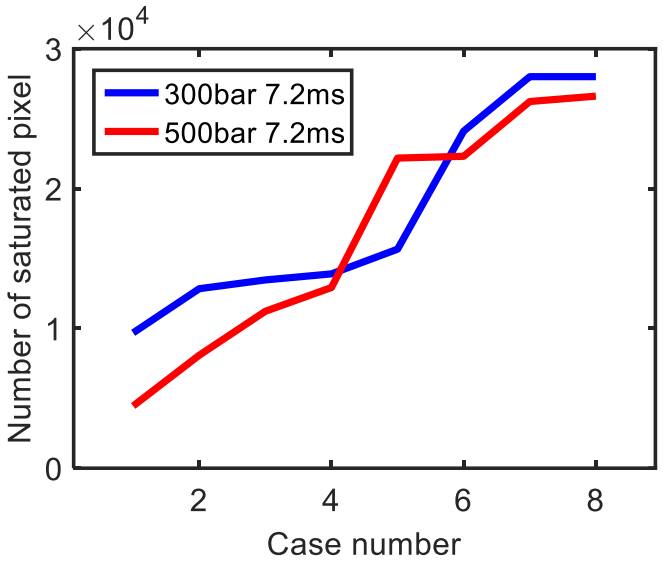

(a) Number of saturated pixel

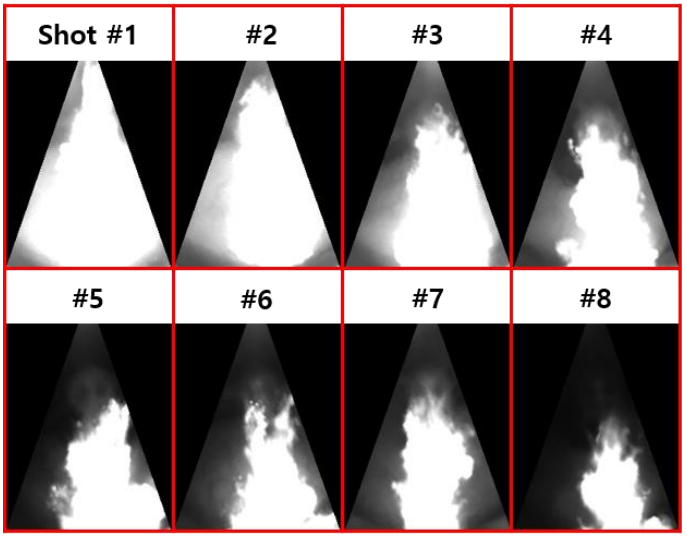

(b) Variation in flame structure (300 bar, 7.2 ms injection)

Figure 4.8 Existence of stochastic behavior in PRF70 combustion

4.4 Flame development in PRF70 combustion

4.4.1 Radially averaged intensity for analysis

From precedent analysis explained above, it is guessed that there are stochastic behaviors in spray combustion of PRF 70 in several conditions, related with soot production or flame structure. To clearly demonstrate the stochastic behavior which would dominates overall flame properties, additional tests (more than 20 shots) in each condition were conducted. 20 cases are big enough to reflect stochastic behaviors and profound analysis was done on these new data sets.

To discover the physical properties of spray combustion with PRF 70 fuel, direct measurement of natural luminosity and shadowgraph technique were adopted simultaneously. As explained in Chapter 2, combining two images from each diagnostics helps to understand flame development.

At first, analysis of natural luminosity image was done by RGB separation. Figure 4.9 shows that spatially integrated natural luminosity for 300 bar injection pressure (with 7.2 ms duration). As explained in 4.3, it is confirmed that there are variations large variations in integrated natural luminosity. To comprehend flame developments and soot formation, profiles of radial averaged intensity of penetration length versus time were obtained from RGB component. Figure 4.10 shows that radial averaged profiles for four representative cases of Fig. 4.9. Red zone in figure means region of soot where the signal value is larger than 90% of maximum value. Blue zone in figure means region of blue premixed flame zone derived from Blue component in

pixel value. From the comparison between natural luminosity and shadowgraph images, it was confirmed that premixed flame with blue component is well matched with dark reaction zone in shadowgraph image. Therefore, it is possible that entire reaction zone or flame can be described as blue zone in radial profile. Direct comparing between natural luminosity and shadowgraph images is shown Figure 4.11. Fig. 4.10 shows how flame develops after start of combustion. At first, flame starts by auto-ignition of air-fuel mixture in downstream region with premixed flame. Here, initial combustion points can be more than one, as shown in third case, which means that auto ignition occurs at several points simultaneously in wide downstream region. Regardless of number of initial combustion points, flame propagates to both upstream and downstream direction. In a few moments, red zone begins to appear inside the blue zone and then red zone also propagates both direction like blue zone. As soot propagates as time goes, overall flame with blue zone begins to be covered by red zone, indicating that soot exists in all penetration location.

Prior to analysis of individual shot, flame was divided into two concepts base on apparent feature in radially averaged intensity profile. First concept involves flame which steadily propagates from initial combustion points to upstream direction (Concept A). Second concept includes additional auto-ignition in upstream region few moments (more than 0.5 ms) after initial combustion (Concept B). Feature of these two concepts is also found in Fig. 4.10. In last two cases, flame propagates from initial combustion zone to both directions and finally soot appears (Concept A). In first two cases, during flame propagation from initial points, there are additional auto-ignition occurs in

more upstream position (Concept B). Additional auto-ignition in figure appears as separated auto-ignition zone from initial combustion points or immediate rise in vertical length of blue zone marked by black circle in first two plots.

Difference in flame development between initial combustion and additional auto-ignition is whether it is premixed or diffusive combustion. As shown in four radially averaged intensity profiles, initial combustion zone expands to both upstream and downstream direction. However, additional auto-ignition propagates to only downstream direction. Like conventional diesel combustion, additional auto-ignition involves intensive soot production from upstream. Thus combustion in concept B can be considered as combination of premixed flame in downstream and diffusive flame in upstream.

Figure 4.12 shows extracted intensity profiles from Fig. 4.9 for each concept. From the figures, it can be known that there is also intensity variation in each concept. Not only 300 bar injection case but also 500 bar and 700 bar cases were divided to two concepts, shown in Figure 4.13 and 4.14. To find out stochastic factors which can change intensity or flame structure, several variables were considered, which can be found in radially averaged intensity profiles.

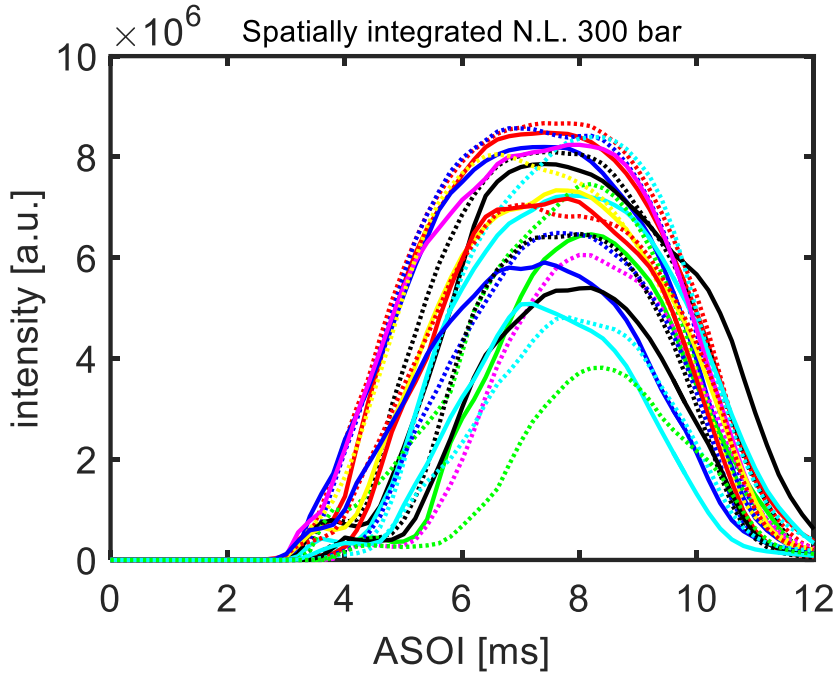

Figure 4.9 Spatially integrated natural intensity

(total 23 shots for 300 bar, 7.2 ms)

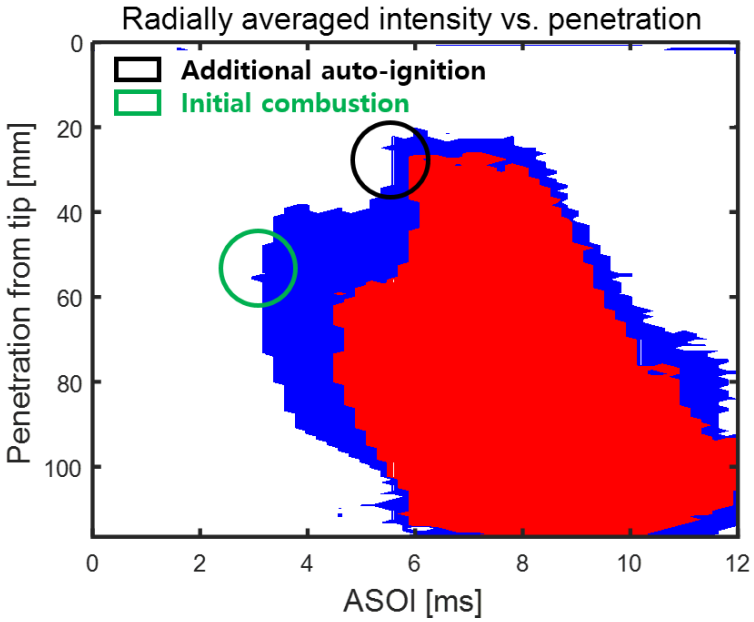
Radially averaged intensity vs. penetration
Additional auto-ignition
Initial combustion
Penetration from tip [mm]
ASOI [ms]
0
20
40
60
80
100
0
2
4
6
8
10
12

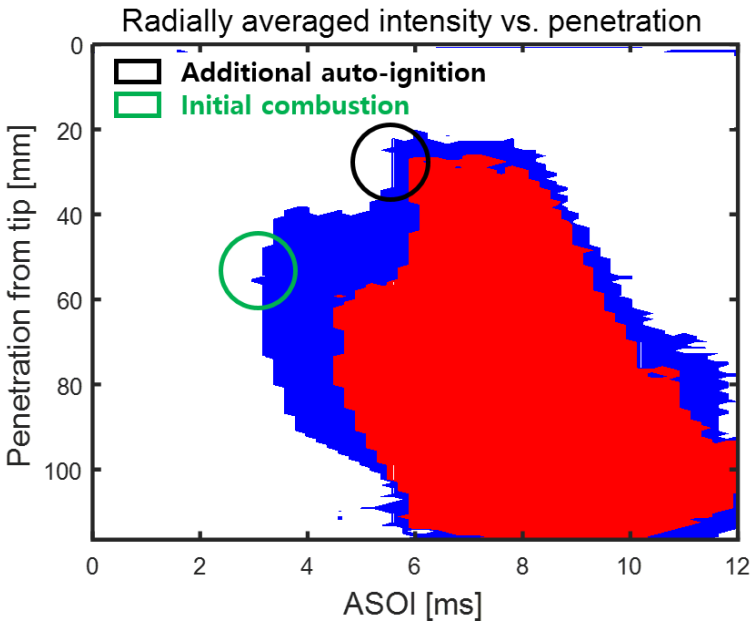
Radially averaged intensity vs. penetration
Additional auto-ignition
Initial combustion
Penetration from tip [mm]
ASOI [ms]
0
20
40
60
80
100
0
2
4
6
8
10
12

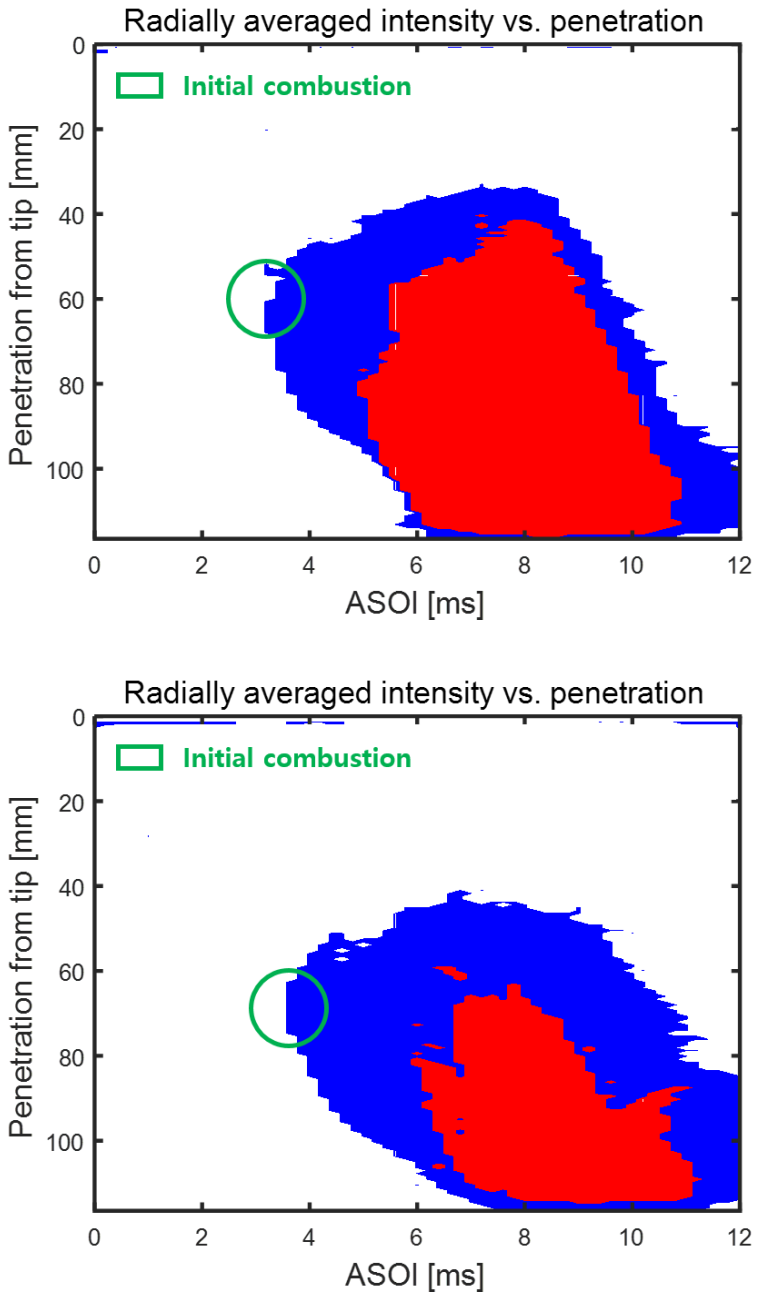

Figure 4.10 Radially averaged intensity for four representative shots

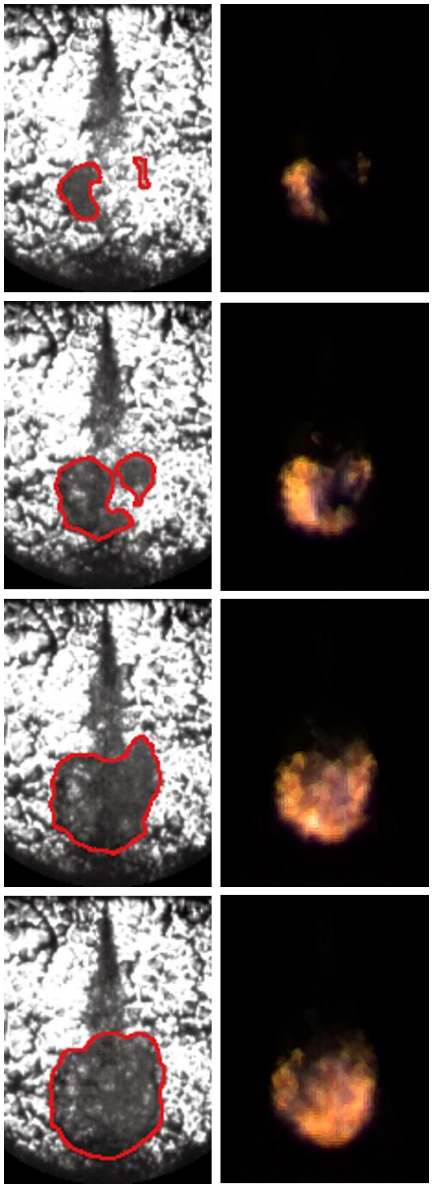

Figure 4.11 Comparison of natural luminosity and shadowgraph images

Left: shadowgraph images and flame boundary

Right: natural luminosity images from color camera

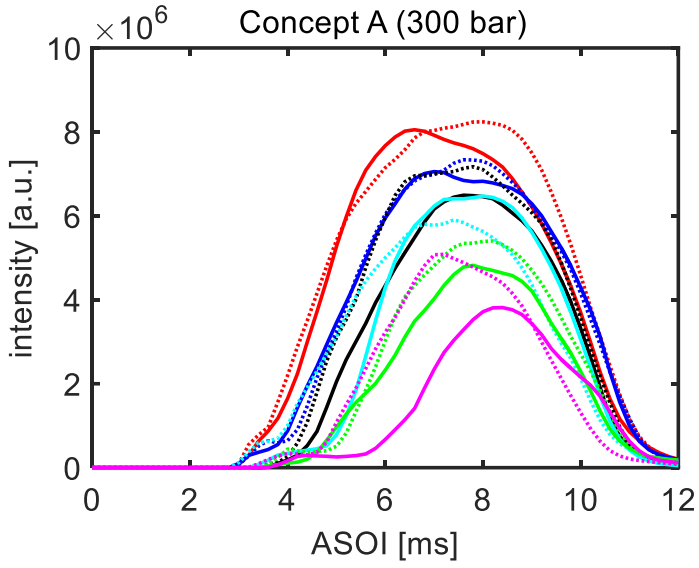

(a) Concept A (12 shots)

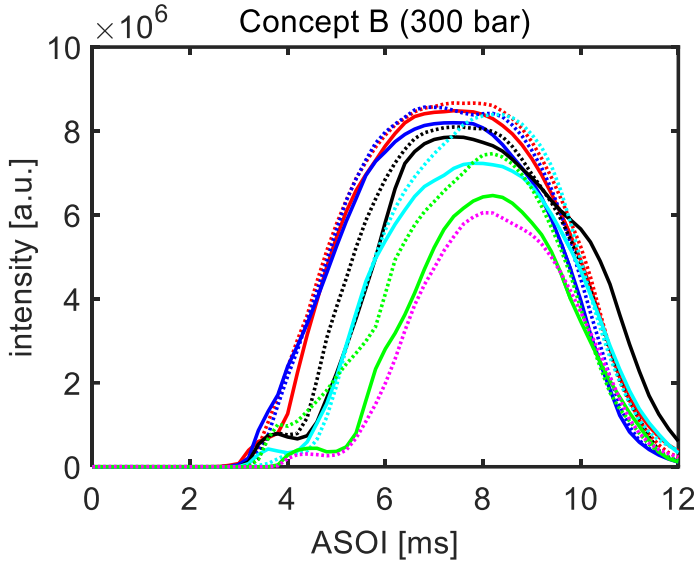

(b) Concept B (11 shots)

Figure 4.12 Spatially integrated natural luminosity for 300 bar injection

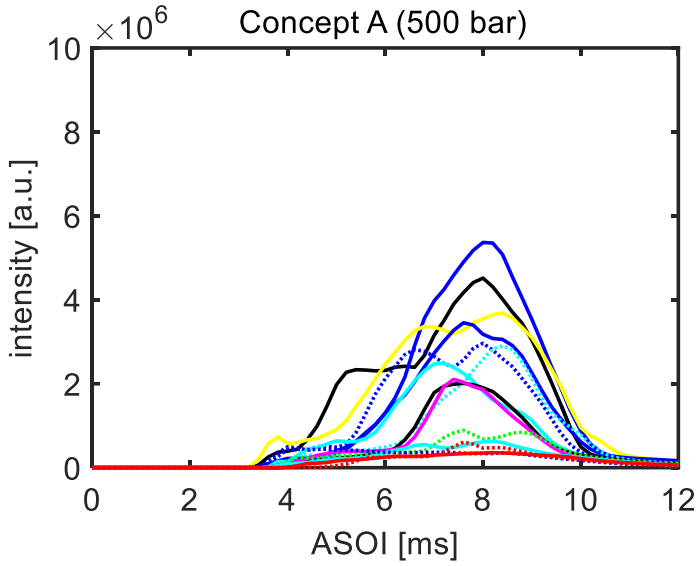

(a) Concept A (14 shots)

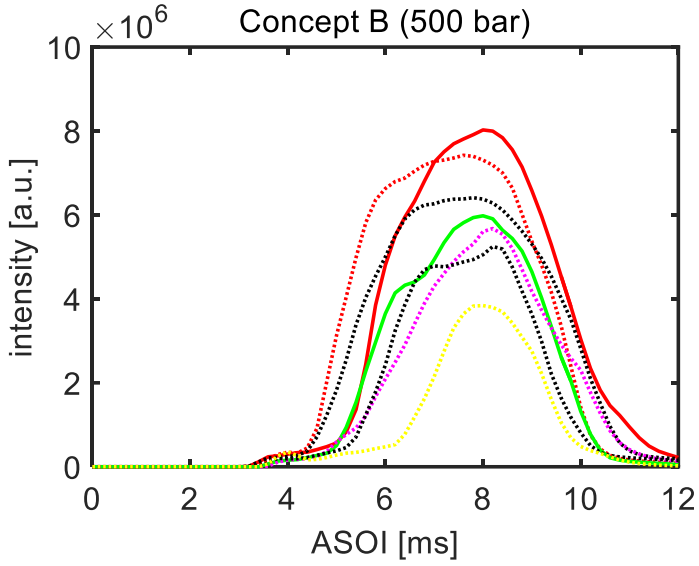

(b) Concept B (7 shots)

Figure 4.13 Spatially integrated natural luminosity for 500 bar injection

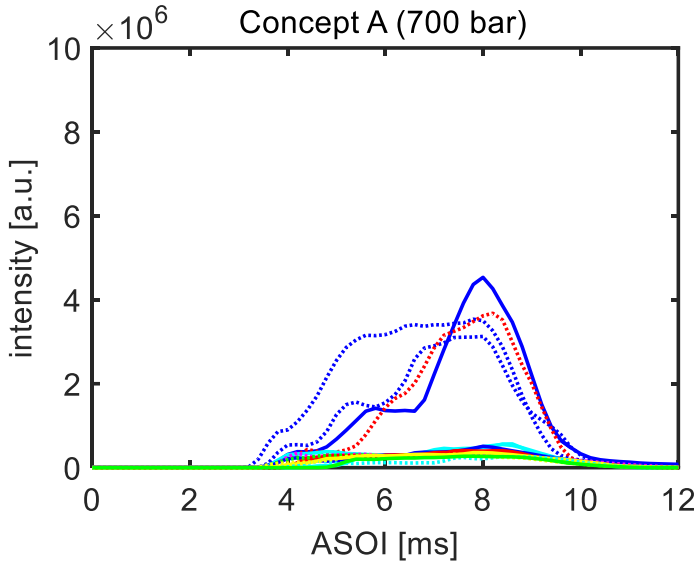

(a) Concept A (16 shots)

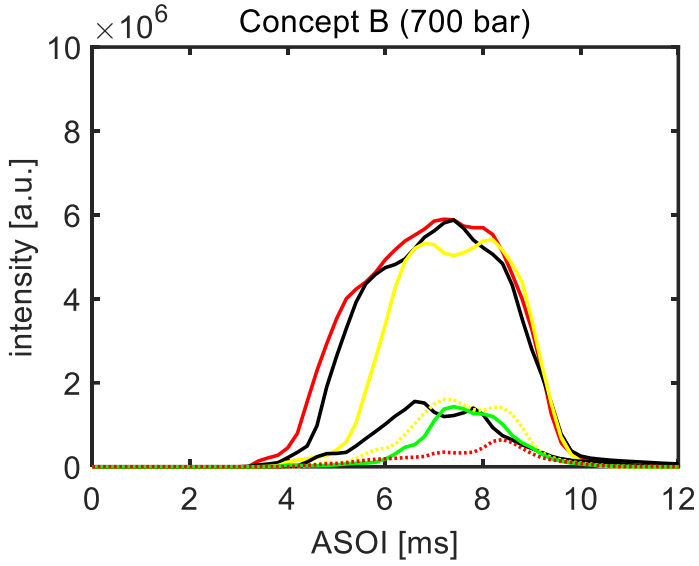

(b) Concept B (7 shots)

Figure 4.14 Spatially integrated natural luminosity for 700 bar injection

4.4.2 Concept A

Firstly, relation between spatially-temporally integrated intensity and initial combustion location was considered. It means that as location of initial combustion changes, overall flame structure would be changed. Here, spatially-temporally integrated intensities are derived by integrating profiles in Fig. 4.12, 4.13 and 4.14 with time. Figure 4.15 shows spatially-temporally integrated intensity of 12 cases included in concept A of 300 bar injection. Each case was given number in accordance with descending order of intensity (A#1, A#2, A#3…). Figure also shows distance from injector tip to initial combustion zone defined as closest flame from injector tip at first frame equivalent to ignition delay. From the figure, it can be known that overall intensity of flame has negative correlation with initial combustion zone from tip, that is, as combustion starts far from injector tips, combustion intensity goes weak. Figure 4.16 show minimum distance from injector tip to flame and soot region during whole combustion duration, respectively. As flame propagates more upstream, also region of soot production moves upstream. Strong connection exists between two values and both values have positive correlation with initial combustion position. Consequently, as initial combustion starts more close to injector tip, flame can propagate more upstream and soot is produced more. For 500 and 700 bar injection pressure, combustion is also divided to two concepts. Figure 4.17 shows spatially-temporally integrated intensity of 500 bar injection cases. Similar with result of 300 bar condition, integrated intensity decreases as initial combustion occurs far from injector tip. In Figure 4.18, flame

propagation and soot region from injector are shown. As shown in figure, flame propagation and soot region go far from injector tip, as intensity decreases. From more detailed exploring for individual shot, it can be realized that A#9, A#11 and A#13 stay away from main trend in flame propagation. In those cases, flame propagates as much as low numbered cases with high intensity, but it does not have effect on flame intensity or soot production. The reason of this phenomenon will be explained chapter 6. Disappearance of marker with high numbered cases in Fig. 4.18 means that there is no saturated soot signal during combustion duration. Thirdly, for concept A in 700 bar injection tests, Figure 4.19 shows integrated intensity and initial combustion location. As shown in figure with intensity, first four cases have moderate intensity and the others have very low intensity. It is also shown in Figure 4.20 where soot is only detected in first four cases. Considering closest flame location from tip shown in Figure 4.20, there are also abnormal cases (e.g. A#5, A#8 and A#9) like A#9, A#11 and A#13 in 500 bar condition. From comparing integrated intensity and soot production of concept A for three injection pressures, it is verified that as injection pressure increases, ratio of non-soot or non-saturated signal increases. Because of relatively high injection pressure, initial combustion occurs in more downstream region and then flame cannot propagate to close to injector although there is a little variation. It means that it is possible to achieve premixed burn without soot though injection duration is longer than ignition delay if injection pressure is higher than 500 bar.

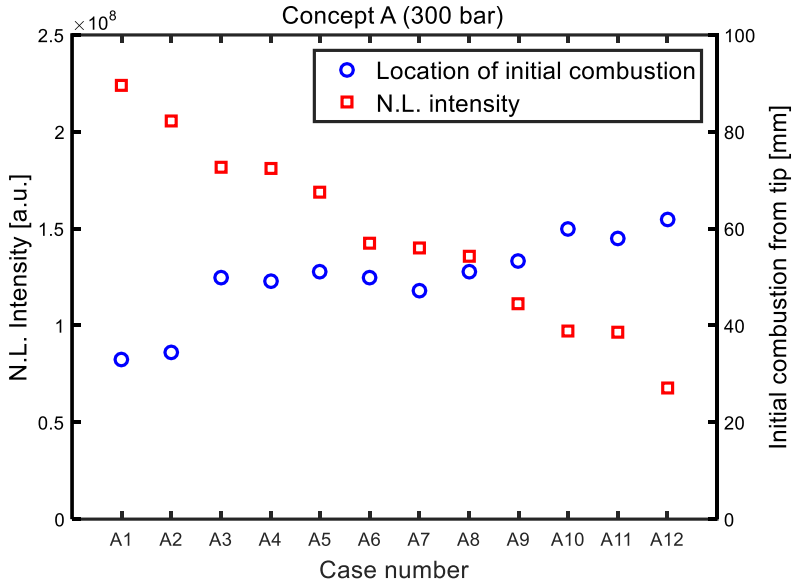

Figure 4.15 Combustion intensity and initial combustion location

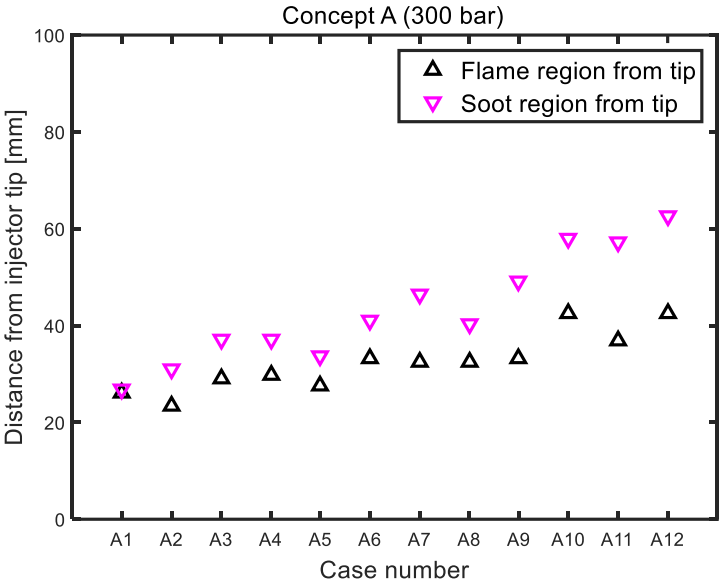

Figure 4.16 Distance from injector tip to flame and soot region

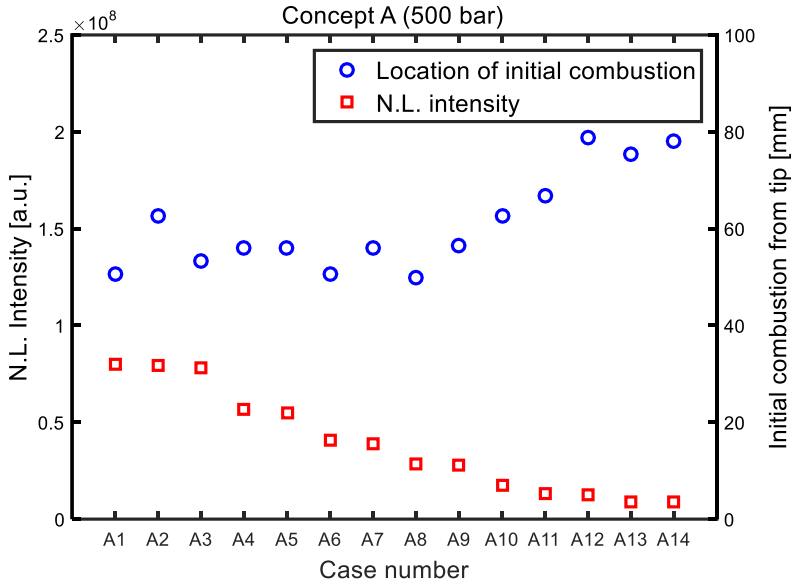

Figure 4.17 Combustion intensity and initial combustion location

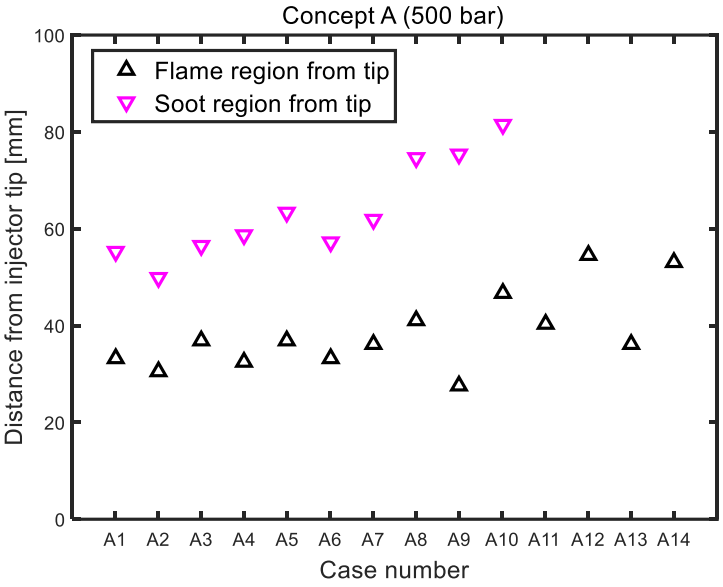

Figure 4.18 Distance from injector tip to flame and soot region

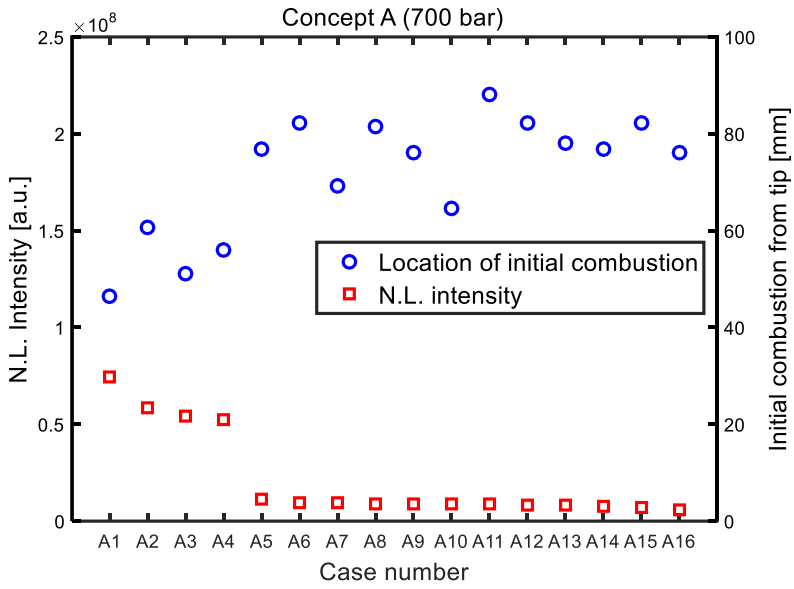

Figure 4.19 Combustion intensity and initial combustion location

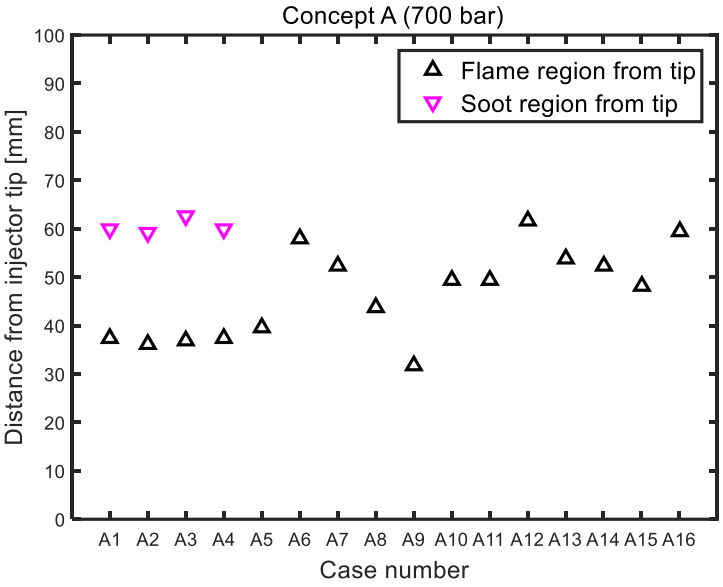

Figure 4.20 Distance from injector tip to flame and soot region

4.4.3 Concept B

As explained in 4.4.1, combustion in concept B involves additional separated auto-ignition in upstream region. From the results that initial combustion location has strong correlation with integrated intensity, it was expected that location of additional combustion has effect on flame structure or soot production. Figure 4.21 shows integrated intensity and location of separated auto-ignition for 300 bar injection pressure cases. Among the total 23 cases for 300 bar injection cases, 11 cases have combustion of concept B. Each case was given number in accordance with descending order of intensity (B#1, B#2, B#3…). It is shown that as additional combustion occurs far from injector tip, intensity decreases. This trend can be found in Figure 4.22. As shown in figures, flame propagation and region of soot have strong positive correlation with position of additional auto-ignition. From further observation, other two factors can make soot production trend different (e.g. initial combustion location as in concept A and timing of additional auto-ignition). Like B#6 and B#7 shots in Fig. 4.21(a), they have lower intensity than B#1 and B#2 shots in spite of similar additional combustion position. For B#6 shot, because additional auto-ignition occurs about 2.2 ms after start of combustion, timing of soot appearance in upstream is later than that of #B1 and #B2. For #B7 shots, initial combustion location has effect on intensity of early stage. For #B1 and #B2, because initial combustion occurs closer to tip rather than #7, soot is produced in early stage by initial combustion. Figure 4.23 shows four intensity profiles during combustion duration for B#1, B#2, B#6 and B#7. Last two plots

show that rise of intensity is delayed when compared with first two, because two factors proposed above have effect on flame intensity. Plots in Figure 4.24 and 4.25 shows seven shots included in concept B of 500 bar injection tests. Equally, trend in location of separated region, flame propagation and soot production have very similar shape. Figure 4.26 and 4.27 show results of eight shots from 700 bar tests. First three shots have higher intensity than last five shots. Although last five shots have low intensity nearly similar to that of non-soot combustion in concept A, soot occurs sparsely in locally fuel-rich zone in practice. However, it is not enough to induce bulk production.

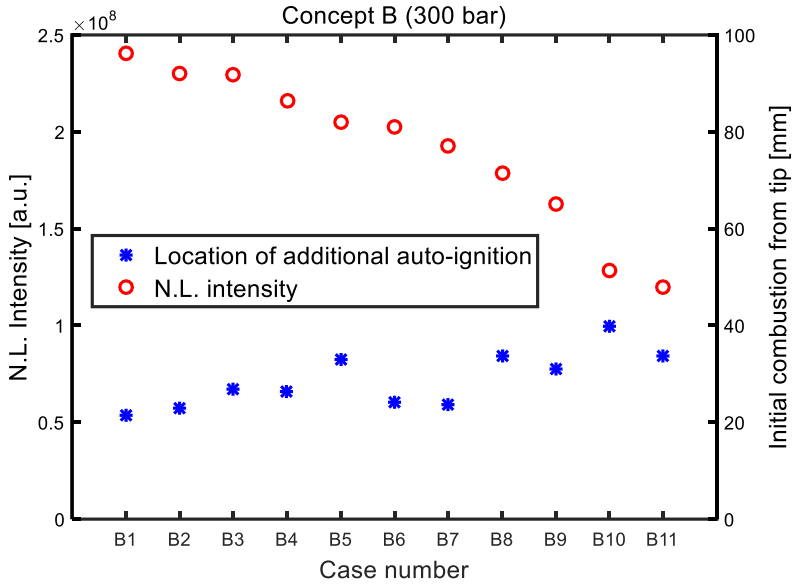

Figure 4.21 Combustion intensity and additional auto-ignition

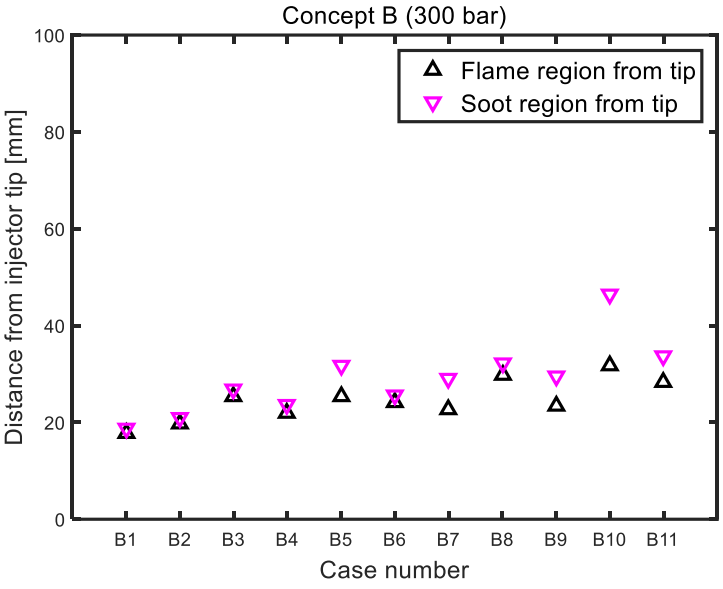

Figure 4.22 Distance from injector tip to flame and soot region

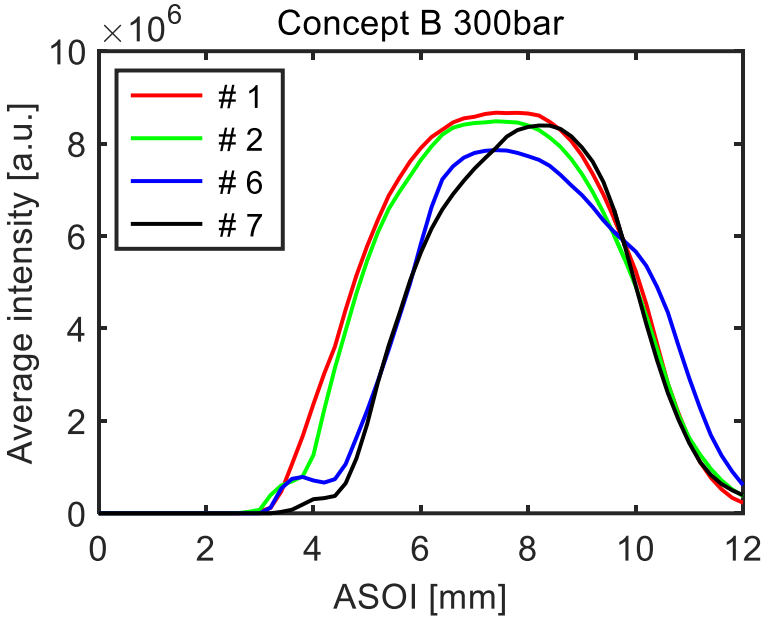

Figure 4.23 Spatially integrated natural luminosity intensity for abnormal cases

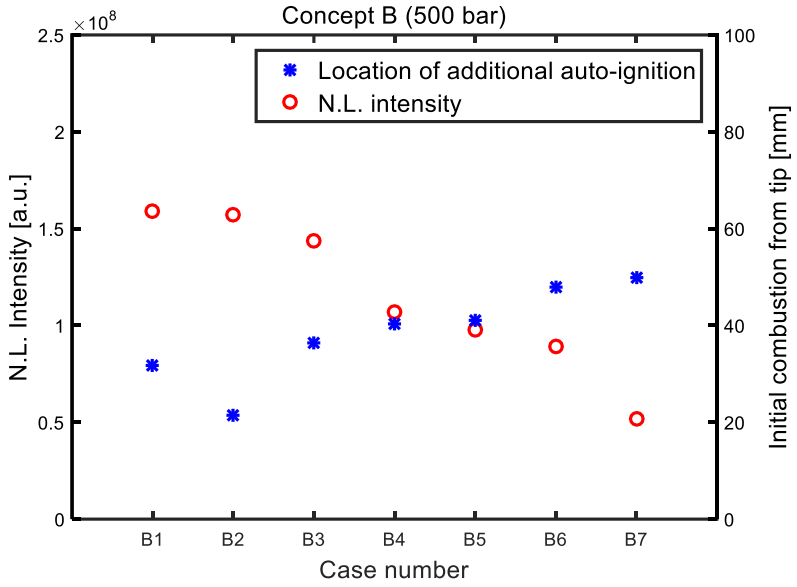

Figure 4.24 Combustion intensity and additional auto-ignition

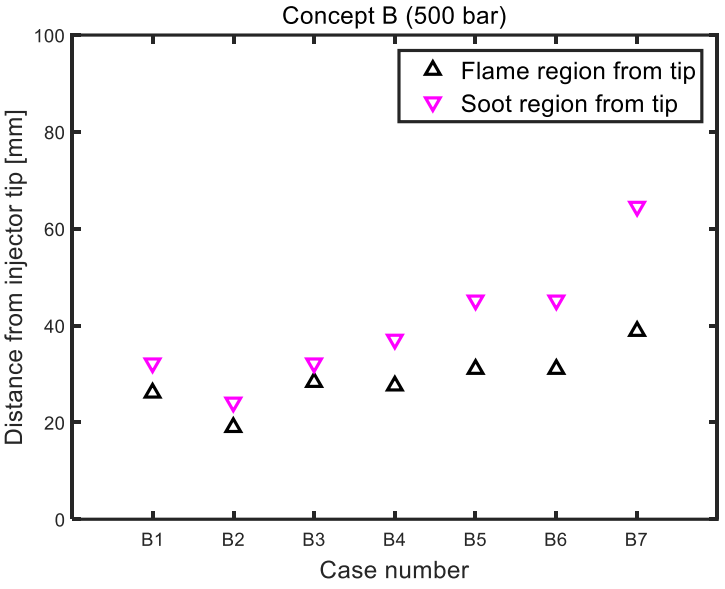

Figure 4.25 Distance from injector tip to flame and soot region

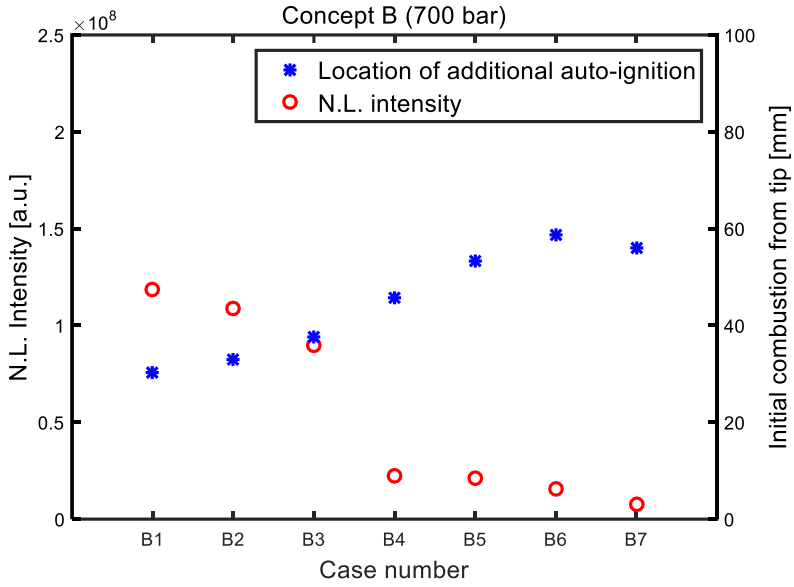

Figure 4.26 Combustion intensity and additional auto-ignition

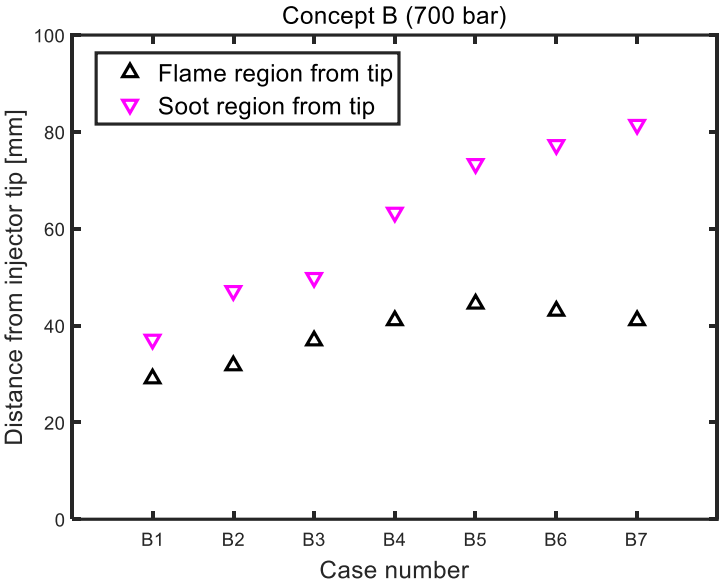

Figure 4.27 Distance from injector tip to flame and soot region

4.5 Summary

In this chapter, flame development was analyzed using filtered natural luminosity image. At first, combustion regime was divided to 'premixed combustion zone' and 'diffusive combustion zone'. Considering conventional diesel combustion cannot be marked on present regime, it was verified that there are three combustion types. With Excepting 'premixed combustion zone' and 'conventional diesel combustion', which can be described by existing conceptual models like LTC model by Musculus and Heavy-duty diesel model by John Dec, respectively. Thus, this new combustion behavior called diffusive combustion zone was focused in present work and expected to suggest new idea for understanding distinctive phenomenon. For fixed injection duration to 7.2 ms, injection pressure was changed from 300 bar to 700 bar. From the apparent feature of averaged intensity contour, combustion type in diffusive combustion zone was divided to two concepts. Concept A involves initial combustion at particular points in spray region and following flame propagation. Concept B has not only behavior of concept A, but also additional auto-ignition in upstream region, few moments after initial combustion.

In concept A, combustion structure and development are determined by initial combustion position. As first ignition occurs at more upstream region, combustion tends to have high intensity with more soot. If first ignition occurs lower than particular position, flame propagation cannot propagate enough to produce soot duration combustion duration.

In concept B, combustion intensity mainly due to soot signal is dominated

by position of additional auto-ignition in upstream region. Additional auto-ignition usually induces huge amounts of soot with extreme fuel-rich mixture. Although some cases in concept B are influence by timing of additional auto-ignition, concept B generally shows high intensity with wide soot region.

As injection pressure increases, combustion zone moves to downstream whether it is initial combustion or additional auto-ignition, and number of shots with only premixed flame increases. According to conventional definition of PCI or PPCI is that injection has to be completed before SOC. It claims that if there exists time overlap between injection period and combustion duration, soot will be produced by latter part of fuel injected after SOC. In contrast to original definition, large number of shots have only premixed flame even at long injection duration. It means that there is possibility of fully premixed combustion with long injection duration much longer than ignition delay. However, to realize the it's possibility of low soot with long injection duration, stochastic or unsteady combustion behaviors must be fully understood and well regulated.

Chapter 5. Experimental results 3 – Confirmation of flame structure by shadowgraph and Mie-scattering

5.1 Introduction

To validate the natural luminosity images and support my arguments, shadowgraph technique was adopted. In this chapter, analysis of flame development will be reprocessed from shadowgraph results. Spatial features of flame can be explained by shadow graph images like multi ignition zone, radial expansion or cool flame.

5.2 Cool flame and expansion of initial combustion zone

Figure 5.1 shows penetration versus time after start of injection for 300 bar injection pressure. Red line represents penetration length measured in centerline of spray and blue line is length of liquid phase in spray. Penetration length was calculated by averaging process of over twenty shots in Chapter 4. Vapor phase and liquid region are separated right after start of injection. Within 1 ms, liquid length is saturated and maintained with a little fluctuation until injection finish. Vapor phase continues to penetrate across the chamber. Figures show penetration data up to 3 ms when ignition starts and shadowgraph images become complicated to detect spray edgy. There is no distinct gap in liquid

length between three injection pressures. However, vapor penetration clearly shows effect of injection pressure on spray developments. Figure 5.2 shows that shadowgraph images for A#11 shot of 300 bar injection. After start of injection, dark vapor region on the top penetrates to downward. About 2.5 ms ASOI, spray head suddenly disappears, which indicating that first stage combustion or low temperature combustion with cool flame. In chemical aspects, cool flame can be represented by formaldehyde (CH_2O) and small amount of heat is released by partially oxidized reaction. Because refractive index of cool flame region becomes close to ambient condition during the cool flame, cool flame zone looks transparent. Boundary of this transparent vapor zone can be realized by image subtraction. By subtracting two successive shadowgraph images, blurred boundary of cool flame can be leaved in resultant images [53]. 0.5 ms after first stage ignition, initial combustion or reaction occurs in cool flame region. As explained chapter 4, initial combustion can occur at several spots simultaneously. In this case, initial combustion starts at 2 points at 3.2 ms and radially expands. At 4.2 ms dispersed reaction zone combined to single big zone and continue to expand to all direction. When flame expands and passes the particular point, intensive soot occurs from upstream. In contrast to reaction zone with dark texture, soot is visualized as white texture. Indeed, shadowgraph cannot clearly show region of soot like soot boundary or locally produced soot.

Average of radial expansion rate in downstream (u_b) is 20~30 m/s. It is not easy to detect the movement of local flame front, because boundary of premixed zone is too wrinkle to detect. Thus, premixed zone was considered as perfect sphere and averaged radius was calculated. Laminar flame speed in

downstream region (S_L) is ~1 m/s calculated by following equation [5].

From inverse operation with $\rho_u/\rho_b \cong 3$, it can be derived that ratio of laminar burning area(A_L) to spherical burning area(A_b) is 7 ~ 10. This range is reasonable for flame expansion in premixed combustion. Equations between u_b, S_L, A_L, and A_b are listed below.

$$S_L = S_{L.0}(T_u/T_0)^{\alpha}(p/p_0)^{\beta} \quad \text{(EQ. 5.1)}$$

$$S_b A_b = S_L A_L \quad \text{(EQ. 5.2)}$$

$$u_b = S_b(\rho_u/\rho_a) \quad \text{(EQ. 5.3)}$$

From the shadowgraph images, it can be known that flame propagation to both upstream and downstream direction in Fig. 4.10 comes from radial expansion of this premixed combustion behavior.

Figure 5.3 shows shadowgraph images of B#2 as representative shot of concept B of 300 bar injection. Similar to Fig. 5.2, initial combustion occurs at downstream region, but about 3.9 ms ASOI, additional combustion near boundary of cool flame. It is difficult to distinguish vapor region and additional combustion zone in upstream, because they have same dark texture. However, reaction zone rapidly expands and get out from narrow boundary of vapor region. Boundary of vapor region in upstream is marked by red line. Finally, all reaction zones are merged to single reaction zone and produce soot signal.

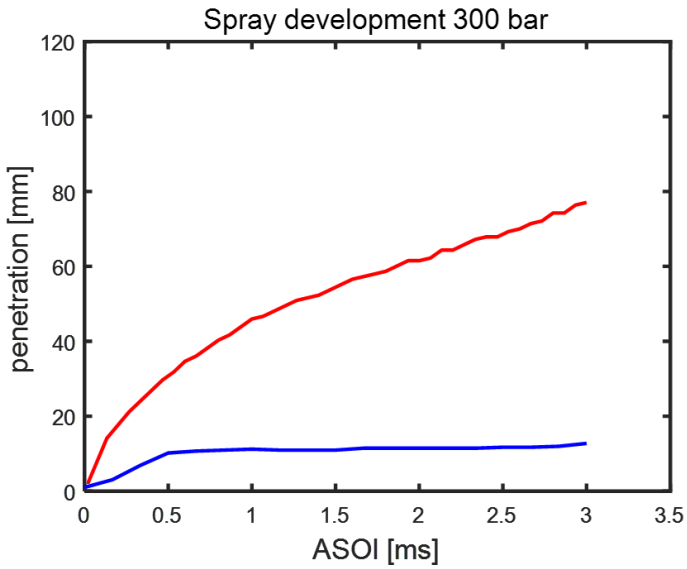

(a) 300 bar

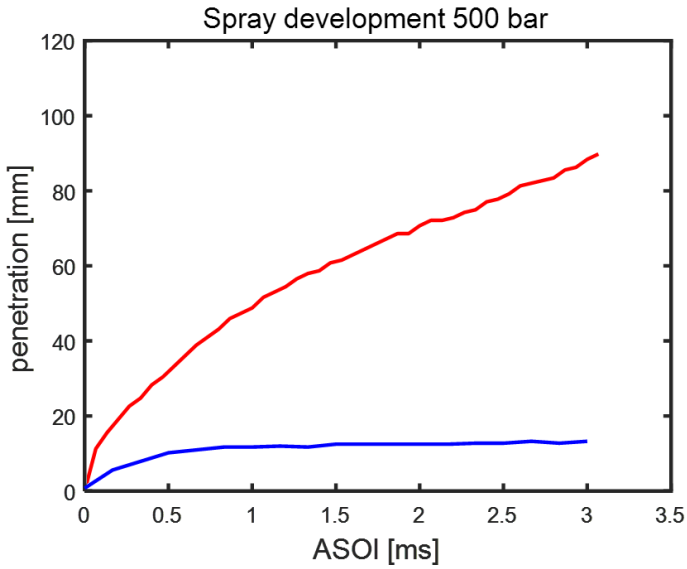

(b) 500 bar

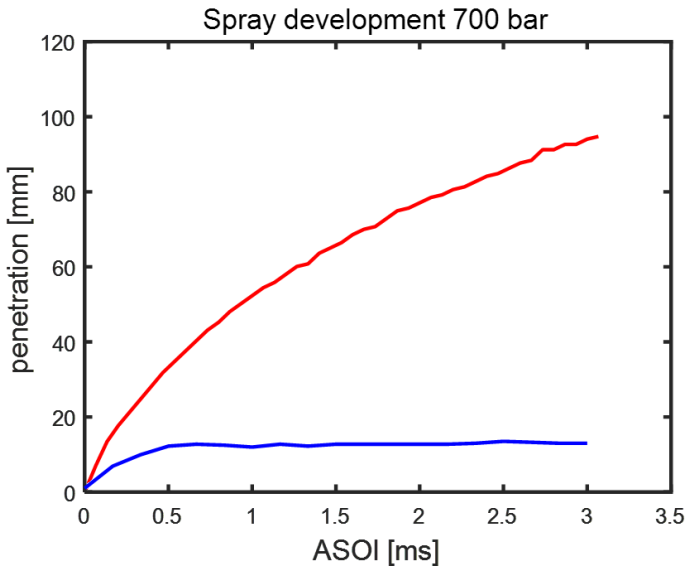

(c) 700 bar

Figure 5.1 Vapor and liquid penetration length from shadowgraph

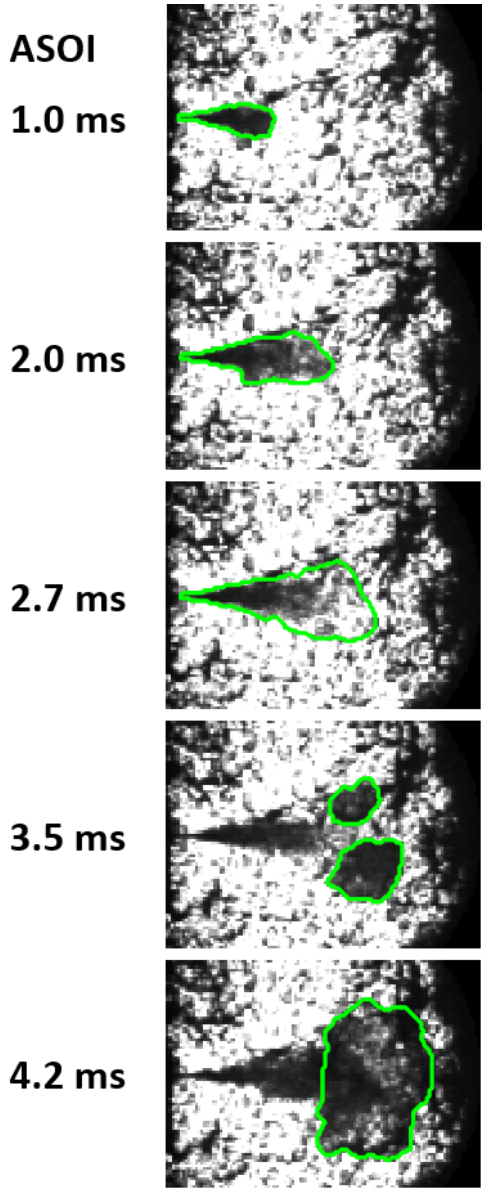

Figure 5.2 Flame development of concept A

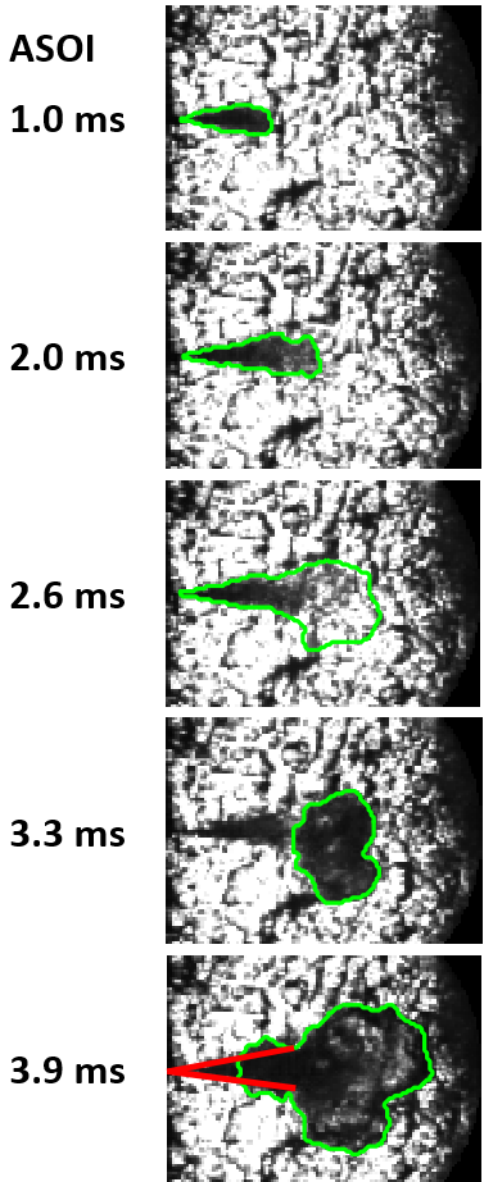

Figure 5.3 Flame development of concept B

5.3 Summary

From the shadowgraph technique, it is possible to know that existence of cool flame, radial expansion of reaction zone. Propensity of soot is well understood by luminosity contours in chapter 4, but, spatial features or hidden reactions of flame are more clearly shown in shadowgraph images. Reaction zone with invisible wavelength can be detected by dark zone in shadowgraph, although it does not give information about what kinds of radical or species exist. Shadowgraph images give evidence that radial expansion of reaction zone in downstream region, which can help to establish new conceptual model for combustion of low octane fuel. Flame from initial combustion in downstream propagates to radially direction as like spark ignition. It means that early stage of combustion in downstream is dominated by propagation of premixed flame.

Chapter 6. Understanding of stochastic combustion behavior with 1-D spray model

6.1 Introduction

To understand more detailed about thermodynamic state inside the spray region, validated one dimensional penetration model was adopted and reproduced. This kind of model was first suggested by Naber and Sieber in 1996 [54]. Assuming that radial velocity profiles in same penetration length as uniform and spray cone angle is maintained constant during injection duration, they solved relation between penetration length and time with non-dimensional form. Entire spray zone at particular time is considered as single control volume and equivalence ratio at spray head can be predicted. Predicted equivalence ratio in this model is cross-sectional average equivalence ratio. Figure 6.1 shows schematic of model with uniform velocity profile suggested in 1996 by Sandia National Laboratory [54].

Several experiments were conducted to show relation between lift-off length (H) and soot production [17, 55-57]. In those researches, lift-off length and soot were measured by OH chemiluminescence and laser-induced incandescence, respectively. By coupling directly measured lift-off length with predicted equivalence ratio, it is possible to predict averaged equivalence ratio

at lift-off length (Φ(H)). Comparing equivalence ratio at lift-off length (Φ(H)) with soot existence shows typical trend in diesel combustion. As lift-off length is increased by high injection pressure or long ignition delay (e.g. low ambient temperature, low oxygen concentration or high EGR), amount of air entrainment before combustion increases. When predicted equivalence ratio at lift-off length becomes lower than two, soot incandescence signal drastically decreases, which is equal to theory that soot does not appear under fully premixed condition with equivalence ratio lower than two [5].

Next, improved prediction model was developed by M. P. M. Musculus and K. Kattke in 2009 [58]. The biggest differences compared to old model are velocity profile and transient behavior. In this new model, to make simple one-dimensional model more realistic, radial distribution of velocity and mass fraction was added. Radial distribution of velocity gives reality of non-homogeneity mixture, especially, existence of locally rich mixture in centerline. In addition to radial variable option, analytical solution for discrete control volume was served. In contrast to uniform profile model where entire spray zone is considered as single control volume, new model with variable velocity profile divide total penetration length (100 mm) to 2000 control volume with same thickness (0.05 mm). Thus, new model can describe the physical properties of individual control volume, like transient behavior during injection opening or closing duration or unsteady injection rate. Indeed, multiple control volume explanation was constructed to simulate the transient behavior, occurring before fully developed or after end of injection [59]. Figure 6.2 shows schematic of model with variable velocity profile.

Considering valid correlation between Φ(H) and soot incandescence in reference results with uniform velocity profile, option of uniform velocity profile was selected. Additionally, to reflect and describe the flame development after end of injection, solution with multiple discrete control volume was used.

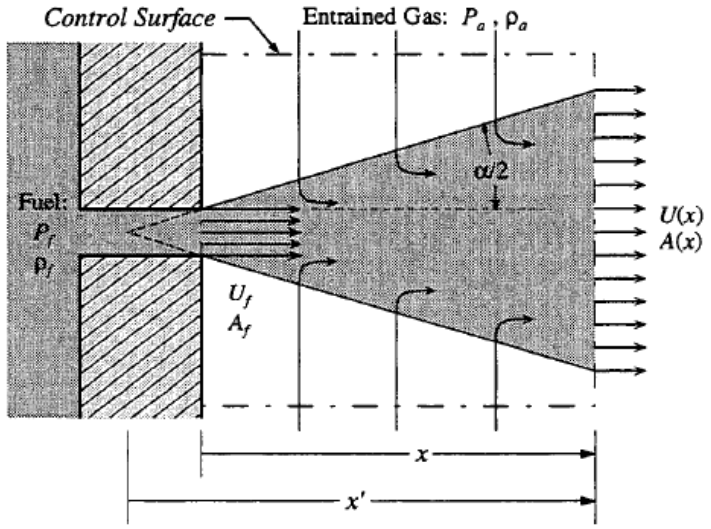

Figure 6.1 Schematic of spray model with uniform velocity profile [54]

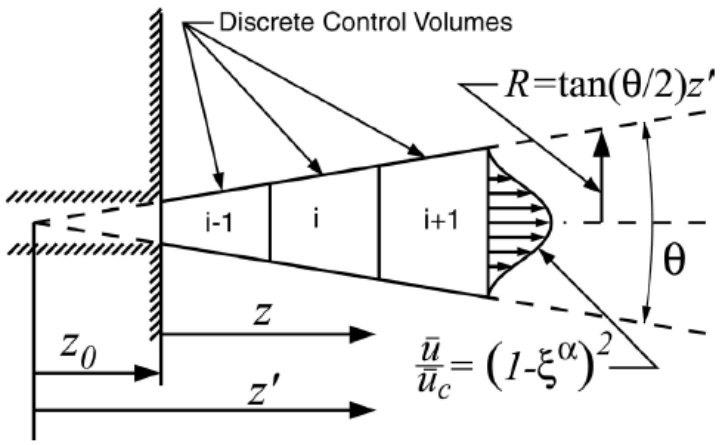

Figure 6.2 Schematic of spray model with variable velocity profile [58]

6.2 Methodology

Figure 6.3(a) shows analytical model of present study, combination of two existing model from Sandia National Laboratory. Figure 6.3(b) shows calculation sequence of find physical properties for each control volume. Mass of control volume at (t + Δt) is determined by mass inflow from front control volume and outflow to next control volume during time interval Δt. As shown in figure, mass outflow from particular control volume work as inflow of next control volume. For first control volume adjoin with injector hole, mass inflow ($m^t_{out,o}$) is fuel injection rate ($\dot{m}_f$) (Equation 6.1). Overall equation expressing mass flow versus time can be simplified as Equation 6.2. Mass flow term in Equation 6.2 is determined by fuel volume fraction ($\bar{\bar{X}}_f$), flow velocity ($\bar{\bar{u}}$) and area (A) [58].

$$m^t_{out,o} = \dot{m}_f \qquad \text{(EQ. 6.1)}$$

$$m^{t+\Delta t}_{f,i} = m^t_{f,i} + \rho_f[\dot{m}^t_{out,i-1} - \dot{m}^t_{out,i}]\Delta t \qquad \text{(EQ. 6.2)}$$

$$m^t_{out,i} = \bar{\bar{X}}_f \times \bar{\bar{u}} \times A \qquad \text{(EQ. 6.3)}$$

Thickness of control volume is 0.01 mm and simulated penetration length is 100 mm, consisting of 10000 control volumes. Number of control volume was arbitrary selected.

Other properties of spray structure were obtained from shadowgraph

measurement. Most important factors from experiments are penetration length versus time and spray cone angle. To acquire two factors, sprays in non-vaporizing condition were obtained to replace original images of reacting spray. Spray images from reacting condition are more complicated to detect penetration after start of combustion, because of wrinkled background and irregular combustion. Non-vaporizing experiments were conducted by injecting fuel into nitrogen charged chamber. In Figure 6.4, penetration length of reacting spray until SOC and that of non-vaporizing spray are compared, and it is found out that two penetrations are well matched until 3 ms ASOI corresponding to ignition delay. Black dotted line in figure is self-developed fitting curve for non-vaporizing penetration to obtain initial fuel velocity near the nozzle exit. From the fitting curves, velocity at nozzle exit was obtained as 214, 274 and 325 m/s for 300, 500 and 700 bar injection, respectively.

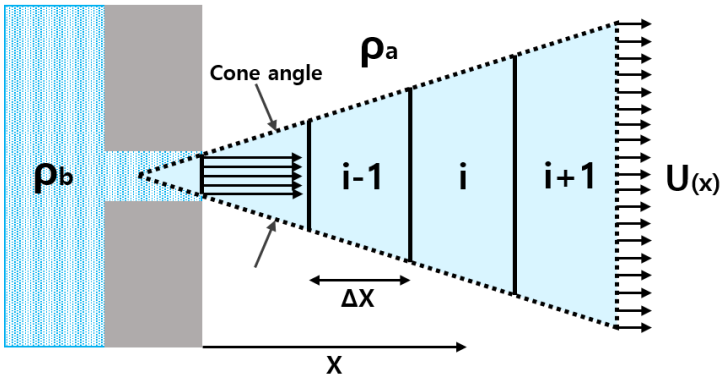

(a) Schematic of spray model in present research

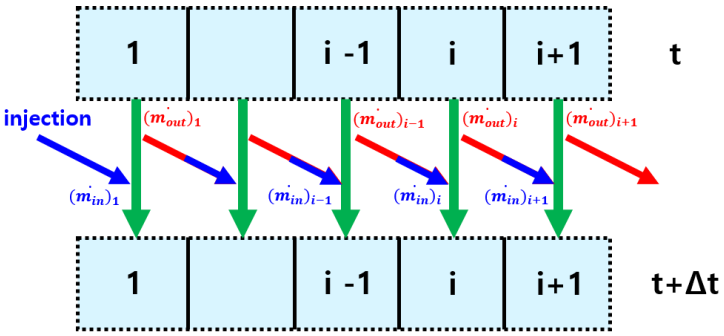

(b) Sequence of mass flow calculation

Figure 6.3 Concept of spray model

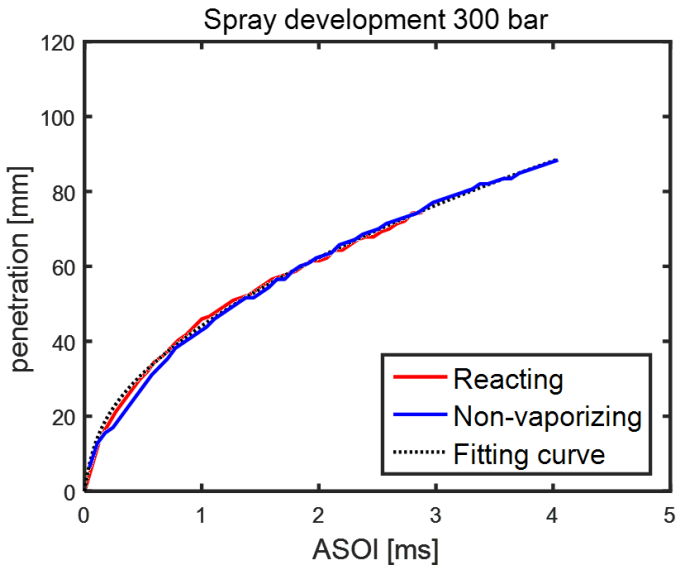

(a) 300 bar injection

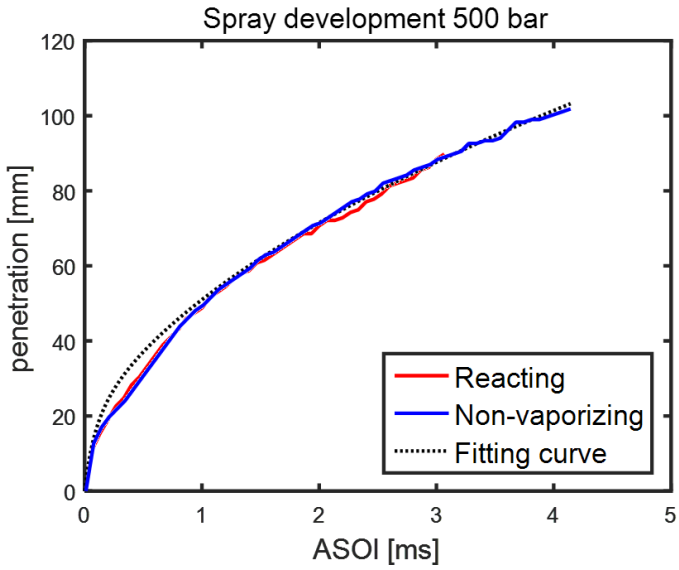

(c) 500 bar injection

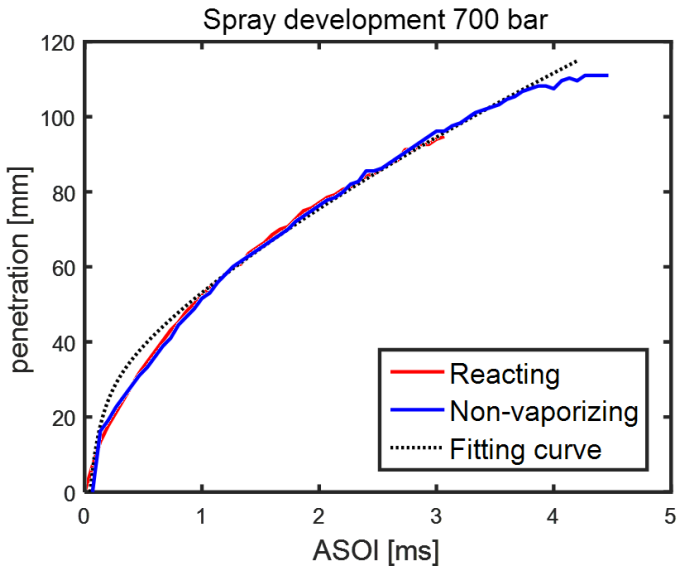

(c) 700 bar injection

Figure 6.4 Penetration length for reacting condition from 5.1 (red), non-vaporizing condition (blue) and fitting curve (black) for calculation of nozzle exit velocity

6.3 1-D model for equivalence ratio prediction

Fuel is injected first control volume with velocity at nozzle exit, and penetrates up to maximum simulated length 100 mm. Figure 6.5 shows penetration length versus time ASOI. Comparing with experiments data of non-vaporizing and reacting condition, simulated penetration length also well matched not only in 300 bar injection but also in 500 bar and 700 bar injections. Fuel has initially high momentum with nozzle exit velocity and begins to lose momentum, so velocity decreases as fuel penetrates. Because of losing momentum while penetrating across the chamber, slop in penetration plot becomes small in downstream region.

Most important results can be obtained from this simulation research is prediction of equivalence ratio in spray. Figure 6.6 shows cross-sectional averaged equivalence ratio from simulation. Figures includes equivalence ratio distribution at particular time ASOI. For 300 bar injection pressure, penetration length is 26 mm at 0.4 ms ASOI, which also can be shown in previous penetration plot. The first control volume right next to the nozzle exit has infinite equivalence ratio, because control volume is filled with fuel only. As far from injector tip, equivalence ratio drastically decreases. From the visualization research in previous chapter shows ignition delay of PRF70 is about 3~3.2 ms ASOI (chapter 3). At 3 ms ASOI, fuel penetration length reach 77 mm from tip and spray head, the leanest zone in spray, has equivalence ratio about 1.1. For 500 and 700 bar injection tests, fuel penetrates more than 300 bar injection in same period, because of high momentum. As shown in Fig.

6.6(b) and (c), penetration lengths are 87.5 mm and 95.5 mm at 3 ms ASOI for 500 bar and 700 bar, respectively. Corresponding equivalence ratios at those penetration lengths are 0.93 and 0.86. Consequently, as injection pressure increases, spray head zone expected to accompany the first reaction would be leaner. Thus, it is convinced that averaged intensity of first combustion is higher in 300 bar rather than other two conditions.

By applying results of equivalence ratio, it is possible to understand experiment results in chapter 4 again, especially relation between soot production and flame propagation. In chapter 4, it is confirmed that flame propagation close to injector tip leads to more soot production. Referring past reference researches showing that whether equivalence ratio at lift-off length is bigger or smaller than two is critical to soot production, penetration location 42.3 mm where averaged equivalence ratio is two is designated as reference position (dashed vertical line in Fig. 6.6). By comparing flame propagation length of individual with this reference position, it is expected to get evidence that there is critical boundary determining soot production in both concepts A and B. Plots from Figure 6.7 to 6.9 show comparison of flame propagation before end of injection with reference position. Because flame propagation after end on injection has little effect on soot production, flame propagation was chosen in injection period and named as effective flame propagation, that is, effective flame propagation means closest distance from tip to flame during 7.2 ms duration. Evidence of this effective flame propagation will be explained in this chapter with equivalence ratio contour. Fig. 6.7 shows effective flame propagation for concept A and B of 300 bar injection. Like the results of natural

luminosity analysis, flame propagates more upstream in concept B. All shots with 300 bar injection pressure have effective flame propagation lower than reference position except once case. As shown in Fig. 4.15 and 4.21, all 23 shots have high integrated intensity with intensive soot. Thus, it was little verified that if flame propagates and passes the reference position, soot is more produced. For 500 bar injection pressure, 7 shots in concept B, accompanying intensive soot production, have lower effective flame propagation than reference position like 300bar injection pressure. However, among the 14 shots in concept A, last six shots have higher effective propagation than reference position, which means flame occurs in region where equivalence ratio is below 2. Actually, they have low integrated intensity with low soot production or without soot. This trend is more clearly shown in 700 bar injection pressure. For concept B in Fig. 6.9(b), last four cases have effective propagation very close or higher than reference position. As shown in Fig. 4.26, these four cases have low intensity with locally soot production. For concept A, 12 shots of total 16 shots have much higher effective flame propagation than reference position. As shown in the Fig. 4.20, these 12 shots have very low integrated intensity relative to other shots. By comparing effective flame propagation with reference position, it is proved that 42.3 mm can be considered as critical position, determining whether soot would appear in spray or not. Additionally, like great agreement of modeling and experiments results in other references, equivalence ratio prediction with one dimensional is well matched with visualization data.

In practice, some shots have sooty region in spite of high effective flame

propagation. This deviation results from inhomogeneity of mixture in spray region. Although one dimensional model gives value of cross-sectional averaged equivalence ratio, fuel component is not uniformly distributed in real spray. Directly measurement of mixture fraction with Rayleigh scattering said that fuel is concentrated in spray centerline indicating equivalence ratio is higher in spray core region [59, 60, 61]. Thus, effective flame location with cross-sectional averaged equivalence ratio lower than two has the possibility of having zones with local equivalence ratio bigger than 2. These locally fuel-rich zones can produce soot even at little high effective flame propagation. Figure 6.10 and 6.11 shows several exemplary shots with effective flame propagation much lower and little higher than reference position, respectively. In Fig. 6.10, soot is produced with bulk motion, but, in Fig. 6.11, soot occurs discontinuously because soot is only produced in locally fuel-rich regions which occupy very small portion of flame zone.

To understand effective flame propagation used in this chapter, simulations for transient behavior of equivalence ratio before and after end of injection were carried out. As shown in Fig. 6.6, cross-sectional averaged equivalence profiles follow one curve called steady-state curve during injection period. When injection completes 7.2 ms ASOI, equivalence ratio starts to decreases. Figure 6.12(a), 6.13(a) and 6.14(a) show cross-sectional averaged equivalence after end of injection. After end of injection (EOI) 0.2 ms (7.4 ms ASOI), equivalence ratio near injector tip drastically drops to nearly zero. As time goes after end of injection, equivalence ratio plot is detached from steady-state curve. It means that extremely fuel-rich region near injector or upstream

region turns to lean state quickly as soon as fuel supply is stopped. Rapid drop of equivalence ratio was also reported by several researches [62]. Figure 6.12(b), 6.13(b) and 6.14(b) show equivalence ratio contour until 12 ms ASOI for 300 bar, 500 bar and 700 bar injection pressure. Expansion of non-zero equivalence ratio zone is much faster in high injection pressure, because of high momentum. Most important thing in equivalence ratio contour is that mixture near the tip lose their high equivalence ratio. Right after end of injection, upstream region begins to be filled by light color and finally equivalence ratio drops to below two. This can be reason why effective flame propagation is restricted to before end of injection. Also, it can be the answer to question in chapter 4. In chapter 4, it was mentioned that A#9, A#11 and A#13 of 500 bar injection and A#5, A#8 and A#9 of 700 bar injection have abnormal behavior that soot is hardly produced though flame propagates close to injector tip. Because equivalence ratio in upstream is not enough to produce soot after end of injection, too late flame propagation has little effect soot production. These shots have flame propagation quite close to injector during whole combustion process, but effective flame propagation is higher than reference position. It is clearly shown in Figure 6.15. Fig. 6.15 shows radially averaged profile on equivalence ratio contour for two cases among six abnormal cases. Although, there are additional flame after end of injection, flame cannot meet the fuel-rich zone, because of transient behavior in upstream region.

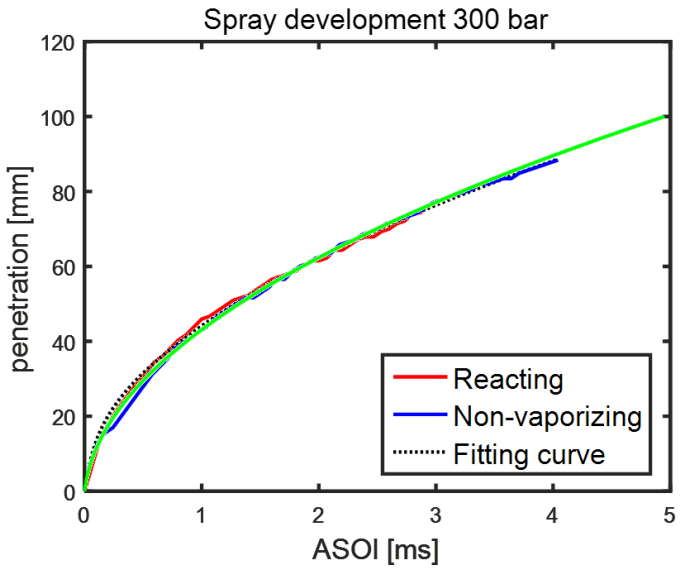

(a) 300 bar injection pressure

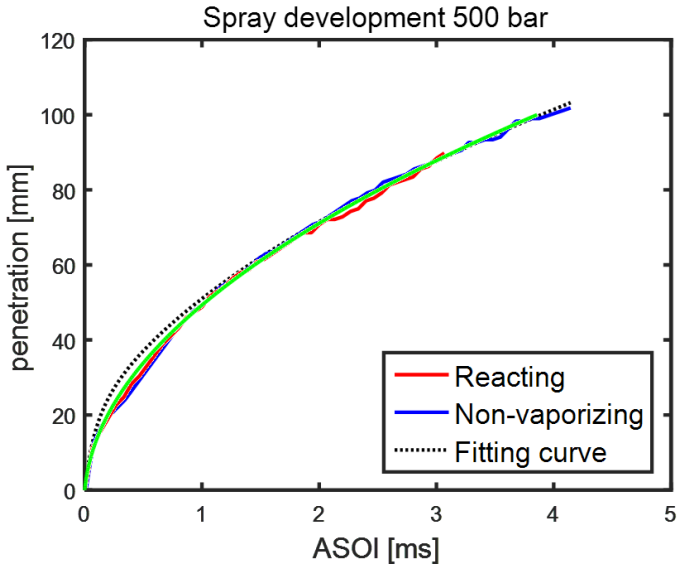

(b) 500 bar injection pressure

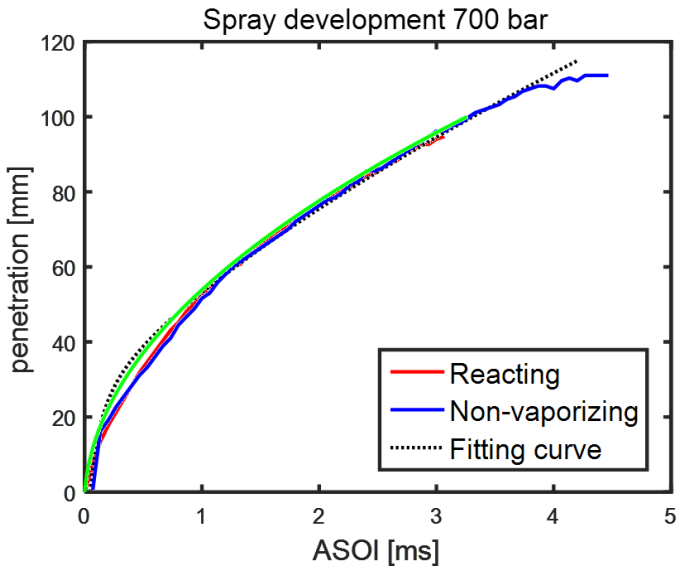

(c) 700 bar injection pressure

Figure 6.5 Penetration length from experiments (Fig. 6.4) and simulation results (green)

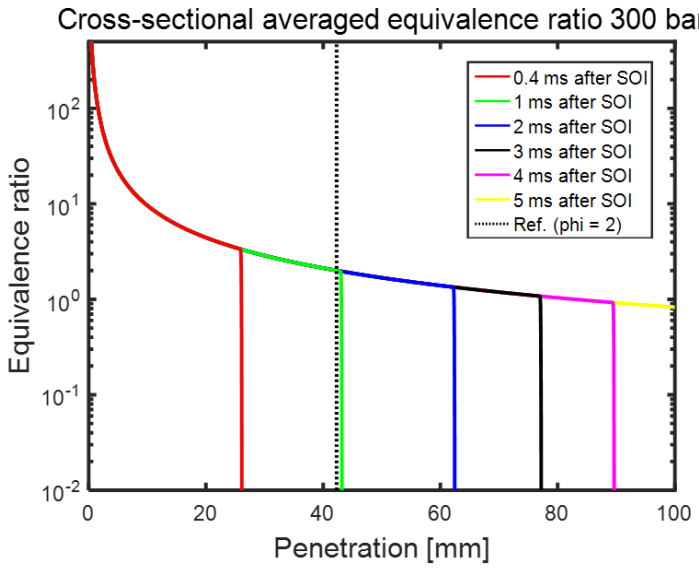

(a) 300 bar injection pressure

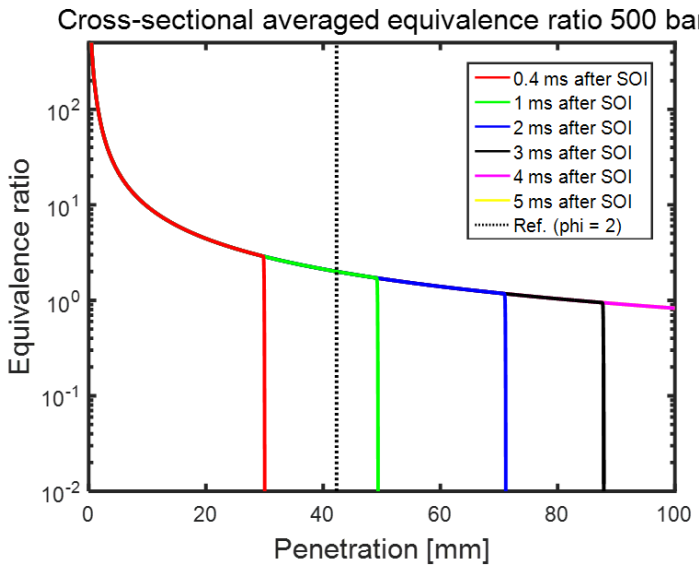

(b) 500 bar injection pressure

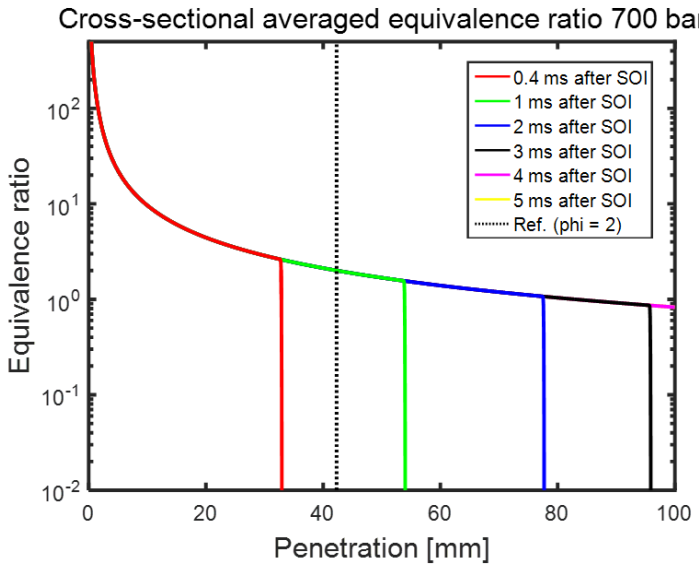

(c) 700 bar injection pressure

Figure 6.6 Cross-sectional averaged equivalence ratio after SOI

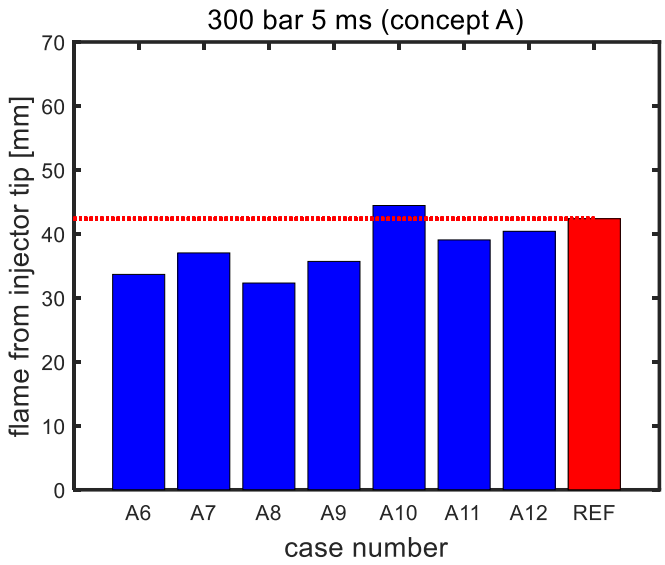

(a) Concept A (7 shots of total 12 shots)

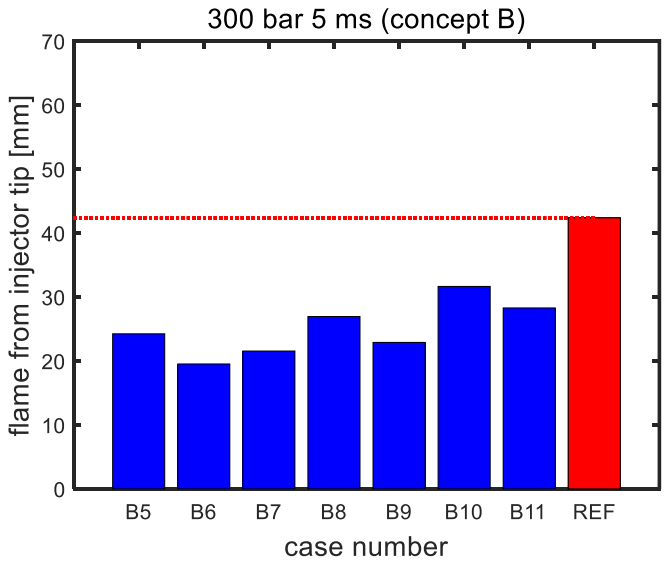

(b) Concept B (7 cases of total 11 shots)

Figure 6.7 Effective flame propagation and reference position (42.3 mm) for 300 bar cases

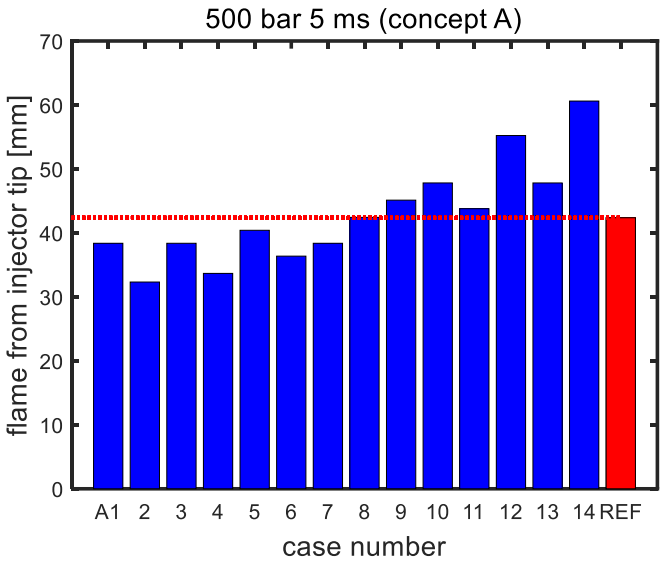

(a) Concept A (all 14 cases)

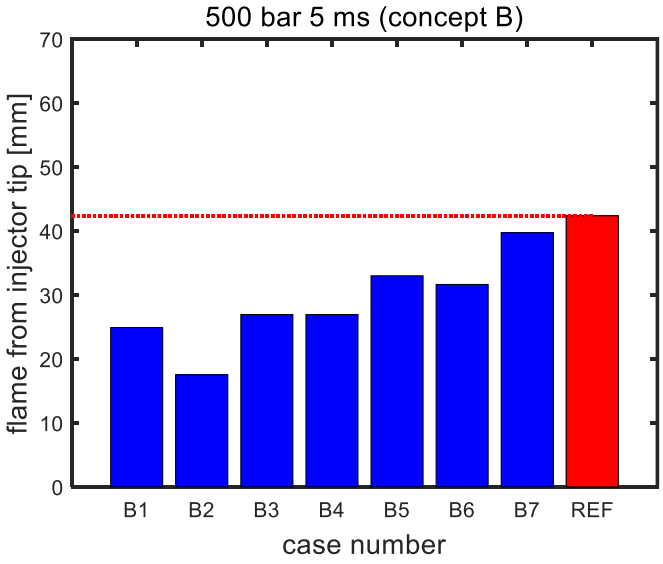

(b) Concept B (all 7 cases)

Figure 6.8 Effective flame propagation and reference position (42.3 mm) for 500 bar cases

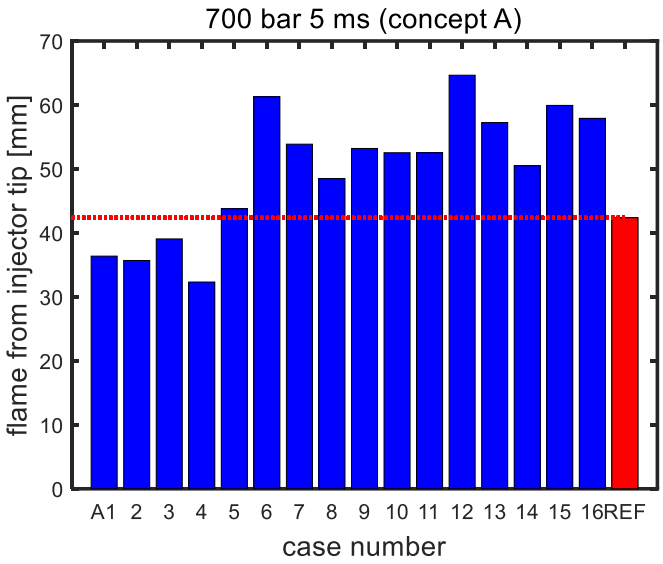

(a) Concept A (all 16 cases)

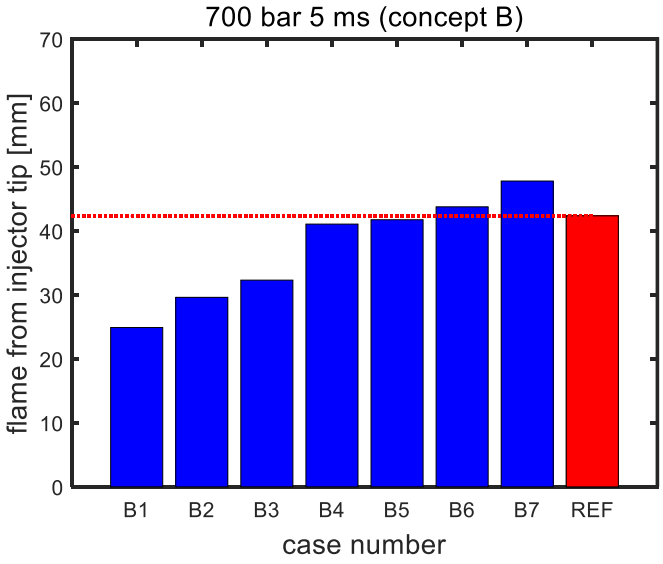

(b) Concept B (all 8 cases)

Figure 6.9 Effective flame propagation and reference position (42.3 mm) for 700 bar cases

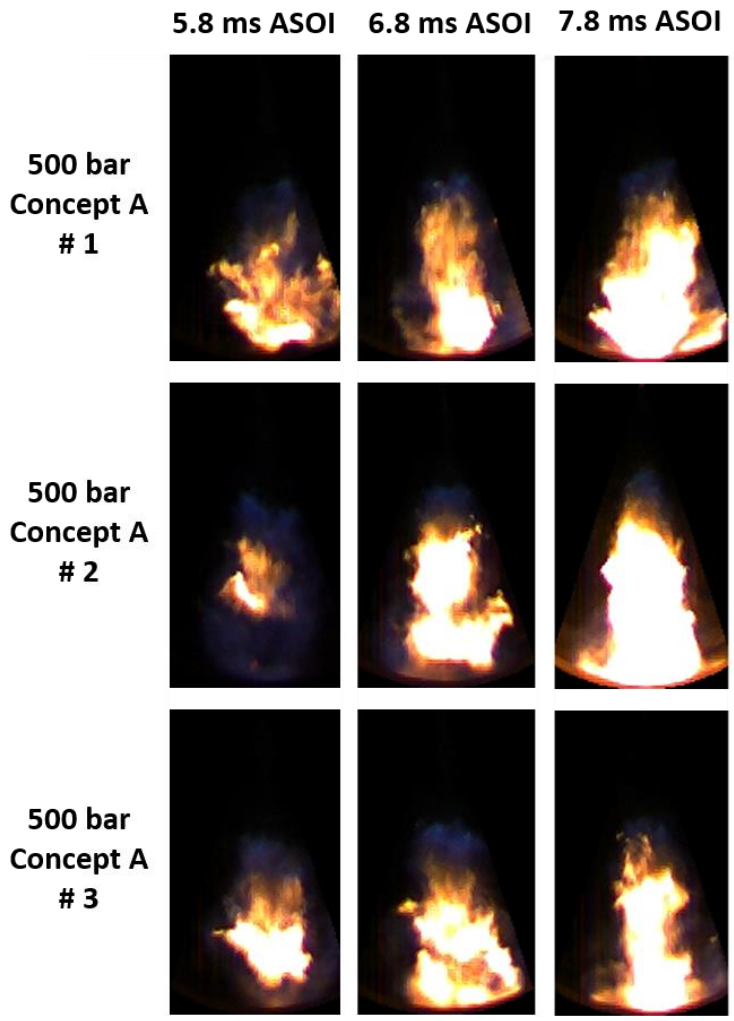

Figure 6.10 Flame with bulk of soot

(Effective flame propagation much lower than 42.3 mm)

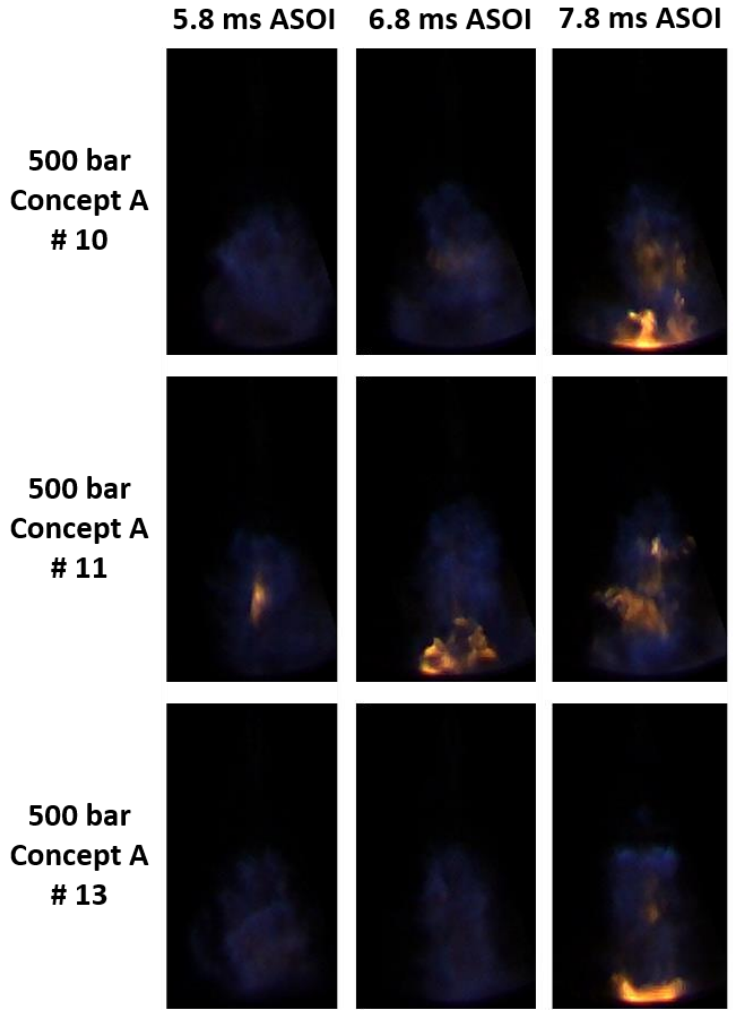

Figure 6.11 Flame with local soot production

(Effective flame propagation little higher than 42.3 mm)

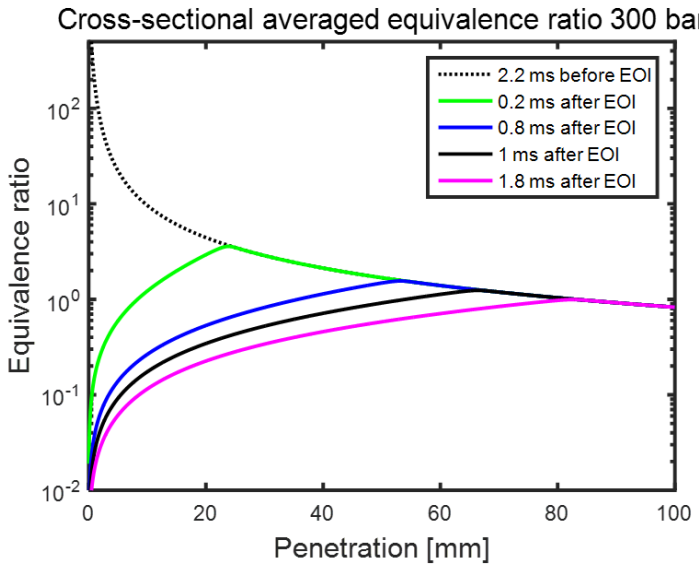

(a) Equivalence ratio after EOI

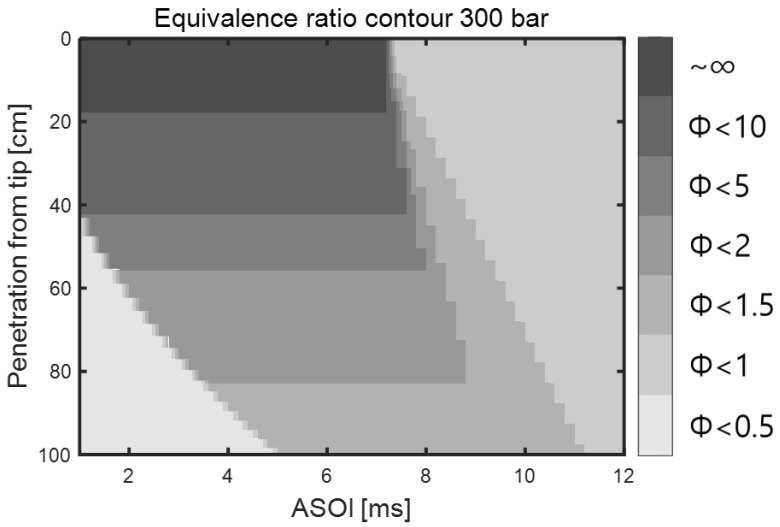

(b) Equivalence ratio contour after SOI

Figure 6.12 Change of equivalence ratio after EOI and equivalence ratio contour ASOI with 300 bar injection

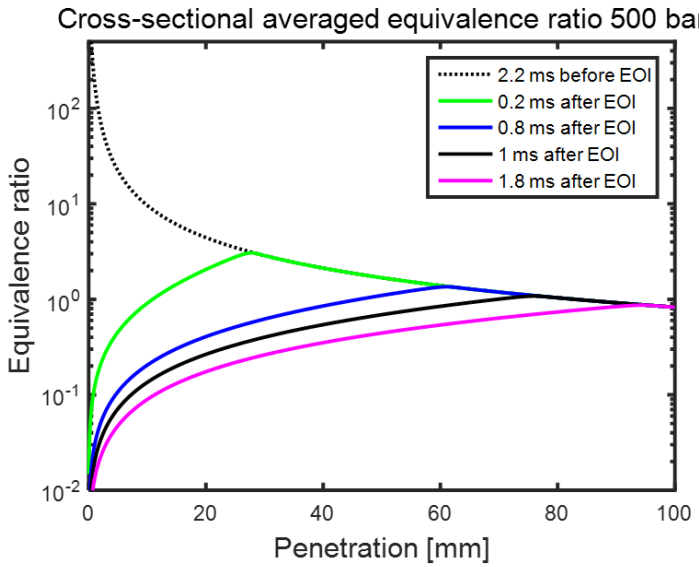

(a) Equivalence ratio after EOI

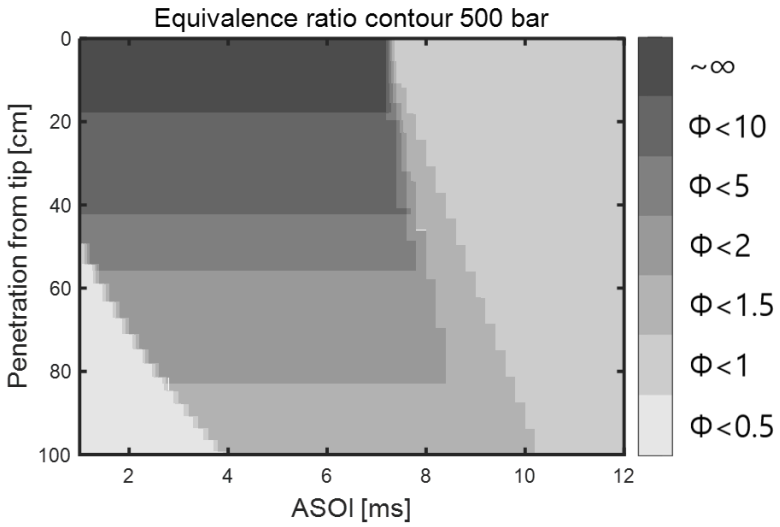

(b) Equivalence ratio contour after SOI

Figure 6.13 Change of equivalence ratio after EOI and equivalence ratio contour ASOI with 500 bar injection

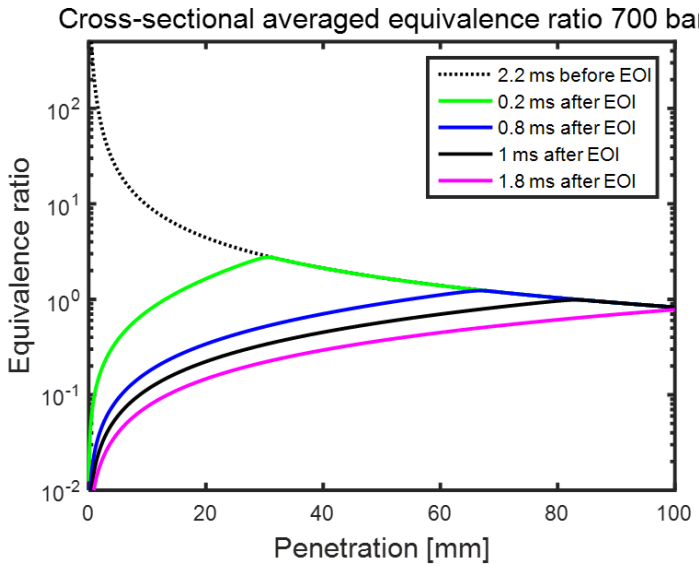

(a) Equivalence ratio after EOI

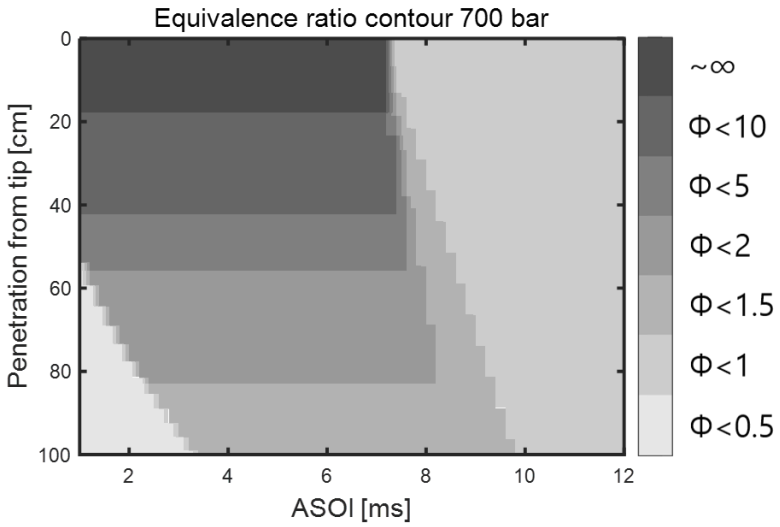

(b) Equivalence ratio contour after SOI

Figure 6.14 Change of equivalence ratio after EOI and equivalence ratio contour ASOI with 700 bar injection

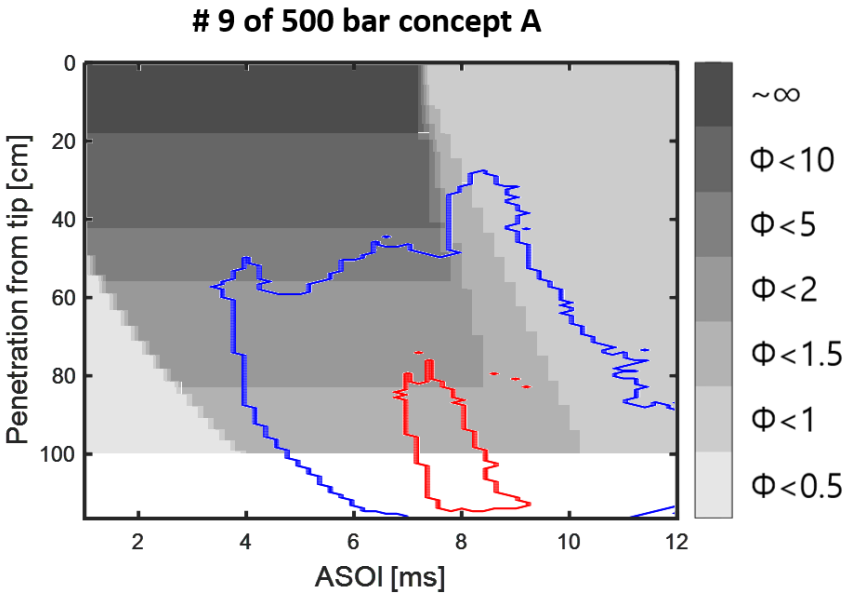

(a) #9 shots of 500 bar concept A

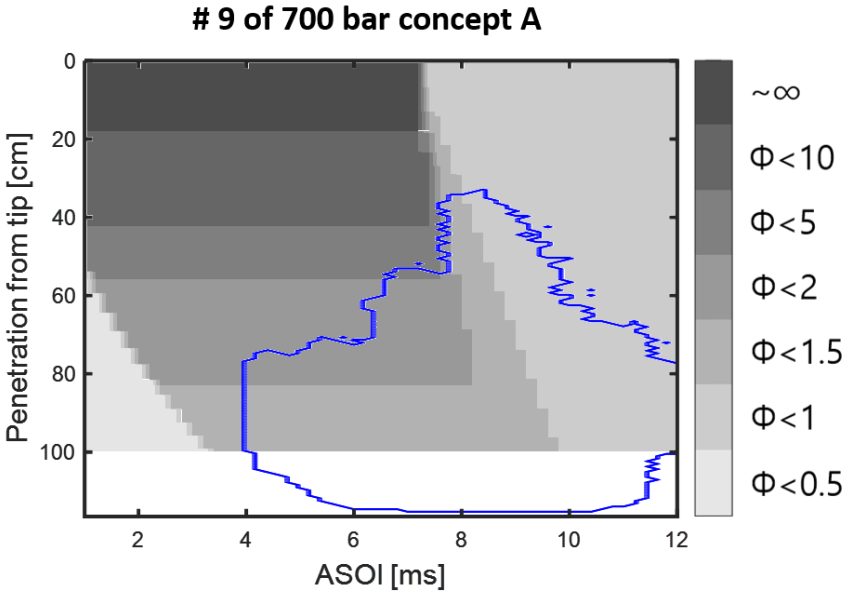

(b) #9 shots of 700 bar concept A

Figure 6.15 Radially averaged intensity on equivalence ratio contour

6.4 Simulation of reacting flow in spray

In previous chapter, it was explained that the as combustion occurs more close to injector whether it is initial combustion or additional auto-ignition, the more soot would be produced. Even at same conditions, there is variation in combustion position and resulting integrated intensity. It was thought that variation in when and where combustion occurs is stochastic behavior and would be determined by variation in thermodynamic state of mixture. Because chamber volume is large enough to cancel out the effect of heat release on pressure, pressure is considered as constant during combustion. Therefore, spatial variation or cyclic variation of temperature was considered as major factor to determine combustion properties. Because of long ignition delay, fuel in downstream zone fairly well mixes with large amount of ambient air. Like homogeneous charge compression ignition where prediction of SOC is quite difficult, auto-ignition of this premixed PRF70-air mixture also can have large variation. Generally, auto-ignition of premixed type mixture is influence by local temperature and occurs in relatively hot spot.

To understand the effect of temperature on soot production, simulation of reacting flow inside the spray was conducted. Initial state of mixture was fixed to thermodynamic state of first control volume. Before this mixture enters the next control volume, air is added to mixture with adiabatic mixing. After mixing with ambient air, chemical reaction progresses while it crosses inside the control volume. Amount of air entrainment added prior to entering control volume is determined by equivalence ratio of each control volume. Equivalence

ratio and time step data came from previous simulation results. Figure 6.16 shows schematic of reacting spray simulation. To evaluate the chemical reactions and thermodynamics properties, Cantera, toolbox for thermo-chemical calculation incorporated in MATLAB, was adopted. To describe the time-evolution of thermodynamic states in control volume, total (3+N) differential equations for pressure, mixture volume, temperature, and masses of N species, are defined as below, and these coupled equations are solved by using MATLAB ode-solver [12, 63]. Temperature of mixture (T_{mix}) was calculated by adiabatic mixing process. (Equation 6.6)

$$mC_p dT + \sum_i \dot{m}_i u_i + PdV = 0 \qquad \text{(EQ. 6.4)}$$

$$\dot{m}_i = \ MW_i[\dot{N}_i]V \qquad \text{(EQ. 6.5)}$$

$$\int_{T_{mix.(i+1)}}^{T_a} C_{p.a} dT = (fuel - air \ \ ratio) \int_{T_{mix.i}}^{T_{mix.(i+1)}} C_{p.f} dT \qquad \text{(EQ. 6.6)}$$

$[\dot{N}_i]$ (kmol/$m^3 \cdot s$) is the rate of mole concentration change and MW_i (kg/kmol) is molecular weight of each species.

To reflect on the reactivity of primary reference fuel, full PRF mechanism, including 1034 species and 7558 reactions was adopted. This mechanism was introduced by combining normal heptane and isooctane mechanisms from Lawrence Livermore National Laboratory [64]. Like in experiments, fuel in simulation was composed of isooctane and normal heptane with volumetric

ratio of 70:30.

As explained above, it is expected that temporal or spatial variation of temperature can make stochastic behavior. It was verified that temperature distribution exists along the penetration by temperature measurements. Figure 6.17 shows ambient temperature distribution used in reacting simulation. As shown in figure, full penetration length 100 mm was divided three zones. The upstream zone near injection and the downstream zone near opposite wall have temperature variation, and central zone has constant temperature. It was assumed that temperature of air-fuel mixture in first control volume was fixed to 840 K.

Figure 6.18(a) and (b) shows temperature profiles with 300 bar injection pressure as function of ASOI and penetration length, respectively. It is verified that there are three major stages in plot, mixing dominant stage, first ignition stage and second ignition stages. In mixing dominant stage, mixture temperature is determined by ambient air temperature. If ambient temperature is higher than 840 K, mixture temperature becomes increases slightly and vice versa. First ignition stage called low temperature combustion is represented by small heat release. In this stage, fuel spices are partially oxidized and prepare for next stage. First ignition stage is also known as cool flame shown in shadowgraph image in chapter 5. Finally, in second ignition stage called high temperature combustion, temperature rapidly increases with large amount of heat release. During this stage, fuel components and oxygen are consumed with exothermic reaction and produce final product like H_2O and CO_2.

Each stage is also well explained by speciation results as shown in Figure

6.19. Fig. 6.19 shows change of species relative to initial total mass. During mixing dominant stage, amount of air in mixture continue to increase because of air entrainment and temperature slightly changes. In first ignition stage, fuel begins to be consumed and partially oxidized. As evidence of cool flame, change of CH_2O is also plotted. During first stage ignition, other small UHC species accumulates as well as CH_2O. Finally, when combustion reaches last stage, oxygen and remained fuel including CH_2O are drastically consumed and results in high temperature rise.

As shown in Fig. 6.18, there are variation in ignition timing or location. With 300 bar injection pressure, ignition occurs between 50 and 70 m except two cases. It means combustion is influenced by temperature of upstream and central zone. When mixture travel in upstream zone, temperature slightly increases or decreases depending on ambient temperature, and it makes difference in low temperature combustion and following high temperature combustion. As shown in figures, earlier low temperature combustion leads to earlier high temperature combustion. It means there is no negative temperature coefficient effect in this simulation. Figure 6.20 shows correlation between low temperature combustion and high temperature combustion. Two combustion stages are linearly connected and it means that if low temperature combustion is determined, high temperature combustion would be determined dependently. Namely, occurrence of high temperature combustion is mostly influenced by low temperature combustion regardless of temperature distribution. To understand the temperature effect of each zones, additional three simulations were conducted. Each simulation has temperature variation in only one zone.

Ambient temperature profiles and corresponding combustion temperatures are shown in Figure 6.21 and 6.22. Injection pressure was fixed to 300 bar. For example, first simulation in Fig. 6.22 shows combustion temperature with only temperature variation in upstream zone. In this case, there are large variation in low temperature and high temperature combustion. It means that variation in low temperature combustion leads to variation in high temperature combustion. If temperature variation exists only in central zone, high temperature combustion is slightly affected. Locations of low temperature combustion are almost same even with different central temperature. And temperature in downstream zone has no effect on combustion location. Consequently, temperature in front of injector tip has dominant effect on low temperature combustion. Moderate temperature variation near injector tip could leads to significant variation in main combustion behavior, especially for low octane fuel. From the results, it is expected that relatively large variation in upstream zone is responsible for variation in experimental results

Figure 6.23 shows temperature profiles with 500 bar injection pressure. From the comparison with 300 bar injection cases, it can be found that there is apparent difference between two injection pressure cases. Here, for 700 bar injection pressure, combustion locations get out of full penetration scale for most of cases. Thus, analysis of reacting simulation was focused on only 300 bar and 500 bar injection cases.

First difference is timing of second stage ignition can be regard as ignition delay. Combustion or second ignition stage of 500 bar injection has occurs at much farther penetration location. As inferred from visualization data, it can be

simply understood that high momentum leads to long travel length before combustion. As explained in previous paragraph, ignition of 300 bar injection pressure is influenced by temperature of upstream and central zone. In contrast, case with 500 bar injection condition has ignition location more than 70 mm. Two cases with longest ignition delay get out of full penetration range 100 mm, considered as combustion does not occur. After mixture passes the central zone, mixture enters the downstream zone with lower ambient temperature. As indicated by vertical dashed line in Fig. 6.18(a) and 6.23(a), residence time in central zone is shorter for 500 bar injection pressure. However, for 300 bar injection cases, mixture continues to stay in central zone until start of combustion. Thus, it can be expected that low temperature of downstream zone begins to have effect on chemical reaction. However, like 300 bar injection cases shown in Fig. 6.22, effect of temperature variation in downstream zone is much smaller than that of upstream and central zone. It is clearly shown in combustion temperature with constant temperature. As shown in Fig. 6.25, main combustion or high temperature combustion is much delayed with high injection pressure even at constant temperature condition (blue arrows). First ignitions occur almost same timing or distance; however, second ignition is more delayed for 500 bar injection pressure. It means that high injection pressure lead to longer ignition delay than low injection pressure even at same constant temperature condition. This effect of injection pressure can be supported by equivalence ratio effects. Changes of equivalence ratio along to penetration can have effect on ignition timing. Even for conditions of constant temperature, 500 bar injection pressure has longer ignition delay rather than

300 bar injection pressure. Different ignition delay in same ambient temperature can be explained by only difference in equivalence ratio. In general, fuel-rich mixture has short ignition delay rather than relative lean mixture. Exemplary data of ignition delay is shown in Figure 6.26. The increase in ignition delay becomes larger per unit decrease in equivalence ratio. As shown in predicted equivalence ratio (Fig. 6.6), mixture becomes lean as it moves to downstream region. From predicted equivalence ratio and ignition delay data, it can be known that as mixture penetrates more distance, equivalence ratio decreases and reactivity of mixture rapidly decreases. Low equivalence ratio resulted from long penetration makes the ignition more difficult. Equivalence ratio effect is valid for not only constant temperature distribution cases but also other variable temperature distribution.

In summary, temperature near the injector tip has significant effect on main combustion timing or location. Because high temperature combustion or main combustion is linearly connected to precedent low temperature combustion, timing or location of low temperature is dominant factor in this condition. From the additional results, low temperature combustion is almost determined by first zone temperature. And equivalence ratio always effects on main combustion event. In constant temperature distribution, equivalence ratio is only factor to determine ignition delay, however, with variable temperature distribution, ambient temperature and equivalence ratio have effect on ignition delay simultaneously. Especially, as mixture moves to downstream, equivalence ratio and ambient temperature continues to decrease, and it make auto-ignition more difficult. Indeed, effect of equivalence ratio is much significant than

temperature of downstream.

Second difference is that high injection pressure has large variation in second stage ignition. Intervals between second ignition timings are wider in 500 bar injection pressure, indicated by red arrows in Fig. 6.25. In previous paragraph, it was mentioned that decrease of equivalence ratio by long penetration makes auto-ignition more difficult. Figure 6.27 derived from Fig. 6.18 and 6.23 shows how ignition time delayed according to injection pressure change. It is verified that cases with late ignition timing in 300 bar injection pressure would be more delayed rather than case with early ignition timing when injection pressure increases. For example, red line having relatively long ignition delay with 300 bar injection is delayed about 1.12 ms when injection pressure increases to 500 bar, but, 0.75 ms for magenta line. Magnitude of increase in ignition delay is not same for each condition. Increase in ignition delay with increased injection pressure is relatively bigger for conditions with longer ignition delay or low upstream zone temperature. Thus ignition gaps between temperature profiles increase when injection pressure increases. This results shows that as injection pressure increases, possibility of large variation in ignition timing or location also increases.

Additional reacting flow simulation with normal heptane was conducted for comparison. Normal heptane is considered as surrogate fuel to simulate diesel fuel. Equivalence ratio was predicted by using same process with PRF70 and reaction was calculated by basing on that equivalence ratio results. Temperature profiles of normal heptane are shown in Figure 6.28. To compare the two fuels, results of PRF70 are replotted on same figures. It is clearly shown

that normal heptane has shorter ignition delay and smaller variation in ignition timing rather than PRF70. When injection pressure increase to 500 bar, ignition delay and variation increases; however, they are much smaller than those of PRF70. From theses comparisons, it is confirmed that PRF70 fuel can have large variation in combustion timing or location rather than high reactivity fuel. On the contrary, normal heptane has little variation though there are ambient temperature distribution. This behavior more clearly shown in high injection pressure condition.

From the figures, it is verified that there can be large variation in ignition timing by temperature variation. Especially, temperature of upstream zone determines initial temperature of mixture before first stage ignition. For three constant temperature variations, temperature difference of 40 K can make difference in ignition timing about 1 ms or difference in ignition location about 15 mm. If injection pressure increases to 500 bar, these differences also increase to 1.5 ms and 20 mm. In real combustion, because there exists heat transfer by conduction or soot radiation from reaction zone, temperature distribution can be changed and makes following ignition of unburned mixture more complicated. Separated reaction zone like in concept B can be induced by heat transfer from early combustion.

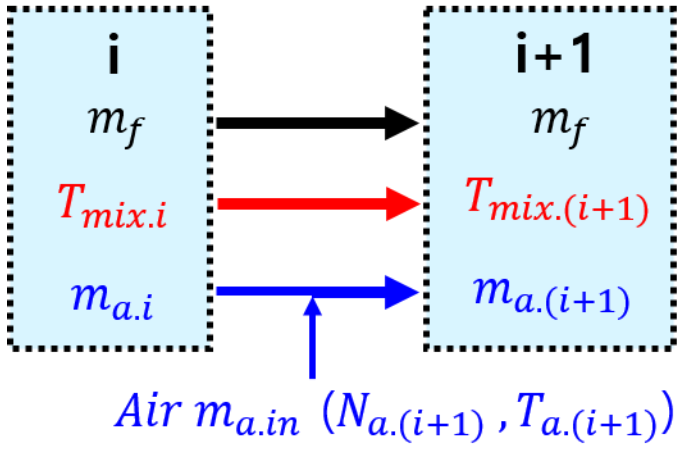

Figure 6.16 Mixture state calculation in reacting flow simulation

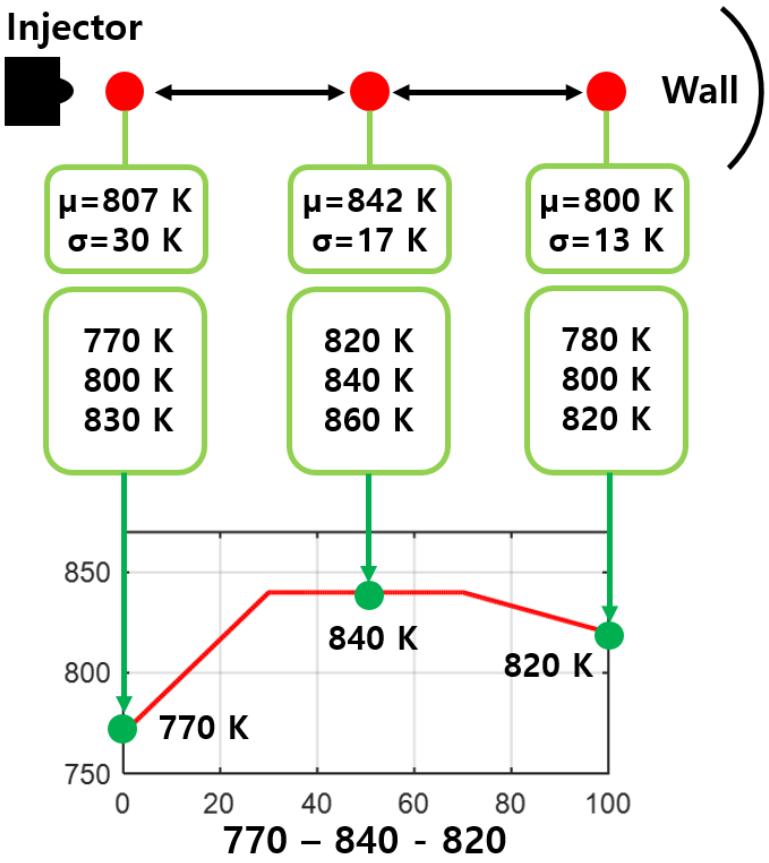

(a) Temperature profiles along the penetration axis in simulation

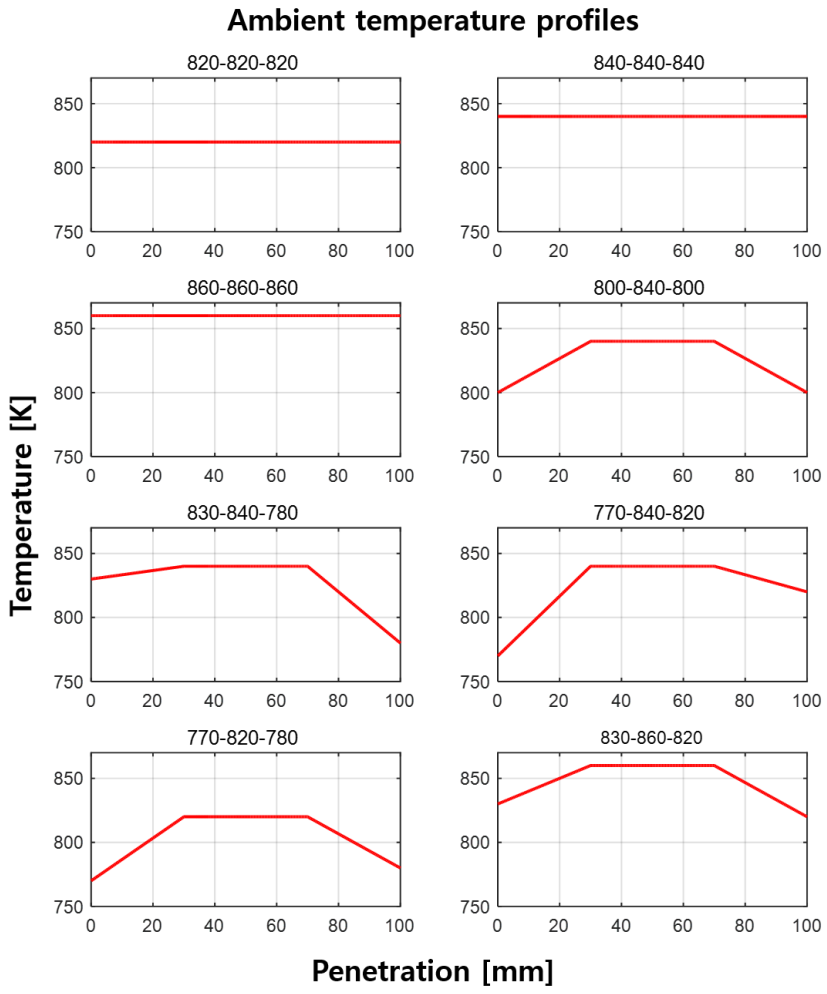

(b) 8 representative temperature profiles for reacting simulation

Figure 6.17 Ambient temperature for reacting simulation

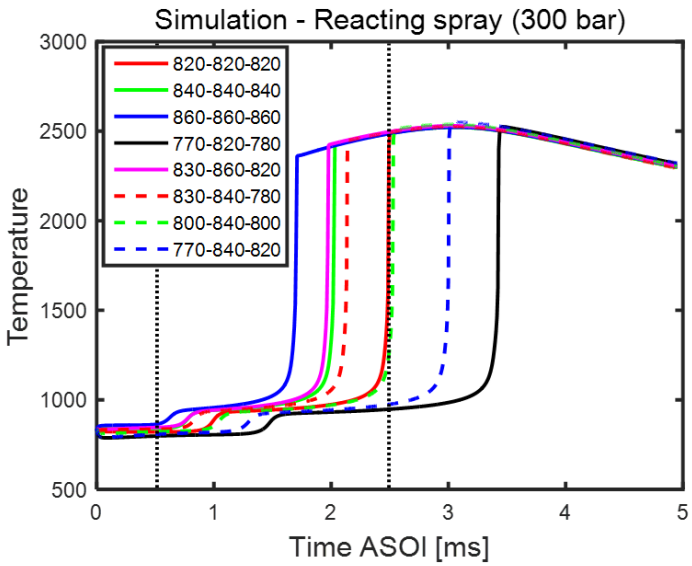

(a) Temperature profiles versus time

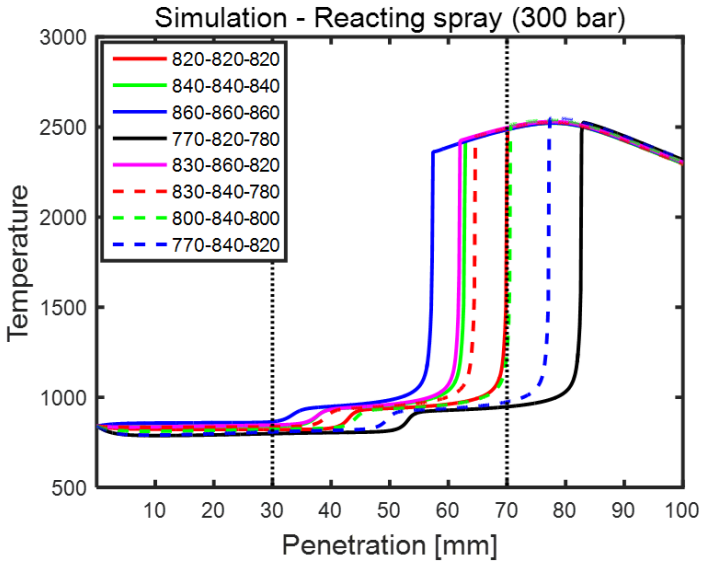

(b) Temperature profiles versus penetration

Figure 6.18 Combustion temperature during reaction process

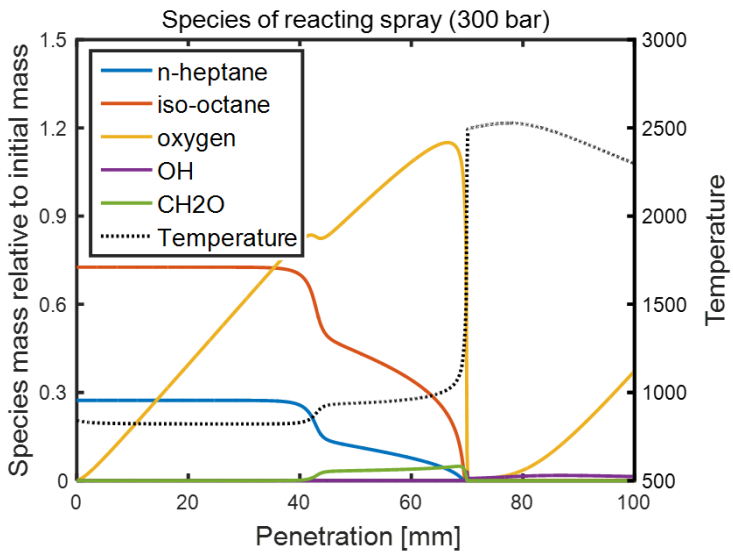

Figure 6.19 Mass of species during reaction process

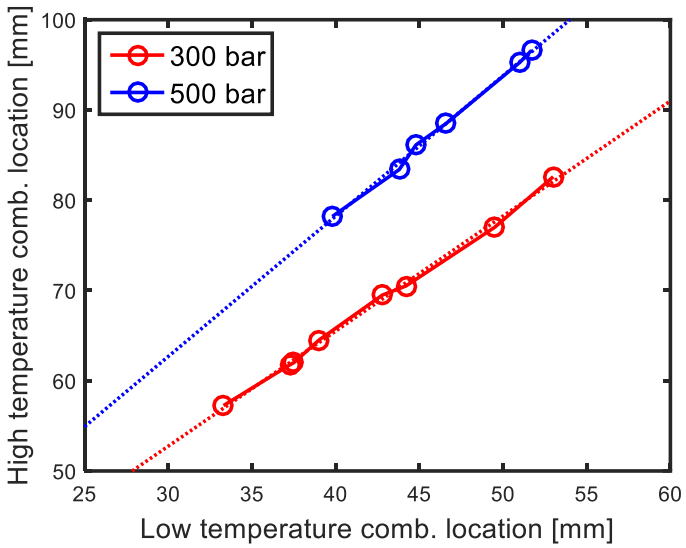

(a) Penetration domain

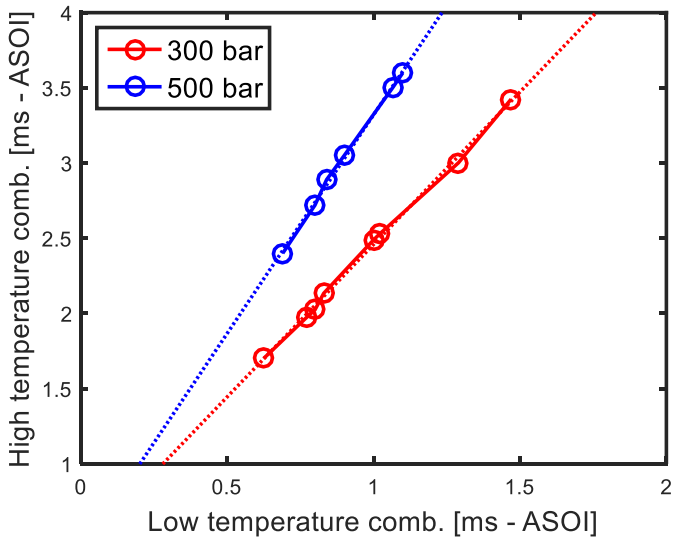

(b) Time domain

Figure 6.20 Relation between high temperature combustion and low temperature combustion

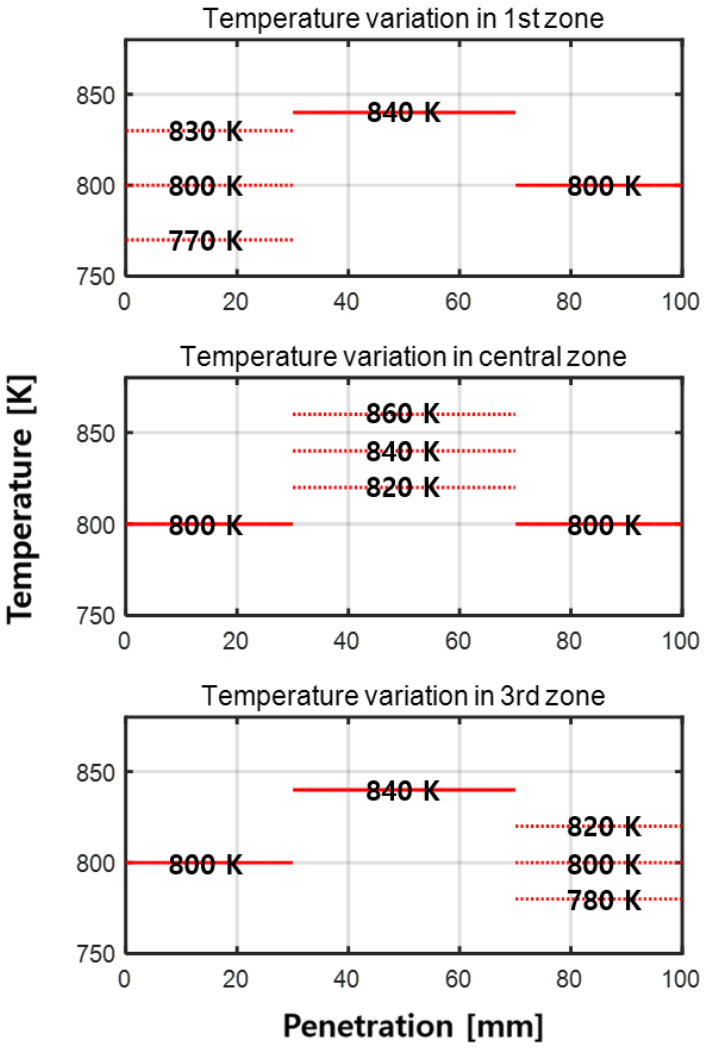

Figure 6.21 Temperature profiles to elucidate the effects of temperature of each zone

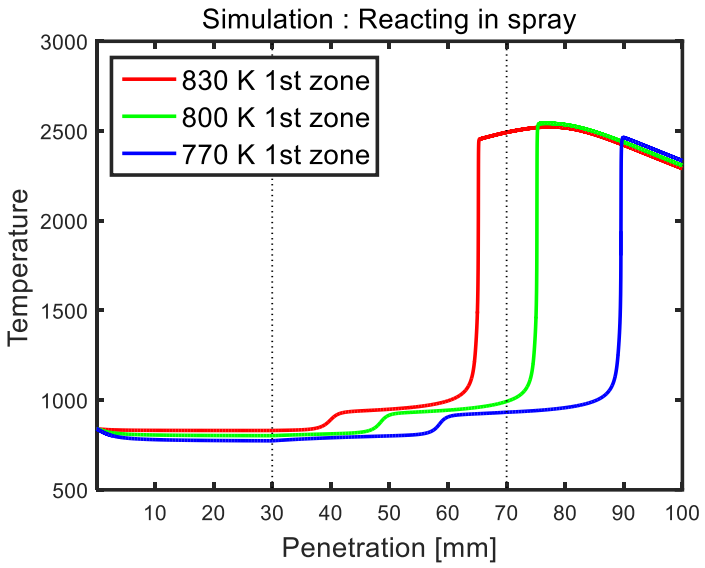

(a) Temperature variation in upstream zone

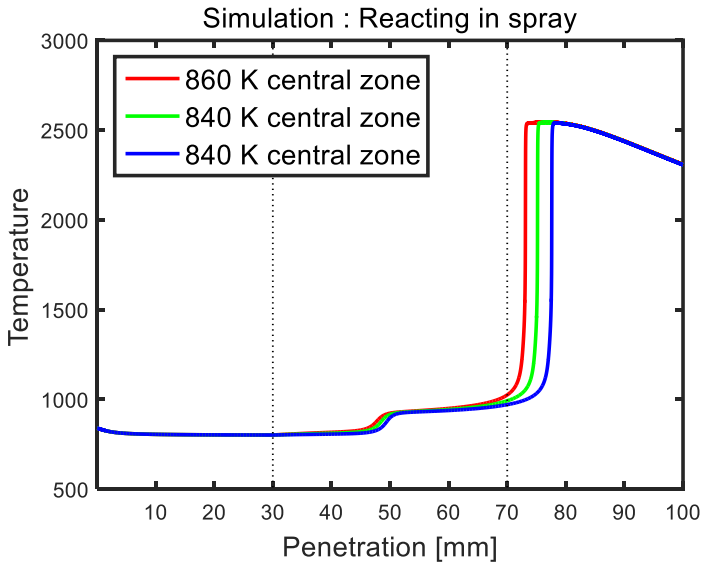

(b) Temperature variation in central zone

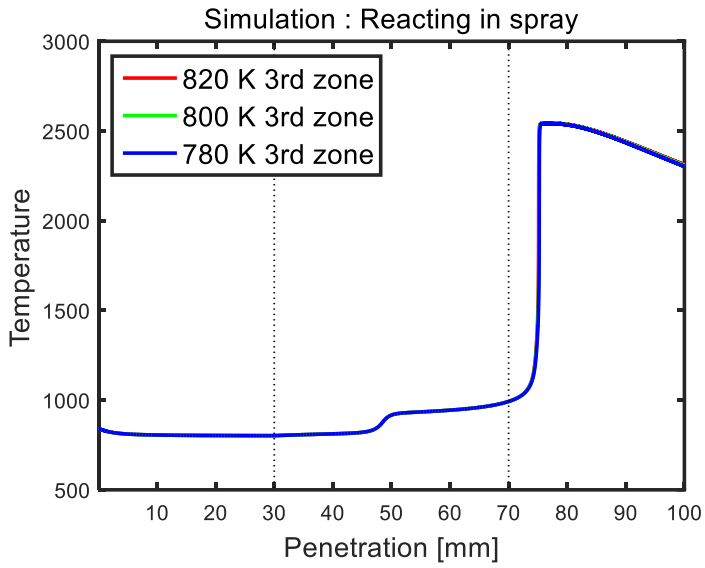

(c) Temperature variation in downstream zone

Figure 6.22 Effects of temperature of each zone on combustion

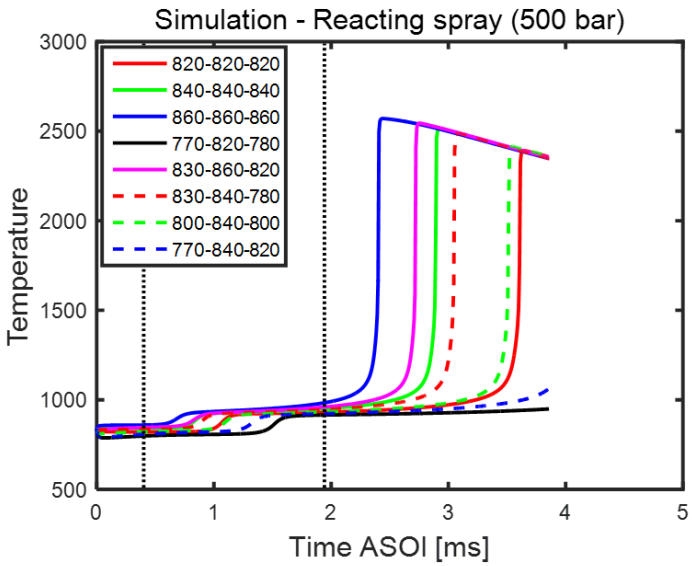

(a) Temperature profiles versus time

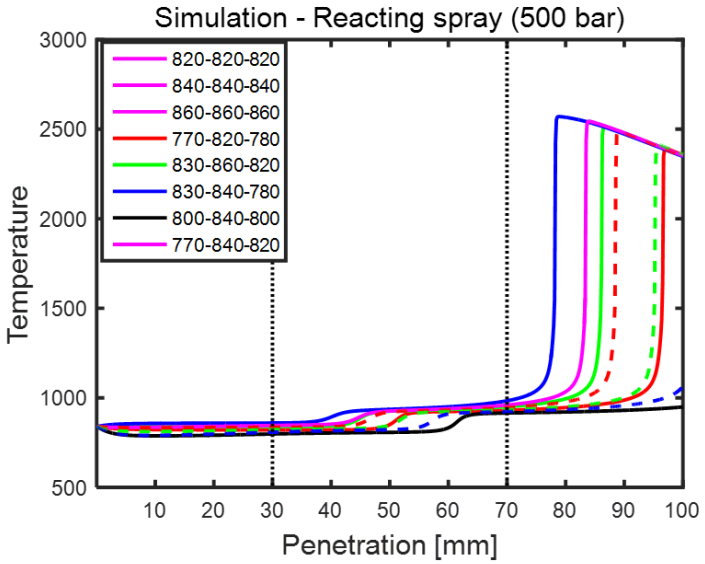

(d) Temperature profiles versus penetration

Figure 6.23 Combustion temperature during reaction process

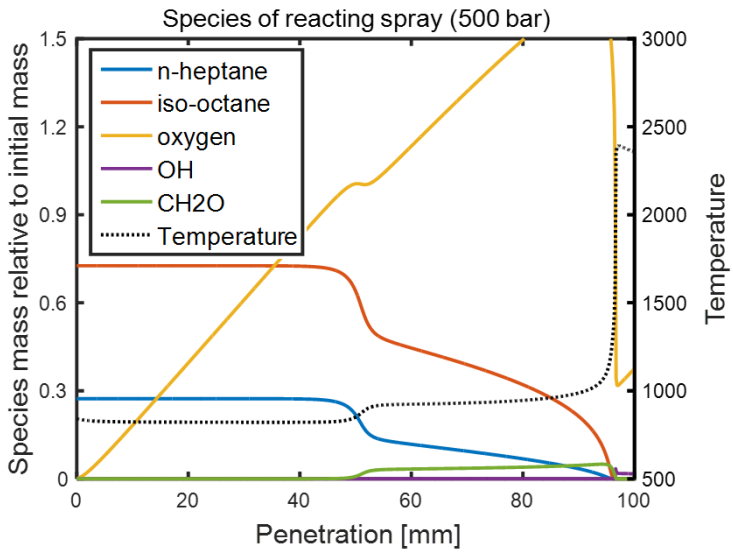

Figure 6.24 Mass of species during reaction process

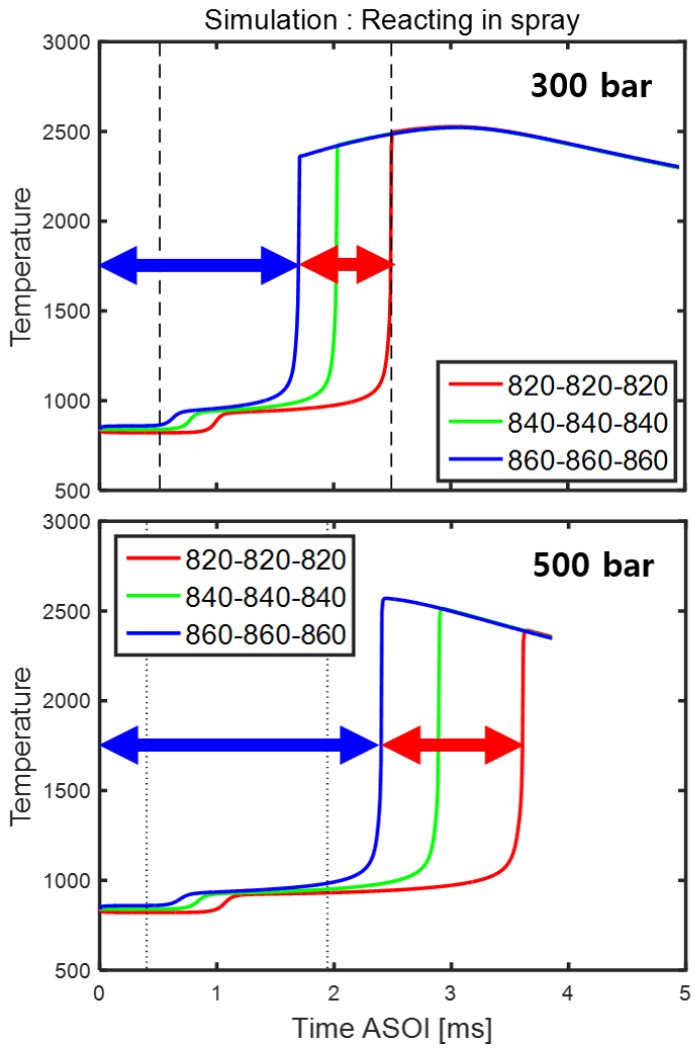

Figure 6.25 Combustion temperature with constant ambient temperature profiles

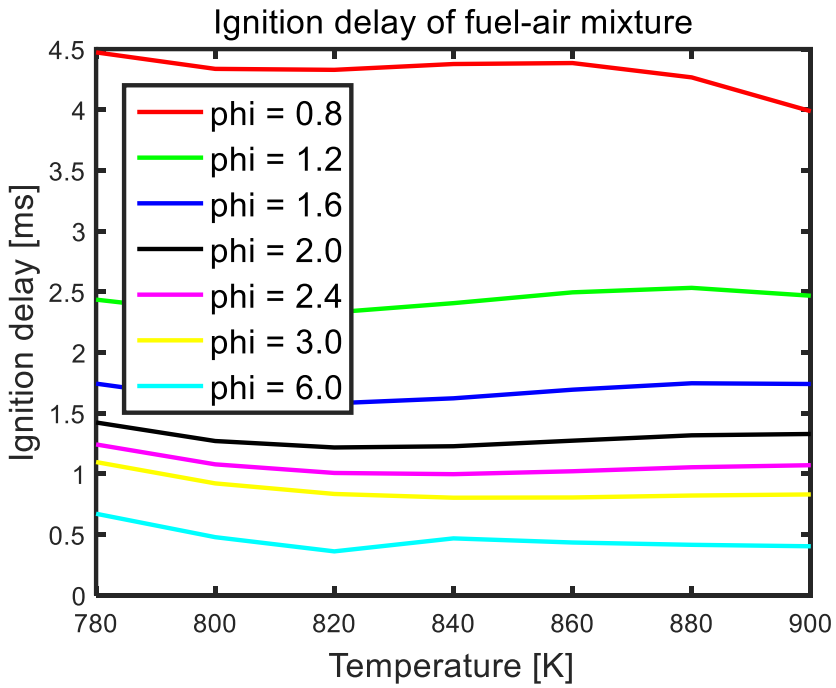

Figure 6.26 Ignition delay of PRF70 with various equivalence ratios

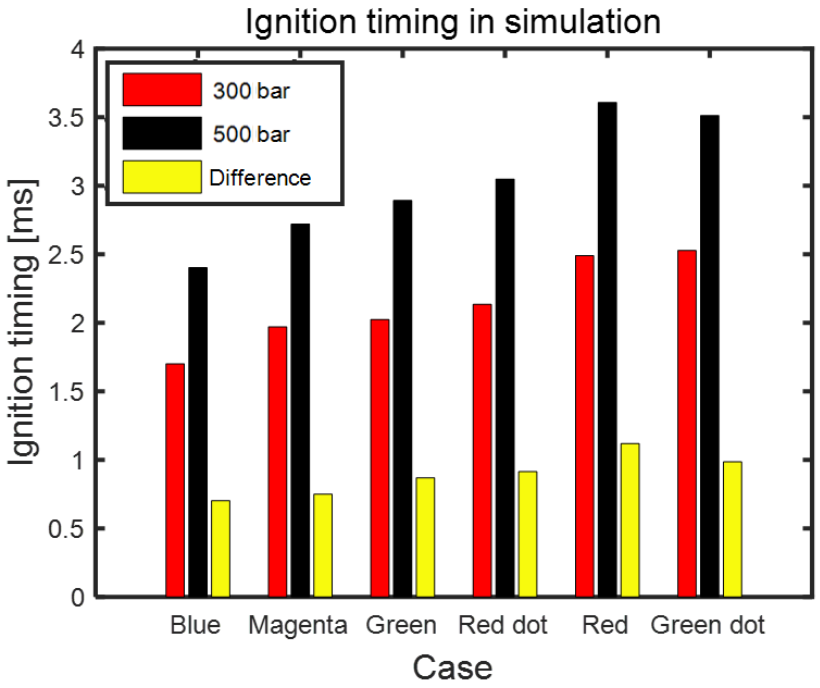

Figure 6.27 Change of ignition timing by injection pressure change

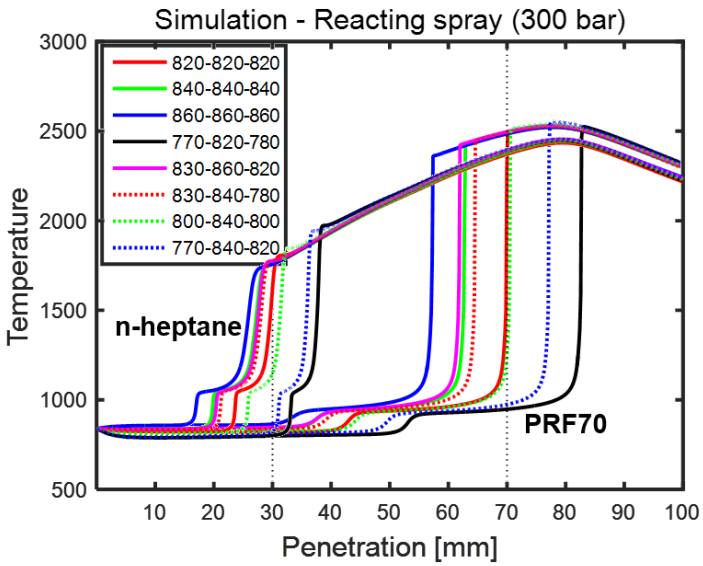

(a) Temperature profiles versus time

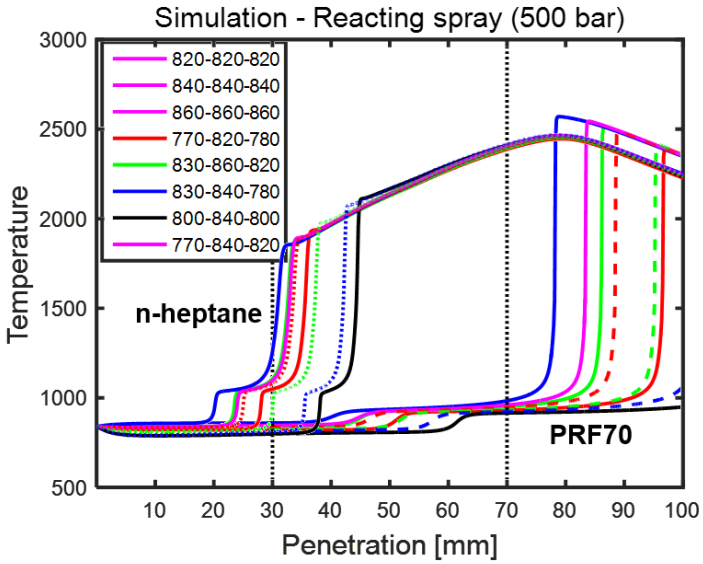

(e) Temperature profiles versus penetration

Figure 6.28 Comparison of PRF70 with normal heptane

6.5 Summary

In this chapter, spray or flame characteristics observed in experiments results was explained by one dimensional penetration model. Model reflects both uniform velocity model and discrete control volume model. From equivalence ratio prediction, it was verified that flame propagation during injection period has effect on soot production. This result is well matched with precedent researches about relation of lift-off length and soot production [17, 55, 56, 57, 65].

To understand the stochastic behavior, reacting spray model using chemical kinetics mechanism was developed. Using predicted equivalence ratio, air entrainment was calculated for fixed fuel mass. From the results, it is confirmed that non-uniform temperature distribution determines first and second ignition. Even at uniform temperature distribution, decrease of equivalence ratio makes traveling mixture more difficult to be auto-ignited. In contrast to PRF 70, normal heptane shows much shorter ignition delay and resultant variation in ignition timing is much smaller than that or PRF 70. It is certain that low octane fuels which have long ignition delay rather than diesel fuels have possibility of high variation in combustion behaviors. To reduce the variation in ignition timing with fixed injection pressure, temperature should be well regulated along the penetration axis.

Chapter 7. Suggestion of combustion model and final conclusion

7.1 Suggestion of new conceptual model

From visualization experiments and computational study, conceptual model which describes combustion behavior of PRF70 is achieved. Figure 7.1 and 7.2 show schematic of conceptual model suggested through the present work.

Right after start of injection, liquid and vapor phase are separated. In 0.2 ms ASOI, liquid length is saturated and vapor zone continues to move forward. Before high temperature combustion, cool flame or first stage ignition occurs, indicated by gray region. Cool flame in fuel spray is realized as sudden change of spray head to transparent in shadowgraph images. During cool flame, partially oxidized species exist like CH_2O and H_2O_2. About 3 ms ASOI, high temperature combustion occurs in downstream zone with premixed flame form. Number of first ignition points can be more than two. Several small combustion zones are united into one combustion zone, and radially expands. According to visualization tests, there are two types in PRF70 combustion. First, in concept A, flame developed with radial expansion of initial combustion zone. However, in concept B, additional auto-ignition occurs in upstream region, few moments after initial combustion. As show in Fig. 7.1, concept A follows left stream at turning point and concept B follows right. In concept B, because of auto-ignition in upstream, soot is produced earlier than concept A. Finally, flame

with intensive soot from additional auto-ignition and radially expanded initial combustion zone meet and make singular diffusive flame. In concept A, there is another subordinate feature. As shown in Figure 7.2, there is also case without bulk of soot production, because flame does not propagate to upstream enough

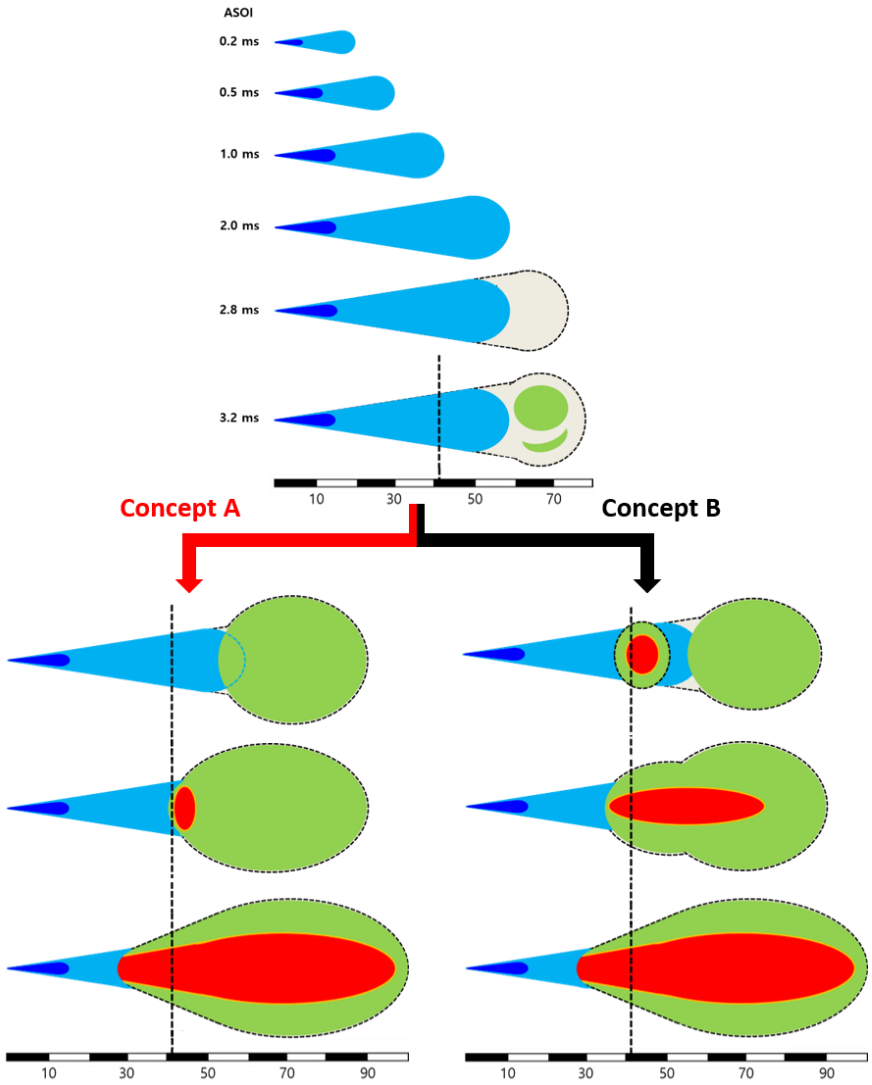

Figure 7.1 Conceptual model for PRF70 spray combustion

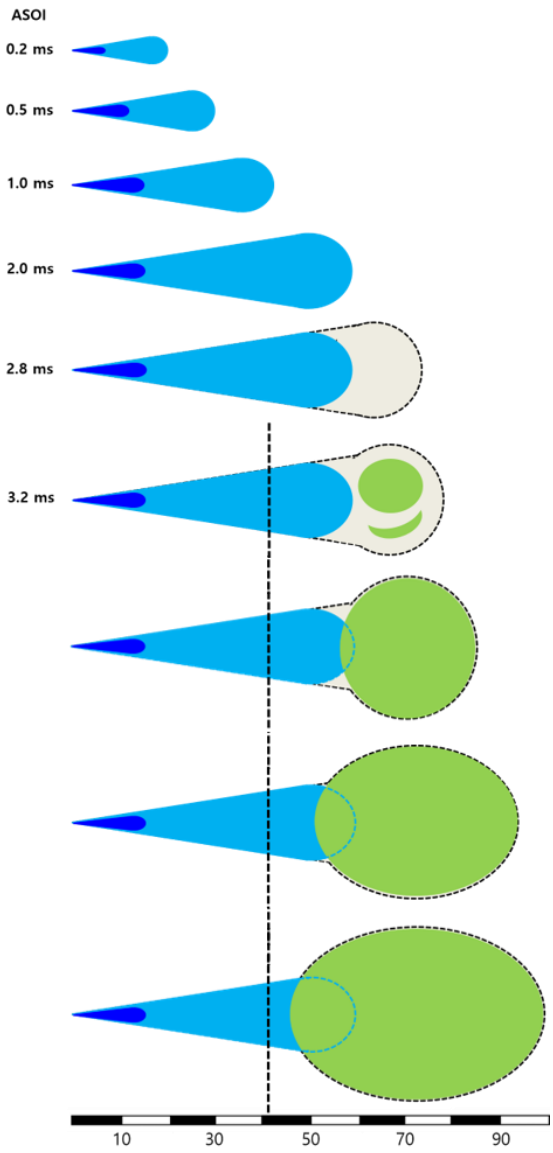

Figure 7.2 Conceptual model for PRF70 spray combustion without soot

7.2 Final conclusion and summary

As a pilot research for gasoline compression ignition, fundamental study to understand combustion of low octane fuel was conducted by using primary reference fuel with octane number 70. By injecting fuel to constant volume chamber, basic properties of fuel spray were measured.

Firstly, PPCI operation regime based on natural luminosity. From the operation regime, it was clearly shown that as injection duration increases or injection pressure decreases, combustion mode shifts to non-premixed zone with high intensity. Regime can be divided to 'premixed combustion' and 'partially premixed combustion' zone. Combustion characteristic of premixed zone is similar with that of low temperature combustion. However, partially premixed combustion zone is different to conventional diesel flame though it has intensive soot production. Because combustion start at more downstream region rather than diesel, flame development is unusual.

To understand this interesting behavior, (filtered) natural luminosity visualization and shadowgraph technique were applied simultaneously to visualize spray development and soot production. By separating blue and red components in natural luminosity images, it can be confirmed that premixed flame with blue signal occurs spontaneously and propagates both upstream and downstream direction. As initial combustion occurs more close to injector tip, flame propagates more close to tip and resultant soot production increases. Sometimes, there is additional auto-ignition in upstream, few moments after SOC. In this case, soot production is determined by location of additional auto-

ignition. From averaged radial averaged intensity, it was shown that there is high correlation between flame intensity, soot production, location of initial combustion, maximum flame propagation and additional auto-ignition.

From shadowgraph images taken simultaneously with natural luminosity images, radial expansion of initial combustion zone can be confirmed. Combining with Mie-scattering signal from liquid phase, spray development before combustion is well understood. Saturation of liquid length and cool flame can be shown in combined images.

To understand more detailed about thermodynamic state inside the spray region, validated one dimensional penetration model was developed. Empirical values were obtained from visualization tests and all values are fixed to the same condition with experiments. From equivalence ratio prediction, it was verified that flame propagation during injection period has influence on soot production. Additionally, reacting spray using chemical reaction mechanism was conducted. Results of this simulation give information of stochastic behavior in spray region. Non-uniform temperature in chamber can leads to difference of ignition delay, especially, temperature near the injector tip has significant effect on main combustion. Not only temperature, but also equivalence ratio has effects on ignition delay. In spray, because mixture becomes leaner as it travels to downstream, mixture in downstream has long ignition delay. Comparing with simulation of normal heptane, it is verified that gasoline-like fuel including low octane fuel has possibility of high variation in combustion behaviors.

In contrast to convention definition of PCI or PPCI where injection has to

be completes before SOC, long injection duration also leads to moderated premixed flame without intensive soot signal. If propagation of premixed flame to upstream direction is restricted by applying a well regulated ambient condition not to pass the threshold position, soot cannot be produced even at long injection duration. Indeed, in operation regime of Fig. 3.6, cases with injection pressure over 800 bar hardly show soot signal even at much longer injection duration. Because main combustion occurs enough downstream region to assures that flame cannot propagate to threshold in finite time.

Reference

1. Hairuddin, A. A., Wandel, A. P., & Yusaf, T. (2014). An introduction to a homogeneous charge compression ignition engine. Journal of Mechanical Engineering and Sciences, 7, 1042-1052.
2. Gardner, R., The Outlook for Energy: A View to 2040, 2012.
3. World Energy Council (WEC). Global transport scenarios 2050. London: WEC, 2011
4. Kosaka, H., Aizawa, T., & Kamimoto, T. (2005). Two-dimensional imaging of ignition and soot formation processes in a diesel flame. International Journal of Engine Research, 6(1), 21-42.
5. Heywood, J., Internal combustion Engines, McGraw-Hill, New Work, 1988.
6. Dec, J. E. (2009). Advanced compression-ignition engines—understanding the in-cylinder processes. Proceedings of the combustion institute, 32(2), 2727-2742.
7. Kalghatgi, G. T. (2014). The outlook for fuels for internal combustion engines. International Journal of Engine Research, 1468087414526189.
8. On-Highway Emissions Regulations, Cummins Emission Solutions.

9. Yanagihara, H., Sato, Y., & Mizuta, J. (1996, April). A simultaneous reduction of NOx and soot in diesel engines under a new combustion system (Uniform bulky combustion system UNIBUS). In *17th International Vienna Motor Symposium* (pp. 303-314).
10. Kimura, S., Aoki, O., Ogawa, H., Muranaka, S., & Enomoto, Y. (1999). New combustion concept for ultra-clean and high-efficiency small DI diesel engines (No. 1999-01-3681). SAE Technical Paper.
11. Hashizume, T. 1998. Combustion and Emission Characteristics of Multiple Stage Diesel Combustion, SAE Paper No. 980505.
12. Lee, J., & Song, H. H. (2014). Experimental and computational study on recompression reaction of pilot-injected fuel during negative valve overlap in a gasoline-fueled homogeneous charge compression ignition engine. International Journal of Automotive Technology, 15(7), 1071-1082.
13. Kalghatgi, G. T., Risberg, P., & Å ngström, H. E. (2006). Advantages of fuels with high resistance to auto-ignition in late-injection, low-temperature, compression ignition combustion (No. 2006-01-3385). SAE Technical Paper.
14. Hildingsson, L., Johansson, B., Kalghatgi, G. T., & Harrison, A. J. (2010). Some effects of fuel autoignition quality and volatility in premixed

compression ignition engines. SAE International Journal of Engines, 3(2010-01-0607), 440-460.

15. Kalghatgi, G. T. (2014). Fuel/engine interactions. Training, 1998, 09-21.
16. Kalghatgi, G. T., Hildingsson, L., Harrison, A. J., & Johansson, B. (2011). Surrogate fuels for premixed combustion in compression ignition engines. International Journal of Engine Research, 1468087411409307.
17. Siebers, D. L., & Higgins, B. (2001). Flame lift-off on direct-injection diesel sprays under quiescent conditions (No. 2001-01-0530). SAE Technical Paper.
18. Risberg, P., Kalghatgi, G., Å ngstrom, H. E., & Wåhlin, F. (2005). Auto-ignition quality of diesel-like fuels in HCCI engines (No. 2005-01-2127). SAE Technical Paper.
19. Kalghatgi, G. T., Risberg, P., & Angstrom, H. E. (2007). Partially pre-mixed auto-ignition of gasoline to attain low smoke and low NOx at high load in a compression ignition engine and comparison with a diesel fuel (No. 2007-01-0006). SAE Technical Paper.
20. Hildingsson, L., Kalghatgi, G., Tait, N., Johansson, B., & Harrison, A. (2009). Fuel octane effects in the partially premixed combustion regime in compression ignition engines (No. 2009-01-2648). SAE Technical Paper.

21. Manente, V., Tunestål, P., & Johansson, B. (2009). Half load partially premixed combustion, PPC, with high octane number fuels. gasoline and ethanol compared with diesel. In Symposium on International Automotive Technology: SIAT 2009.
22. Manente, V., Johansson, B., Tunestal, P., & Cannella, W. (2009). Effects of different type of gasoline fuels on heavy duty partially premixed combustion. SAE International Journal of Engines, 2(2009-01-2668), 71-88.
23. Manente, V., Zander, C. G., Johansson, B., Tunestal, P., & Cannella, W. (2010). An advanced internal combustion engine concept for low emissions and high efficiency from idle to max load using gasoline partially premixed combustion (No. 2010-01-2198). SAE Technical Paper.
24. Sellnau, M., Sinnamon, J., Hoyer, K., & Husted, H. (2011). Gasoline direct injection compression ignition (GDCI)-diesel-like efficiency with low CO2 emissions. SAE International Journal of Engines, 4(2011-01-1386), 2010-2022.
25. Sellnau, M. C., Sinnamon, J., Hoyer, K., & Husted, H. (2012). Full-Time Gasoline Direct-Injection Compression Ignition (GDCI) for High Efficiency and Low NOx and PM. SAE International Journal of Engines, 5(2012-01-0384), 300-314.

26. Borgqvist, P., Tunestal, P., & Johansson, B. (2012). Gasoline partially premixed combustion in a light duty engine at low load and idle operating conditions (No. 2012-01-0687). SAE Technical Paper.
27. Chang, J., Kalghatgi, G., Amer, A., & Viollet, Y. (2012). Enabling high efficiency direct injection engine with naphtha fuel through Partially Premixed Charge Compression Ignition Combustion (No. 2012-01-0677). SAE Technical Paper.
28. Chang, J., Kalghatgi, G., Amer, A., Adomeit, P., Rohs, H., & Heuser, B. (2013). Vehicle demonstration of naphtha fuel achieving both high efficiency and drivability with EURO6 engine-out NOx emission. SAE International Journal of Engines, 6(2013-01-0267), 101-119.
29. Marriott, C. D., & Reitz, R. D. (2002). Experimental investigation of direct injection-gasoline for premixed compression ignited combustion phasing control (No. 2002-01-0418). SAE Technical Paper.
30. Hanson, R., Splitter, D., & Reitz, R. D. (2009). Operating a heavy-duty direct-injection compression-ignition engine with gasoline for low emissions (No. 2009-01-1442). SAE Technical Paper.
31. Weall, A., & Collings, N. (2009). Gasoline fuelled partially premixed compression ignition in a light duty multi cylinder engine: a study of low

load and low speed operation. SAE International Journal of Engines, 2(2009-01-1791), 1574-1586.

32. Weall, A., & Collings, N. (2007). Investigation into partially premixed combustion in a light-duty multi-cylinder diesel engine fuelled gasoline and diesel with a mixture of. SAE technical papers.
33. Ra, Y., Loeper, P., Reitz, R. D., Andrie, M., Krieger, R., Foster, D. E., ... & Szymkowicz, P. (2011). Study of high speed gasoline direct injection compression ignition (GDICI) engine operation in the LTC regime. SAE International Journal of Engines, 4(2011-01-1182), 1412-1430.
34. Manente, V., Zander, C. G., Johansson, B., Tunestal, P., & Cannella, W. (2010). An advanced internal combustion engine concept for low emissions and high efficiency from idle to max load using gasoline partially premixed combustion (No. 2010-01-2198). SAE Technical Paper.
35. Ciatti, S., Johnson, M., Adhikary, B. D., Reitz, R. D., & Knock, A. (2013). Efficiency and Emissions Performance of Multizone Stratified Compression Ignition Using Different Octane Fuels (No. 2013-01-0263). SAE Technical Paper.
36. Zheng, L., Qi, Y., He, X., & Wang, Z. (2012). Visualization of partially premixed combustion of gasoline-like fuel using high speed imaging in a

constant volume vessel. SAE International Journal of Engines, 5(2012-01-1236), 1320-1329.

37. Ogawa, H., Shibata, G., Jin, X., Hirose, T., & Kono, N. (2013). Visualization and Heat Release Analysis of Premixed Diesel Combustion with Various Fuel Ignitabilities and Oxygen Concentrations in a Constant Volume Combustion Vessel (No. 2013-01-0899). SAE Technical Paper.
38. Kim, K., Bae, C., & Johansson, B. (2013). Spray and combustion visualization of gasoline and diesel under different ambient conditions in a constant volume chamber (No. 2013-01-2547). SAE Technical Paper.
39. Baert, R. S., Frijters, P. J., Somers, B., Luijten, C. C., & de Boer, W. (2009). Design and operation of a high pressure, high temperature cell for HD diesel spray diagnostics: guidelines and results (No. 2009-01-0649). SAE Technical Paper.
40. Cung, K., Moiz, A., Johnson, J., Lee, S. Y., Kweon, C. B., & Montanaro, A. (2015). Spray–combustion interaction mechanism of multiple-injection under diesel engine conditions. Proceedings of the Combustion Institute, 35(3), 3061-3068.
41. Meijer, M., Somers, B., Johnson, J., Naber, J., Lee, S. Y., Malbec, L. M., ... & Bazyn, T. (2012). Engine Combustion Network (ECN):

Characterization and comparison of boundary conditions for different combustion vessels. Atomization and Sprays, 22(9), 777-806.

42. Bardi, M., Payri, R., Malbec, L. M., Bruneaux, G., Pickett, L. M., Manin, J., ... & Genzale, C. L. (2012). Engine combustion network: comparison of spray development, vaporization, and combustion in different combustion vessels. Atomization and Sprays, 22(10).
43. Pei, Y., Davis, M. J., Pickett, L. M., & Som, S. (2015). Engine Combustion Network (ECN): Global sensitivity analysis of Spray A for different combustion vessels. Combustion and Flame, 162(6), 2337-2347.
44. Pickett, L. M., Genzale, C. L., Bruneaux, G., Malbec, L. M., Hermant, L., Christiansen, C., & Schramm, J. (2010). Comparison of diesel spray combustion in different high-temperature, high-pressure facilities. SAE International Journal of Engines, 3(2010-01-2106), 156-181.
45. https://ecn.sandia.gov/
46. Kolodziej, C., Kodavasal, J., Ciatti, S., Som, S., Shidore, N., & Delhom, J. (2015). Achieving Stable Engine Operation of Gasoline Compression Ignition Using 87 AKI Gasoline Down to Idle (No. 2015-01-0832). SAE Technical Paper.
47. Kolodziej, C. P., Ciatti, S., Vuilleumier, D., Adhikary, B. D., & Reitz, R. D. (2014). Extension of the lower load limit of gasoline compression

ignition with 87 AKI gasoline by injection timing and pressure (No. 2014-01-1302). SAE Technical Paper.

48. Bobba, M. K., Genzale, C. L., & Musculus, M. P. (2009). Effect of ignition delay on in-cylinder soot characteristics of a heavy duty diesel engine operating at low temperature conditions. SAE International Journal of Engines, 2(2009-01-0946), 911-924.
49. Dec, J. E. A conceptual model of DI Diesel combustion based on laser-sheet imaging, SAE Paper 970873, 1997. There is no corresponding record for this reference.
50. Flynn, P. F., Durrett, R. P., Hunter, G. L., zur Loye, A. O., Akinyemi, O. C., Dec, J. E., & Westbrook, C. K. (1999). Diesel combustion: an integrated view combining laser diagnostics, chemical kinetics, and empirical validation.
51. Musculus, M. P., Miles, P. C., & Pickett, L. M. (2013). Conceptual models for partially premixed low-temperature diesel combustion. Progress in Energy and Combustion Science, 39(2), 246-283.
52. Musculus, M. P. (2006). Multiple simultaneous optical diagnostic imaging of early-injection low-temperature combustion in a heavy-duty diesel engine (No. 2006-01-0079). SAE Technical Paper.

53. Pickett, L. M., Kook, S., & Williams, T. C. (2009). Visualization of diesel spray penetration, cool-flame, ignition, high-temperature combustion, and soot formation using high-speed imaging. SAE International Journal of Engines, 2(2009-01-0658), 439-459.

54. Naber, J. D., & Siebers, D. L. (1996). Effects of Gas Density and Vaporization on Penetration and Dispersion of Diesel Sprays". SAE Technical Paper 960034. Society of Automotive Engineers, Warrendale, PA.

55. Siebers, D. L., Higgins, B., & Pickett, L. (2002). Flame lift-off on direct-injection diesel fuel jets: oxygen concentration effects (No. 2002-01-0890). SAE Technical Paper.

56. Pickett, L. M., & Siebers, D. L. (2004). Non-sooting, low flame temperature mixing-controlled DI diesel combustion (No. 2004-01-1399). SAE Technical Paper.

57. Pickett, L. M., & Siebers, D. L. (2002). An investigation of diesel soot formation processes using micro-orifices. Proceedings of the Combustion Institute, 29(1), 655-662.

58. Musculus, M. P., & Kattke, K. (2009). Entrainment waves in diesel jets. SAE International Journal of Engines, 2(2009-01-1355), 1170-1193.

59. Pickett, L. M., Manin, J., Genzale, C. L., Siebers, D. L., Musculus, M. P., & Idicheria, C. A. (2011). Relationship between diesel fuel spray vapor penetration/dispersion and local fuel mixture fraction. SAE International Journal of Engines, 4(2011-01-0686), 764-799.

60. Idicheria, C. A., & Pickett, L. M. (2007). Quantitative mixing measurements in a vaporizing diesel spray by Rayleigh imaging (No. 2007-01-0647). SAE Technical Paper.

61. Idicheria, C. A., & Pickett, L. M. (2007). Effect of EGR on diesel premixed-burn equivalence ratio. Proceedings of the Combustion Institute, 31(2), 2931-2938.

62. Musculus, M. P., Lachaux, T., Pickett, L. M., & Idicheria, C. A. (2007). End-of-injection over-mixing and unburned hydrocarbon emissions in low-temperature-combustion diesel engines (No. 2007-01-0907). SAE Technical Paper.

63. Song, H. H., & Edwards, C. F. (2009). Understanding chemical effects in low-load-limit extension of homogeneous charge compression ignition engines via recompression reaction. International Journal of Engine Research, 10(4), 231-250.

64. Shi, Y., Ge, H. W., & Reitz, R. D. (2011). Computational optimization of internal combustion engines. Springer Science & Business Media.

65. Pickett, L. M., & Siebers, D. L. (2004). Soot in diesel fuel jets: effects of ambient temperature, ambient density, and injection pressure. Combustion and Flame, 138(1), 114-135.

국 문 초 록

압축 착화 엔진(CI engine)은 연소 특성상 높은 열효율을 가지고 있지만, 입자상 물질(soot)과 질소산화물(NOx)을 많이 배출하는 단점을 가지고 있다. 현재 많은 국가들에서는 자동차 배기가스에 의한 환경 문제를 줄이기 위해 엔진에서 발생하는 오염물질의 배출을 제한하는 규제를 강화하고 있다. 이러한 추세에 맞추어 압축 착화 엔진에서 입자상 물질을 줄이지 위한 많은 연구가 이루어지고 있는데 그 중 하나가 부분 예혼합 압축 착화(PPCI: Partially premixed compression ignition) 방식이다. 압축 착화 엔진에서 입자상 물질은 실린더로 직접 분사된 연료와 내부 공기가 충분히 혼합되지 못한 상태에서 생성되기 때문에 입자상 물질의 생성을 억제하기 위해서는 연소 전까지 공기와 연료의 충분한 혼합을 유도하는 것이 중요하다. 이를 위한 연소 전략 중에 하나인 PPCI 는 물리적인 제어 방식을 통해 당량비가 2 이하인 혼합기의 비율을 높이는 것을 목표로 한다.

다양한 연료들 중에서 가솔린 계열의 연료는 점화 지연이 길기 때문에 연소 시작 전까지 공기와 연료가 혼합될 수 있는 충분한 시간을 보장한다. 이러한 가솔린 계열의 연료들 중에서 옥탄가가 70 전후인 저옥탄 연료의 경우, 낮은 부하, 높은 RPM 에서 고옥탄 가솔린보다 연소 안정성이 뛰어나기 때문에 주목을 받고 있다. 현재 저옥탄 연료를 적용한 압축 착화 엔진에 대한 연구들이 이루어지고

있지만, 기존의 디젤 엔진을 그대로 이용한 것이 대부분이다. 압축 착화 엔진에서의 연료 스프레이 특성은 엔진의 효율, 배기 특성, 구조를 결정하는 주요 변수이지만, 저옥탄 연료의 경우, 이러한 핵심 정보들에 대한 연구가 미미하다. 따라서 저옥탄 연료를 이용한 최적화된 PPCI 엔진을 개발하기 위한 선행 단계로서 가솔린의 스프레이에 대한 연구가 필수적이다. 따라서 본 연구에서는 PRF70 연료를 이용하여 정적연소실에서 저옥탄 연료의 스프레이 연소를 모사하고 계측하는 것을 목표로 한다.

우선, 다양한 조건에서의 연소 모드를 비교한 결과, 기존의 연소 모델로 설명할 수 없는 새로운 연소 모드가 존재함을 확인하였고, 이를 'Partially premixed combustion zone'이라고 명명하였다. 이 조건은 기존의 LTC 연소보다는 분사 기간이 길고, 일반적인 디젤 연소보다 연소 시작 지점이 다운 스트림에 위치하고 있다는 것이 가장 큰 차이점이다. 기존의 디젤 스프레이는 연소는 강한 운동량으로 인해 화염이 앞으로만 전파되는 발달 형상을 보이지만, 이 새로운 연소 모드에서는 저압 분사로 인해 다운 스트림에서의 운동량이 작기 때문에 처음 연소가 시작한 지점에서 모든 방향으로 예혼합 화염 영역의 확장이 발생한다. 화염 영역이 확장이 되면서 스프레이 상류의 특정 지점을 통과하게 되면 최종적으로 강한 발광 신호와 함께 입자상 물질이 생성된다. 반복 실험을 통해 같은 조건에서도 입자상 물질의 발광 세기에 큰

편차가 있음이 확인되었고, 이는 연소 시작 지점의 편차에 기인한 것으로 밝혀졌다. 이러한 확률적인 거동 현상을 이해하기 위해서 시뮬레이션을 통해 스프레이 내부의 열역학적 특성에 대한 정보를 계산하였다. 시뮬레이션 결과, 다운 스트림에서 발생한 화염이 상류의 당량비가 2 인 지점을 통과하는지 여부가 입자상 물질의 생성을 결정하며, 인젝터 앞쪽의 온도 편차가 확률적인 거동을 결정하는 중요 변수임을 알 수 있었다. 만약 스프레이 상류의 배경 온도를 일정하게 제어할 수 있다면, 초기 연소 지점 또한 예측, 제어가 가능할 것이며, 이를 통해 입자상 물질의 생성을 줄일 수 있을 것으로 예상된다. 일반적인 LTC 운전에서는 추가적인 입자상 물질의 생성을 막기 위해 분사 기간을 짧게 가져가는 것이 일반적이지만, 본 연구를 통해서 분사 기간이 길더라도 입자상 물질의 생성을 제한하는 것이 가능하다는 것을 알 수 있다.

본 연구에서는 기존에 알려진 디젤 스프레이 연소와는 다른 저옥탄 연료의 새로운 연소 모드를 확인하였고, 광학계측법을 통해 화염의 발달 과정을 이해하였다. 점화 지연이 긴 연료를 저압으로 분사하였을 경우, 다운 스트림에서의 예혼합 화염이 입자상 물질을 생성을 결정하는 주요 메커니즘이며, 인젝터 앞 쪽, 즉, 스프레이 상류의 온도 구배에 큰 영향을 받는다. 온도 제어를 통해 초기 점화 지점을 충분히 다운 스트림 영역으로 제한할 수 있다면, 연소 기간

동안 상류로의 화염 영역의 확장을 예방하여 입자상 물질의 생성을 줄일 수 있다.